DOCTORAL THESIS

# Distributional analyses of midwater gelatinous zooplankton with ROV-collected videos: a comparative approach using submarine calderas

By

MITSUKO HIDAKA

Supervisor: Adjunct Professor
DHUGAL JOHN LINDSAY

Department of Marine Sciences
Graduate School of Marine Biosciences
Kitasato University
2019

## Acknowledgements

Foremost, I would like to express appreciation to my supervisor Dr. Dhugal Lindsay for his considerable support regarding my PhD research and for his great understanding of my lack of experience when I entered this research field. Thanks to his guidance and patience, I was able to overcome many obstacles to finishing my PhD, such as funding problems and health problems. His generous personality, which attracts many good colleagues, will continue to be an example for me in my future career as a scientist.

Dr. Hiroshi Miyake is the person who gave me the motivation to study gelatinous zooplankton. If I had not met him, I would not have come to think that jellyfishes are such attractive marine creatures. Moreover, he recommended me to work on ROV video analysis at JAMSTEC with his great understanding of my circumstances when I got pregnant with my dearest daughter Yukiko, and he introduced me to Dr. Dhugal Linday.

Dr. Takashi Asahida has been an important person to me to keep me studying ocean science. His words and advice always challenged me to improve my research and move my life forward. One of his comments "Be a specialist, however be a generalist" that I heard in his lecture one day when I was an undergraduate school student is one of the most influential quotes that spoke to me as a scientist.

Dr. Kenichi Hayashizaki has given me some critical advice and heartfelt comments since I was an undergraduate school student. His knowledge-based convictive advice helped me to develop "scientific brain".

Advice from all the other professors at Kitasato University have affected me and improved both my research life and private life. Here I would like to express my appreciation to all the teaching and office staff for their great help.

Dr. Jun Nishikawa gave me advice and his knowledge to help brush up my doctoral thesis, and he has given me a lot of great opportunities to study hydromedusae, ctenophores, and pelagic tunicates. His brilliant students from Tokai University also stimulated my PhD student life.

Dr. Hiroyuki Yamamoto and Dr. Tomohiko Fukushima gave me their great understanding and support for my research, especially allowing me to present my research results overseas by participating in international conferences and publishing in international journals.

Mr. Tsuchiya, Mr. Nitta, Mr. Tanada are people who taught me video technician-like skills. Ms. Watanabe, Ms. Tsuda and Ms. Tabata helped me to follow correctly various office procedures at JAMSTEC. Not only these members but also many other people from JAMSTEC, Marine Works Japan (MWJ), Nippon Marine Enterprises, Ltd (NME) helped me in relation to my PhD research results. Here I would like to sincerely express my appreciation to all staff from these companies.

Lastly, I would like to express my gratefulness to my father Hiroto Hidaka, my mother Yoshiko Hidaka, my twin sisters Yuko Ota, Ayako Ota, and my uncles for all your patience and understanding about my research life and for all the help you have given to take care of my daughter Yukiko.

To Yukiko, hereby your mother finishes her doctoral thesis. As in your name "志子", please never give up on your dreams if you have found something that you want to accomplish. You do not have to fight alone, you can find the people who will

help you realize your dreams, as happened with your mother. I am so sorry that I often came back home late, and thank you for your patience from your early childhood. I will always love you and I wish that you are always happy.

# Table of Contents

# General Introduction

## DEEP-SEA MINING AND ENVIRONMENTAL IMPACT ASSESSMENTS (EIAs)

Both the land and the oceans provide humankind with multiple resources such as oil, gas and metals. However, the resources are finite, and the depletion of these resources is one of the most profound issues in the modern world. Indeed, terrestrial ore mining already faces problems such as deterioration of ore grade and increasing mining costs (Prior et al. 2012). As alternative mineral resources to terrestrial ores, deep-sea minerals are receiving a large amount of attention in recent times. To this date, three types of minable deep-sea mineral sources (manganese nodules, cobalt-rich ferromanganese crusts and seafloor massive sulfides) have been recognised, and they contain industrially valuable elements (Petersen et al. 2016). Kotlinski (2001) predicted that commercial exploitation of deep-sea mineral resources would not start until after 2020. However, the Japan Oil, Gas and MEtals national Corporation (JOGMEC) successfully excavated minerals from seafloor massive sulfide (SMS) deposits at the Izena Hole, Okinawa Trough (about 1600 m depth), with continuous lifting to the surface for the first time, during an expedition from mid August to late September in 2017. The economic evaluation for commercialisation will take place in 2019 (Ministry of Economy, Trade and Industry 2017). From a global perspective, twenty-nine contractors from France, Russia, Japan, China, Korea, Germany, UK, and so on, have already made contracts for

future deep-sea mining in waters beyond national jurisdiction (International Seabed Authority (ISA): www.isa.org.jm (2018)).

During the prospecting and mining processes, a multitude of potential impacts on ocean environments have been predicted and discussed (e.g. review in Glover & Smith 2003, Van Dover 2014). In response to these accumulated arguments, the International Seabed Authority (ISA) produced a document entitled "Recommendations for the guidance of contractors for the assessment of the possible environmental impacts arising from exploration for marine minerals in the Area" (ISA 2013; https://www.isa.org.jm/sites/default/files/files/documents/isba-19ltc-8_0.pdf). The document refers to the acquisition of baseline data and monitoring for the biological, chemical, geological and physical components from the surface to the bottom beyond areas of national jurisdiction.

## MINING DEEP-SEA SEAFLOOR MASSIVE SULFIDE (SMS) DEPOSITS AND RELATED ENVIRONMENTAL IMPACT ASSESSMENTS IN JAPAN

Seafloor Massive Sulfides (SMS) deposits were the last deep-sea mineral resource type to be discovered after manganese nodules and cobalt-rich ferromanganese crusts, and are known to contain a higher grade of deep-sea minerals, such as copper, zinc, gold and silver, than land-based volcanogenic massive sulfide (VMS) deposits. SMS are formed through underwater volcanic hydrothermal activity. Therefore, the deposits develop on divergent or convergent tectonic plate boundaries, such as Mid Ocean Ridges (MORs) or Island Arc systems (Cherkashov 2017). Based on known or suspected active deposits, 59% are located beyond areas of national

jurisdiction, 39% within Exclusive Economic Zones (EEZ), and 2% are included in proposals for extensions of continental shelves by different countries (Peterson et al. 2016). The EEZ of Japan includes two major typical Arc systems, namely the Izu-Bonin Arc and the Okinawa Trough, where many hydrothermal fields have been identified (Ishibashi & Urabe 1995, Fujikura et al. 2008).

Hydrothermal vents are widely known to form the foundations of unique habitats for chemosynthetic organisms – so-called chemosynthetic ecosystems. Fauna living at hydrothermal vents gain their energy through microbial chemoautotrophic primary production, not from photosynthetic primary production, and most of the species are endemic to vent sites (Tunnicliffe et al. 2003). Representative organisms include tubeworms, brachyuran crabs, mytilid mussels and other benthic invertebrates, and they have been actively investigated by scientists since their discovery in 1977 (reviewed in Lutz & Kennish 1993). Hydrothermal vent environments often contain an extremely high biomass of organisms when compared to seafloors far from such highly productive vents. Consequently, hydrothermal vents are of vital importance both for future human economic activities and for deep-sea organisms that rely on chemosynthesis as an energy source. Possible environmental impacts of mining SMS deposits at hydrothermal vents have been actively discussed and reviewed (e.g. Van Dover 2011, Boschen et al. 2013), and the expected impacts are relatively high at the seafloor, though also reaching to the ocean surface. Therefore, targeting the entire water column during surveys at the mining site is a strongly prerequisite for EIAs. Indeed, section III (15:e: iii) expressly states the requirement for baseline data to "assess pelagic communities in the water column and in the benthic boundary layer that may be impacted by operations" (ISA 2013).

In 2014, a program targetting next-generation technology for ocean resources exploration ("Zipangu in the Ocean" program) was kicked off under the cross-ministerial Strategic Innovation Promotion program (SIP) driven by the Cabinet office in Japan (JAMSTEC 2014). The project is intended to facilitate the launch of commercial-based exploration for ocean resources and to help establish global standards concerning technologies for mineral extraction and environmental assessments. For the EIA section, baseline surveys around SMS deposits have been carried out and some investigation protocols have been developed (JAMSTEC 2017).

## GELATINOUS MACROZOOPLANKTON COMMUNITY ABOVE SEAFLOOR MASSIVE SULFIDE DEPOSITS

Gelatinous macrozooplankton are relatively large-sized (>1 cm) zooplankton that have fragile gelatinous bodies, and include "jellyfishes" such as pelagic cnidarians, ctenophores and tunicate chordates. They are ubiquitous and well-adapted to a variety of environments, exponentially increasing in number when the environment changes to being ecologically favourable. Their feeding habits can be categorised into three groups, filter feeding (e.g. phytoplankton or marine snow), crustacean feeders (e.g. copepods and euphausiids) and gelatinous feeders (e.g. salps, cnidarian and ctenophoran jellyfishes), respectively. Pelagic tunicates are filter feeding, most cnidarian jellyfishes and ctenophores are crustacean feeders, and some ctenophores and cnidarians feed on other gelatinous zooplankton (e.g. Madin 1974, Purcell 1991, 2003, Choy et al. 2017).

The regions where SMS deposits occur within the Japanese EEZ are oligotrophic, with extremely low primary productivity near the ocean surface (e.g. McClain et al. 2004). Within such oligotrophic waters, primary production is dominated by extremely small phytoplankton, so-called pico- (<2 μm) or nano-plankton (<20 μm), instead of larger diatoms (Acevedo-Trejos et al. 2013). These phytoplankton are too small to be fed upon directly by grazing copepods (which mainly rely on diatoms), and filter-feeding tunicates can instead become dominant (Sommer et al. 2002) (Fig 1). Therefore, the "jelly web", which refers to a food web based on predator-prey relationships between gelatinous zooplankton, can be more developed than in higher productivity areas. Notwithstanding, the species distribution of gelatinous zooplankton in oligotrophic areas has not yet been studied to any degree.

The high productivity of hydrothermal vent ecosystems can affect the gelatinous zooplankton community above SMS deposits. Burd and Thomson (1994) revealed that enhanced zooplankton biomass extended throughout the water column above hydrothermal vents on the Endeavour Ridge (Pacific Ocean). They also revealed a relatively high biomass of gelatinous zooplankton (medusae) at the same site, and suggested that the medusae in the vent region were generally larger taxa than those captured off-vent (Burd & Thomson 2000). Vereshchaka and Vinogradov (1999) also observed high concentrations of zooplankton just above and below a vent plume and revealed a high relative proportion of gelatinous zooplankton (medusae and ctenophores) using the manned submersibles "Mir-1" and "Mir-2" at the Broken Spur vent field (Atlantic ocean), which is also in an ultra-oligotrophic area. All of this research points to the high food availability (e.g. bacteria, organic particles or

local zooplankton aggregations) at hydrothermal vents as the cause for an enriched gelatinous zooplankton community, especially in oligotrophic areas.

## INVESTIGATION OF GELATINOUS MACROZOOPLANKTON USING ROVS AND DATA MINING OF ARCHIVED VIDEOS

Much of the taxonomy, biology and ecology of gelatinous macrozooplankton remains unknown, especially concerning deep-sea species, because their fragile bodies are easily destroyed by conventional collection methods such as plankton nets. Raskoff et al. (2010) revealed that the taxon composition of gelatinous zooplankton (jellyfishes) caught by a plankton net and observed by a Remotely-Operated Vehicle (ROV) was different, and that net sampling methods were more effective for small sized taxa (mm size). In-situ observation methods such as Human Occupied Vehicles (HOV) or ROVs have been used since the late 20th Century, leading to the discovery of new species, revealing aspects of the ecology of many gelatinous zooplankton, and characterizing their distribution at some localities (e.g. Madin & Harbison 1978, Pugh & Youngbluth 1988, Toyokawa et al. 1998, Haddock et al. 2005, Lindsay & Hunt 2005, Choy et al. 2017). The effectiveness of HOV or ROV investigations for studying gelatinous macrozooplankton is readily apparent from such previous studies. However, investigation protocols remain largely uncharacterized (with the notable exception of Hunt & Lindsay (1999)). Significant differences between HOVs and ROVs are direct observations by the human eye in the former (but usually with low-quality video) and repeatable observations through reference to high-quality videos in the latter. ROVs are superior with respect to repeatability and quality control of the data produced.

Over the past few decades, several thousand ROV dives have been carried out by the Japan Agency for Marine-Earth Science and Technology (JAMSTEC), formerly the Japan Marine Science Technology Center, for many different scientific purposes. However, only a small proportion of the data from these ROV dives has so far been published in research papers. The primary reason for this is a problem with the way shiptime is provided to researchers. Dive time for ROV surveys is costly, so usually only limited surveys can be done during a single research cruise. Ideally, for mid-water ROV surveys, at least three dives should be done at a single station – one mainly concentrating on taxonomic work to characterize the major taxa at the dive site, one where quantitative transects at set depth strata (the same strata regardless of geographic location) are run, and one where the strata for transects are set at depths based on the physico-chemical parameters of the water column vs depth at that particular station. Furthermore, researchers who work on mid-water organisms consider that three or more quantitative dives at the same location should be performed for statistical analyses, since differences in abundance of up to 35-fold have been reported at the same dive site on consecutive days (Lindsay & Hunt 2005). However, because of the reason described above, adequate ship time cannot be ensured. In addition, cancellation of planned dives due to bad weather conditions also happens frequently. As a consequence, only one dive at a locality is often what happens, and because of this, most of the past mid-water ROV dive video records have become betwixt and between states useful for either, but not both, quantitative and taxonomic work. However, if we could properly utilise such video records, we could provide useful baseline data for Environmental Impact Assessments (EIAs)

through data mining. Analyses of legacy data should also be valuable for assessing long-term variations in the ecosystems.

## COMPARATIVE ROV IMAGE-BASED SURVEYS OF GELATINOUS MACROZOOPLANKTON INSIDE AND OUTSIDE DEEP-SEA CALDERAS

When collecting baseline data for Environmental Impact Assessments (EIAs), different elements among the natural habitats should be taken into consideration. For Seafloor Massive Sulfide (SMS) mining, whether the study site is at an active vent site or not, and the sensitivity of the site to disturbances are particularly important. Deep-sea calderas can contain large amounts of high-quality SMS ore (Ishibashi et al 2015.) and hydrothermal vents. The stability of the environment inside calderas is high when compared to the environment outside calderas, because of the semi-closed geography. Indeed, uniform temperature and density water masses inside calderas have been reported from the Izu-Bonin Arc (Iwabuchi et al. 1989, Shitashima & Maeda 2005). These facts indicate that the environment inside calderas could be easily affected by anthropogenic disturbances, such as those accompanying deep-sea mining. Calderas are also ideal study sites to investigate the effects of extremely different environment conditions on biological communities at essentially the same biogeographic location.

The complex topographies of vent sites and calderas has hampered investigations on the resident zooplankton communities using plankton nets. Therefore, the importance of non-destructive, image-based ROV investigations has been considered of great value. Nevertheless, there is limited data on the gelatinous macrozooplankton community at active vent sites based on ROV image-based

surveys (exceptionally Lindsay et al. (2015)) but there is effectively no information at all on the communities within non-active deep-sea calderas. Moreover, the only information on zooplankton at vent sites from within Japan's EEZ is from the Okinawa Trough (Lindsay et al. 2015), and there is no data from the Izu-Bonin Arc. To assess environmental impacts on gelatinous macrozooplankton, more baseline data is necessary. In the context above, the present study attempts to collect baseline data on gelatinous macrozooplankton in the Izu-Bonin Arc, utilising the unique features associated with deep-sea caldera environments. In particular, it focuses on the relationship between hydrothermal ecosystems and gelatinous macrozooplankton communities. Concretely, image-based analyses were carried out on the video records of six ROV dives both inside and outside of three different deep-sea calderas (two hydrothermally active and one inactive) on the Izu-Bonin Arc, and the vertical distribution of gelatinous zooplankton taxa was determined.

**AIM OF THIS STUDY**

This doctoral thesis aims to establish a protocol to analyse archived mid-water ROV dives, and provide baseline data on gelatinous macrozooplankton around Seafloor Massive Sulfide (SMS) deposit areas. The specific goals of the study were to: (1) describe the analysis protocol for archived ROV video records; (2) reveal and compare the gelatinous macrozooplankton communities inside and outside of hydrothermally active and inactive deep-sea calderas.

Accordingly, this doctoral thesis is composed of three chapters. Chapter 1 describes the analysis protocol for archived ROV video records and additional results; Chapter 2 describes the gelatinous zooplankton community both inside and

outside of an inactive deep-sea caldera, and Chapter 3 describes the gelatinous zooplankton community inside and outside of an active deep-sea caldera. Finally, general discussion is made and conclusions are drawn.

**REFERENCES**

Acevedo-Trejos E, Brandt G, Merico A, Smith SL (2013) Biogeographical patterns of phytoplankton community size structure in the oceans. Global Ecol Biogeogr 22: 1060–1070.

Boschen RE, Rowden AA, Clark MR, Gardner JPA (2013) Mining of deep-sea seafloor massive sulfides: A review of the deposits, their benthic communities, impacts from mining, regulatory frameworks and management strategies. Ocean Coast Manage 84: 54–67.

Burd BJ, Thomson RE (1994) Hydrothermal venting at Endeavour Ridge: effect on zooplankton biomass throughout the water column. Deep-Sea Res Part 1 41(9): 1407–1423.

Burd BJ, Thomson RE (2000) Distribution and relative importance of jellyfish in a region of hydrothermal venting. Deep-Sea Res Part I 47: 1703–1721.

Cherkashov G (2017) Chapter 4: Seafloor massive sulfide deposits: Distribution and prospecting. In: Deep-Sea Mining: Resource Potential, Technical and Environmental Considerations (ed Sharma R). Springer International Publishing, Cham, Switzerland,

pp. 143–164. ISBN 978-3-319-52556-3, ISBN 978-3-319-52557-0 (eBook), DOI 10.1007/978-3-319-52557-0

Choy CA, Haddock SHD, Robison BH (2017) Deep pelagic food web structure as revealed by in situ feeding observations. Proc R Soc B 284: 20172116. http://dx.doi.org/10.1098/rspb.2017.2116

Fujikura K, Kojima S, Hashimoto J (2008) Chapter 3, Chemosynthesis-based communities around Japan. In: Deep-sea Life – Biological observations using research submersibles (eds Fujikura K, Okutani T, Maruyama T). ISBN 978-4-486-01787-5. Tokai University Press, Kanagawa, pp. 57–83. (in Japanese)

Glover AG, Smith C (2003) The deep-sea floor ecosystem: current status and prospects of anthropogenic change by the year 2025. Environ Conserv 30(3): 219–241.

Haddock SHD, Dunn CW, Pugh PR (2005) A re-examination of siphonophore terminology and morphology, applied to the description of two new prayine species with remarkable bio-optical properties. J Mar Biol Assoc UK 85: 695–707

Hunt JC, Lindsay DJ (1999) Methodology for creating an observational database of midwater fauna using submersibles: results from Sagami Bay, Japan. Plankton Biol Ecol 46(1): 75–87.

International Seabed Authority (2013) Recommendations for the guidance of contractors for the assessment of the possible environmental impacts arising from exploration for marine minerals in the Area. Available at: https://www.isa.org.jm/sites/default/files/files/documents/isba-19ltc-8_0.pdf (accessed on 14 November 2018)

International Seabed Authority (2018) Deep seabed minerals contractors. Available at: https://www.isa.org.jm/deep-seabed-minerals-contractors (accessed on 14 November 2018)

Ishibashi J, Urabe T (1995) Hydrothermal activity related to arc-backarc magmatism in the Western Pacific. In: Backarc Basins: Tectonics and Magmatism (ed Taylor B). Springer Science+Business Media, New York, pp.451–495.

Ishibashi J, Ikegami F, Tsuji T, Urabe T (2015) Chapter 27, Hydrothermal activity in the Okinawa Trough Back-Arc Basin: geological background and hydrothermal mineralization. In: Subseafloor biosphere linked to global hydrothermal systems; TAIGA Concept (eds Ishibashi J., Okino K. and Sunamura M). ISBN 978-4-431-54864-5. Tokyo, Springer, pp. 337–359. DOI 10.1007/978-4-431-54865-2_27.

Iwabuchi Y, Ashi J, Fujioka K (1989) Geological and geomorphological survey of the Kurose Hole, north of the Hachijo Island. JAMSTEC J Deep Sea Res 5: 37–41. (in Japanese)

JAMSTEC (2014) Ecological surveys and long-term monitoring, SIP Protocol series No.1–6. Available at: https://www.jamstec.go.jp/sip/en/index.html (accessed on 15 November 2018)

JAMSTEC (2017) Ecological surveys and long-term monitoring, SIP Protocol series No.1–6. Available at: https://www.jamstec.go.jp/sip/en/resultList.html (accessed on 15 November 2018)

Kotlinski R (2001) Mineral resources of the world oceans - their importance for global economy in the 21st century. In: Proceedings of fourth ISOPE ocean mining symposium, International Society for Offshore and Polar Engineers, Szczecin, Poland, pp. 1–7.

Lindsay DJ, Hunt JC (2005) Biodiversity in midwater cnidarians and ctenophores: submersible-based results from deep-water bays in the Japan Sea and north-western Pacific. J Mar Biol Ass UK 85: 503–517.

Lindsay D, Umetsu M, Grossmann M, Miyake H, Yamamoto H (2015) Chapter 51, The gelatinous macroplankton community at the Hatoma Knoll hydrothermal vent. In: Subseafloor biosphere linked to global hydrothermal systems; TAIGA Concept (eds Ishibashi J., Okino K. and Sunamura M). ISBN 978-4-431-54864-5. Tokyo, Springer, pp. 639–666. DOI 10.1007/978-4-431-54865-2_51.

Lutz RA, Kennish MJ (1993) Ecology of deep-sea hydrothermal vent communities: a

review. Rev Geophys 31(3): 211–242.

Madin LP (1974) Field observations on the feeding behavior of salps (Tunicata : Thaliacea). Mar Biol 25: 143–147.

Madin LP, Harbison GR (1978) *Bathocyroe fosteri* gen. nov., sp. nov.: a mesopelagic ctenophore observed and collected from a submersible. J Mar Biol Ass UK 58: 559–564.

McClain CR, Signorini SR, Christian JR (2004) Subtropical gyre variability observed by ocean-color satellites. Deep-Sea Res II 51: 281–301.

Ministry of Economy, Trade and Industry (2017) World's first success in continuous ore lifting test for seafloor polymetallic sulphides. Available at: http://www.meti.go.jp/english/press/2017/0926_004.html (accessed on 26 February 2018)

Petersen S, Krätschell A, Augustin N, Jamieson J, Hein JR, Hannington MD (2016) News from the seabed – Geological characteristics and resource potential of deep-sea mineral resources. Mar Policy 70: 175–187.

Prior T, Giurco D, Muddb G, Mason L, Behrisch J (2012) Resource depletion, peak minerals and the implications for sustainable resource management. Glob Environ Change 22: 577–587.

Pugh PR, Youngbluth MJ (1988) A new species of *Halistemma* (Siphonophora: Physonectae: Agalmidae) collected by submersible. J Mar Biol Assoc UK 68: 1–14.

Purcell JE (1991) Predation by *Aequorea victoria* on other species of potentially competing pelagic hydrozoans. Mar Ecol Prog Ser 72: 255–260.

Purcell JE (2003) Predation on zooplankton by large jellyfish, *Aurelia labiata*, *Cyanea capillata* and *Aequorea aequorea*, in Prince William Sound, Alaska. Mar Ecol Prog Ser 246: 137–152.

Raskoff KA, Hopcroft RR, Kosobokova KN, Purcell J, Youngbluth M (2010) Jellies under ice: ROV observations from the Arctic 2005 hidden ocean expedition. Deep-Sea Res II 57: 111–126.

Shitashima K, Maeda Y (2005) Behaviour of hydrothermal plumes and tidal currents in the Suiyo Seamount caldera (Geochemistry). Oceanography in Japan 14(2): 297–307.

Sommer U, Stibor H, Katechakis A, Sommer F, Hansen T (2002) Pelagic food web configurations at different levels of nutrient richness and their implications for the ratio fish production: primary production. Hydrobiologia 484: 11–20.

Toyokawa M, Toda T, Kikuchi T, Nishida S (1998) Cnidarians and ctenophores

observed from the manned submersible *Shinkai 2000* in the midwater of Sagami Bay, Pacific coast of Japan. Plank Biol Ecol 45: 61–74.

Tunnicliffe V, Juniper SK, Sibuet M (2003) Chapter 4, Reducing Environments of the deep-sea floor. In: Ecosystems of the Deep Oceans (ed Tyler PA). Elsevier Science B.V., Amsterdam, pp. 81–110.

Van Dover CL (2011) Mining seafloor massive sulphides and biodiversity: what is at risk? ICES J Mar Sci 68(2): 341–348.

Van Dover CL (2014) Impacts of anthropogenic disturbances at deep-sea hydrothermal vent ecosystems: A review. Mar Environ Res 102: 59-72.

Vereshchaka AL, Vinogradov GM (1999) Visual observations of the vertical distribution of plankton throughout the water column above Broken Spur vent field, Mid-Atlantic Ridge. Deep-Sea Res I 46: 1615–1632.

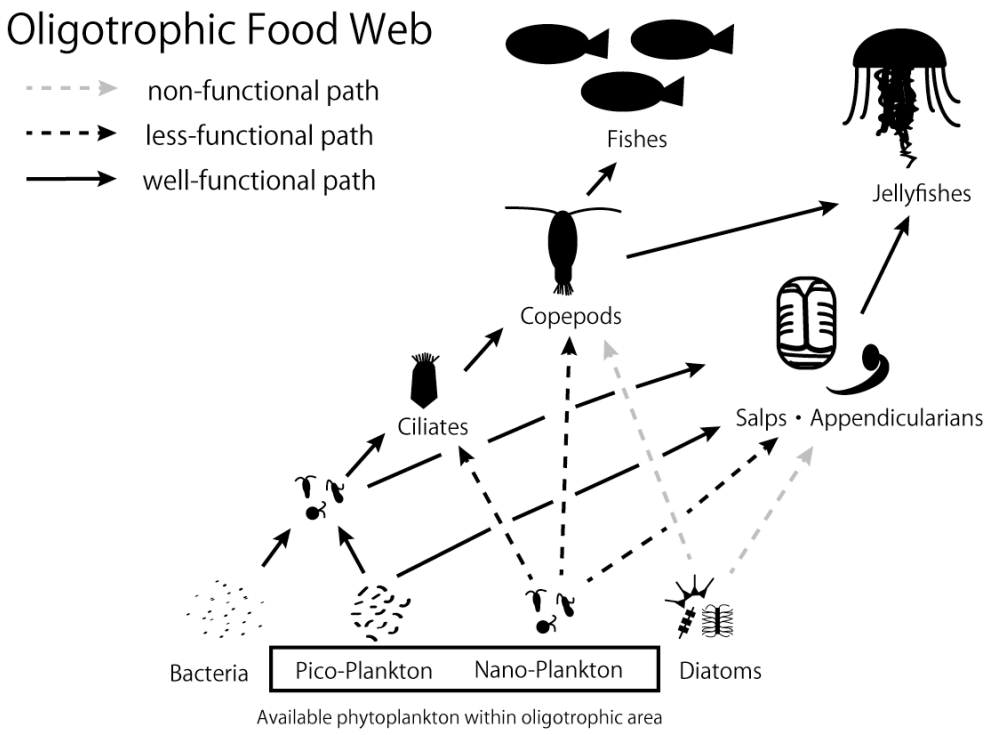


Fig. 1. The food web schema within oligotrophic areas, based on the theory of Sommer et al 2002.

# **CHAPTER 1:** Analysis protocol for archived ROV video records: case study at the Kaikata seamount using the ROV *Hyper-Dolphin*


## ABSTRACT

To extract as much data as possible from legacy ROV dives, a management and analysis protocol based on past JAMSTEC ROV video records was established, using two ROV *Hyper-Dolphin* dives at the Kaikata Seamount. Videos were synchronized to frame-accuracy (<34 msec) using embedded "Timecodes" to maintain consistency in data management. Four examples are given of taxonomic identification methodology using images collected by the ROV. All of the observed gelatinous zooplankton were identified to the lowest possible morphotaxon and their depth distribution recorded. A total of 81 morphotaxa of gelatinous macrozooplankton (23 ctenophores, 24 siphonophores, 21 hydromedusae, 6 scyphozoans and 7 thaliaceans) were observed and identified during dives HPD0081 and HPD0082. The importance of an accurate timestamp (in the present study timecode) and objective morphotaxa designations for analysis and data management were discussed.


## INTRODUCTION

One of the benefits of an in situ image-based survey technique, such as using an ROV, is that it allows us to append information such as depth, salinity, temperature and so on precisely to every observed individual if a CTD or other physico-chemical sensors have been attached to the ROV. Therefore, ROV image-based investigations can reveal the taxon-specific distribution of mid-water

gelatinous zooplankton and the environmental conditions surrounding them (their habitat) throughout the water column, not as mixed samples in a bottle caught by a plankton net. For ROV video analyses, the definition of the "Sample" corresponds to the entire recorded video file or movie sub-clips for each observation, and these movie files will be the vouchers for data analyses that include taxonomic work. To establish a protocol for accurately analysing and managing these movie files was one of the most critical elements to enhance the reliability of the analyses. However, the precise methodology (excepting Hidaka-Umetsu et al. 2015) and actual analytical procedures for ROV video data have not yet been published. Chapter 1 describes the protocol to manage and analyze legacy JAMSTEC ROV mid-water survey records based on *Hyper-Dolphin* dives both inside and outside the Kaikata Seamount, as an example, in preparation for the comparative studies on mid-water gelatinous zooplankton introduced in Chapters 2 and 3.

## MATERIAL AND METHODS

Two mid-water surveys using the ROV *Hyper-Dolphin* (Fig. 2) were selected from archived JAMSTEC ROV dive records from cruise KY02-03 of the R/V *Kaiyo* (from 18 February–13 March 2002) at the Kaikata Seamount (26°40' N, 141° 00' E). The seamount has a caldera on the east crest. The caldera is around 3 km in diameter, with a rim depth of 500–600 m, and hydrothermal activity occurs inside the caldera (Naka 1989, Japan Meteorological Agency 2018). Dive HPD0081 was conducted above the east slope of the outside of the caldera on 7 March 2002 (launched at 26˚42' 16.83"N 141˚06'42.53"E) and dive HPD0082 was conducted on the central

cone inside the caldera on 8 March 2002 (launched at 26˚42' 30.00"N 141˚05'67.61"E) (Fig. 3).

The ROV *Hyper-Dolphin* was equipped with an HDTV (high-definition television) camera integrating an ultra-sensitive super HARP (High gain Avalanche Rushing Photo-conductor) tube. Camera sensitivity was F 1.8 at 2 lux, the gain was variable at 4-200 times, the signal to noise ratio was 43 dB, and the resolution was 800 TV lines. The zoom lens had a minimum focal length of 5.5 mm and a 5× zooming ratio. There were five 400-W SeaArc HMI/MSR metal halide lamps. Two were situated on the port swing arm, and one on the starboard swing arm. These arms were usually opened such that the lights optimised the field of view of the high-definition camera, but were sometimes moved to optimise lighting when making observations of individual organisms in situ. The remaining two lights were forward-pointing and fixed to the frame of the vehicle. Video footage was recorded continuously and simultaneously on BCT-124HDL HDCAM tapes via a native digital signal at 1080i and 29.97 frames (dropframe setting) and was also down-converted to an analogue composite NTSC signal and recorded with depth/time overlay on Sony BCT-D124L Digital BetaCam tapes. Physico-chemical data were collected using a SeaBird SBE19 CTD (Conductivity, Temperature, and Depth profiling system) and an SBE13 dissolved oxygen sensor attached to the vehicle on both dives. The vertical profiles of the physico-chemical data were plotted in Fig 4. CTD data from dive HPD0081 was missing below 690.3 m depth due to a CTD malfunction.

**RESULTS**

## 1. Video data management protocol

### *1.1. Video Data Digitizing and Preparation*

Original video records for HPD0081 and 0082 have been stored on HDCAM and Digital BetaCam tapes. Therefore, these video records need to be digitised to be analysed on a computer. When the video records are digitised, appropriate movie file formats should be chosen so as not to lose any scientific information. The file format depends on what device was used for digitisation, and what software will be used for the analyses. The software package QuickTime Player Pro 7.6.6 was chosen for the video analysis, because it can show "Timecode" in the user interface. Timecode is a time stamp that allows repeatability of analyses because it is based on frames (still images) rather than arbitrary time values, so a given timecode value will always refer to exactly the same still image (i.e. the analysis will always be frame accurate). Original videotapes were played back on a Sony HDW-M2100 (HDCAM) or DVW-A510 (Digi-Beta) video deck, and the video records were digitized in drop frame (Apple ProRes 4:2:2 codec, QuickTime Movie container [.mov]) using an AJA Ki Pro. The original timecode embedded in the video files was replaced using qtChange2.26 (videotoolshed.com) to match the time shown in the video overlay on the digitised NTSC movie files to frame-level accuracy. Therefore, by matching the depth information on the video overlay to the depth information recorded by the CTD, temperature, salinity, density and dissolved oxygen were able to correlated to the presence of organisms. Through the above procedures, scientifically-sound video data can be prepared. For extraction of short voucher movie clips from the entire movie records, Switch Pro 3.1 (Telestream, LLC) was used without media conversion. These movie files were renamed following the rules described below,

and then stored on a Network-Attached Storage (NAS) system (QNAP TVS-871 with four REXP-1000Pro enclosures) in the JAMSTEC High-Quality video data subdirectory.

*1.2. Giving File Names to Digitised and Captured Data*

To manage tens of thousands of ROV-collected video files, arbitrary file names such as those given by serial numbering is just not practical. This is because many different ROVs are used, many different types of cameras are installed on each ROV, and the images are recorded on many different types of media. In some cases, several different types of camera are attached to an ROV at the same time. To efficiently and accurately manage such a complicated data set, metadata should be included for every single file, like a label on a sample bottle. Therefore, a file-naming rule was established (emended from Hidaka-Umetsu et al 2015: Appendix 1). File names incorporated, in the following order, submersible name (HPD= *Hyper-Dolphin*), dive number, date (YYYYMMDD), local time (time of the first appearance of a target in frame as HHMMSS), camera type, camera position, resolution_media type, media reel number, start timecode to end timecode/captured frame timecode, presence/absence of text overlay, taxon name, taxonomist/person responsible for species ID, common Japanese name, co-occurring species ID (if applicable), co-occurring species common Japanese name, and comments for the image, with all fields separated by hyphens. For example, a movie clip of the hydromedusa *Solmissus incisa* s.l. that is eating a fish at 573m depth, which was filmed by the front/forward mounted HDTV camera, recorded on the first of three HDCAM video tapes with no overlay, and was observed between timecode

11:55:39;16 and 12:02:13;20DF (DF=drop frame) where the animal first appeared in the video at 11:55:39 during dive 81 of the ROV *Hyper-Dolphin* and where it was identified by Mitsuko Hidaka, would be given a file name of HPD0081-20020307-115539-SHHD-Front-1920x1080_HDCAM-1of3-TC11553916to12021320DF-NoImpose-Solmissus_incisa_s.l.-Mitsuko_Hidaka-KAPPAKURAGE---eating_fish_573m_24T.mov.

## 2. Analysis protocol

### *2.1. Investigate Dive Profiles and Decide Analysis Strategy*

To decide on the best plan for analyses, it is first necessary to assess the expected usefulness of data collected during any given ROV dive. For this reason, ROV dive profiles of time versus depth need to be graphed. In the present case, the CTD malfunctioned below 690.3 m depth during dive HPD0081, and therefore the black dots in the dive profile for HPD0081 are CTD data, while the blue dots were added based on the occurrence depths of organisms identified during the video analysis (Fig 5). During dive HPD0081, the ROV *Hyper-Dolphin* descended to about 540 m depth at a relatively stable, average speed of 7 m/min, then the descent slowed and irregular observations continued to 640 m depth before it descended to the bottom at approximately 970 m depth at an average speed 18 m/min. After leaving the seafloor, it ascended to 560 m depth very fast (4 m/min) and then irregularly stops were made between 560 and 500 m depth for taxonomic observations, before it finally ascended to the surface at high speed. The entire dive took about 6 hours. In contrast, despite including some short transects with nominal ascents at 200, 280 and 420 m depths, HPD0082 was short and relatively simple. Descent to the bottom took

an hour at an average speed of 9 m/min, then the ROV stayed for 1 hour and thirty minutes at the sea floor, before rapidly ascending to the surface. Based on the dive profiles above, some parts of the dives seem they can be analyzed semi-quantitatively, while in other parts the rapid flow of particles and organisms past the camera will make it impossible to analyze. In order to get as comparable a data set as possible, only the descent was used for semi-quantitative work, while ascent and horizontal transects, where many observations included pan-tilting and/or zooming of the camera, were used only for taxonomic work. Portions where ROV speed was too fast were excluded from the analyses.

*2.2. Video Analysis*

Movie files were analysed on an Apple Mac computer using QuickTime Player Pro 7.6.6, with reference to the embedded timecode. Both high-quality HDTV video with no text overlay (Fig 6) and NTSC video with text overlay were analysed (Fig 7) to determine precise depth information and to match/check data, including the CTD-determined environmental parameter data (Fig 8). For the first analysis, the video records of HPD0081 and HPD0082 were played back at the native speed of the original videos and organisms were searched for in the target depth strata. If an individual of a gelatinous zooplankter occurred, it was identified to the lowest taxonomic level possible. The video record between the first frame where the organism was visible and the last frame before it left the field of view was captured into a small movie clip, as outline above. When an individual was observed by zooming in with the camera or when it was tracked/followed, the time spent doing so was excluded from the lapsed time values used for normalization of the data set.

These movie clips were not only used for taxon identification checks by the second observer (Dr Dhugal J Lindsay) but the clips are also kept in the JAMSTEC High-Quality Video Database server as voucher clips for the investigation. The taxon identifications of individuals were documented in the metadata sheets in two columns, named "Animal identification (100%)" and "Animal identification (50%)". These percentages indicate the reliability of the identification. For example, if the observer was 100 % sure in their identification of a siphonophore (cnidarian jellyfish) as belonging to the genus *Forskalia,* but some doubt remained as to whether it was the species *Forskalia formosa* Keferstein & Ehlers, 1860, or not, then the records would be *Forskalia* sp. in the Animal identification (100%) column and *F. formosa* in the Animal identification (50%) column. For data analysis in the present study, only entries in the Animal identification (100%) column were used to reduce the chance of errors.

*2.3. Data Normalization*

Due to the rarity of ROV-collected data, as much of the collected data and results of analyses as possible, should be utilised to gather baseline data for Environmental Impact Assessments (EIAs). However, trying to do a quantitative analysis with as much of the data as possible is also quite important, especially when attempting to determine the relative vertical distributions of the fauna based on ROV surveys. Kaikata Seamount is located in an oligotrophic area, so water transparency is very high in the upper sea surface layers and the high ambient light and clear water obfuscate transparent gelatinous zooplankton, causing them to disappear into the ambient background. Thus, to ensure the reliability of the analyses, observations at

depths shallower than 100 m depth were omitted for the comparative analyses. Further, the time spent observing in each depth strata was unequal both betwixt and between dives. Therefore, data was normalized by summing the observation time, excluding time spent zooming and tracking organisms, for each 50 m-thick depth stratum during the descent (Fig. 9), and the number of individuals observed for each taxon was divided by that time.

## 3. Results

### *3.1. Taxonomic Identification of Gelatinous Macrozooplankton based on ROV Video Records*

Traditional species identifications are usually done through referring to hierarchical taxonomic keys and other taxonomic guides. Most such keys are based on characters visible in captured specimens, and include observations of microscopic characters or internal structures. However, during *in-situ* ROV image-based investigations, microscopic analyses are unable to be carried out, and most observed organisms will not be caught. Therefore, taxon identification has to be based on characters visible in video images. Some examples of taxon identification protocols for identifying gelatinous zooplankton used in the present study are herein described. The taxonomic terminology for gelatinous zooplankton used in these results primarily refers to that of Lindsay et al. (2015) (Fig. 10 and Appendix 2).

#### 3.1.1. A case study for ctenophores: species identification of *Cestum veneris* Lesueur, 1813

Ctenophores that possess a ribbon-like, long, flattened body without lobes are assignable to the family Cestidae. This family includes two species, *Cestum veneris* (Fig. 11A, B, C) and *Velamen parallelum* (Fol, 1869) (Fig. 11D). These two species belong to two different genera based on their different internal canal connections. The four subtentacular meridional canals (SMCs) of *C. veneris* arise from the stomodaeum and run towards the aboral end, then curve immediately outward at the mid-point of the body, before running along the mid-line of the body to the distal ends (Fig. 11C). On the other hand, the four subtentacular meridional canals (SMCs) of *V. parallelum* are connected to the interradial canals midway between the oral and aboral ends of the latter (Fig. 11D). In the present study, only *C. veneris* was identifiable to species level. In many of the cestid ctenophores in the video record it was impossible to determine the internal canal structure and they were therefore identified as Cestidae spp. The maximum body size of *C. veneris* (<1.5 m) is much larger than *V. parallelum* (<20 cm), and the body size difference may be one reason that it is relatively easy to observe the internal canal structure of *C. veneris.*

3.1.2. A case study for narcomedusae: species identification of *Solmissus incisa* sensu lato vs. *Solmissus marshalli* Agassiz & Mayer, 1902

During dives HPD0081 and HPD0082, two morphotypes of narcomedusan jellyfish assignable to the genus *Solmissus* were observed (Fig. 12). They were clearly distinguishable in the video records by the number of tentacles and colour/shape of the stomach pouches. The first morphotype (Fig. 12A) possessed a disk-like bell shape with a concave top and without external nematocyst patches. It had 17 tentacles, and 17 trapezium-shaped, yellow-coloured stomach pouches that

were closely spaced. The second observed morphotype of *Solmissus* (Fig. 12B) also possessed a disk-like bell shape with a concave top and without external nematocyst patches. However, its body was entirely transparent, it had 18-24 tentacles (in some individuals with whitish distal tips), and it had 18-24 pentagonal stomach pouches that were not closely spaced. Up to the present date, six species of jellyfishes that are assignable to the genus *Solmissus* have been described. These are *Solmissus albescens* (Gegenbaur, 1857), *Solmissus incisa* (Fewkes, 1886), *Solmissus marshalli* Agassiz & Mayer, 1902, *Solmissus faberi* Haeckel, 1879, *Solmissus bleekii* Haeckel, 1879 and *Solmissus atlantica*, Zamponi, 1983. Only the initial three species are widely accepted (Hidaka-Umetsu & Lindsay 2018: Appendix 3). *S. albescens* possesses nematocyst patches on its exumbrella and the maximum number of tentacles is 16, with their only reported habitat so far being the Mediterranean Sea. Therefore, the two morphotypes observed in the present study were not assignable to this species. Both *S. incisa* and *S. marshalli* have been reported from the Pacific Ocean. *S. marshalli* possesses 8-20 tentacles (usually 16), and has square or trapezium-shaped, yellowish stomach pouches (Minemizu et al. 2015). Therefore, the first morphotype we observed (Fig. 12A) was identifiable as *S. marshalli* due to the homology of corresponding characters. *S. incisa* is one of the most commonly observed deep-sea cnidarian jellyfish, but the definition of the species is still uncertain, because the original description by Fewkes (1886) was based on an amalgamation of broken samples that were collected by a net. Hidaka-Umetsu & Lindsay (2018) described morphotype diversity in *S. incisa*, and they made mention of one morphotype that they called "white socks". Some of the *Solmissus* individuals in the present study were obviously the same morphotype as "white socks" (see Fig.

12B), due to the whitish-colored tentacle tips. However, it was not possible in all cases to tell whether the distal tips of the tentacles were white for all observed *S. incisa*, so all morphotypes that possessed a transparent body and where the number of tentacles was between 18-24 were identified as *S. incisa* sensu lato (s.l.).

3.1.3. A case study for siphonophores: species identification of *Forskalia asymmetrica* Pugh, 2003 vs. *Forskalia formosa* Keferstein & Ehlers, 1860

Siphonophorae is an Order of Hydrozoa characterised by having a colonial asexual stage with sexual stages either remaining attached to the colony or being released as "eudoxids". The siphonophoran taxa that are assignable to the genus *Forskalia* possess spirally-arranged zooids in both the nectosome and the siphosome, so that the congeners are clearly distinguished from other genera. In the present study, two species of *Forskalia* were observed in the same depth range, specifically *F. asymmetrica* (Fig. 13A) and *F. formosa* (Fig. 13B). These two species are able to be distinguished by the colonial morphologies. *F. asymmetrica* possesses fewer orange-pigmented gastrozooids and has a sparse-looking siphosome, while *F. formosa* possesess a regularly-arranged, greater number of orange-pigmented gastrozooids than *F. asymmetrica*.

3.1.4. A case study for Pyrosomatida: Colonial morphotaxa of the pelagic tunicate family Pyrosomatidae

Pelagic tunicates are filter-feeding macrozooplankton and the group includes salps, doliolids, pyrosomes and appendicularians. Pelagic tunicates belonging to the order Pyrosomatida were the most abundant filter-feeders in the present study. Some

individuals were identified as *Pyrosoma atlanticum* Péron, 1804, by their possession of a yellowish or pinkish cylindrical colony with numerous processes that taper into tips and bend in towards the open end of the colony. However, in most other cases, the organisms were too far away to observe details of the colony morphology. Nevertheless, three distinct colonial morphologies were observed – namely "Oblong", "Cylindrical" and "Long & Pointy "(Fig. 14A-C). The vertical distributions are illustrated in Fig. 15, based on the three types of colony morphologies. According to these results, "Cylindrical" pyrosomatida were clearly distributed at shallower depths than "Long & Pointy", and "Oblong" occurred at depths in between "Cylindrical" and "Long & Pointy".

### *3.2. Biodiversity of Gelatinous Macrozooplankton at Kaikata Seamount:* A *Taxon List*

According to the image-based, taxonomic identification as described in the preceding paragraphs, 81 morphotaxa of gelatinous macrozooplankton (23 ctenophores, 24 siphonophores, 21 hydromedusae, 6 scyphozoans and 7 thaliaceans) were observed during dives HPD0081 and HPD0082. All identified morphotaxa are listed in Table 1 with their depth of distributions during each dive. This list contains all observed individuals, although there are biases in the time spent observating in each depth strata.

### *3.3. Vertical Distribution of Gelatinous Macrozooplankton at the Kaikata Caldera Based on Feeding Types*

An attempt was made to compare the distributions of macrozooplankton of different feeding types at the two study sites (HPD0081 and HPD0082). However, dive HPD0082 was too short and shallow to meaningfully compare with the results for dive HPD0081. Furthermore, based on the graphs of vertical profiles of environmental factors (Fig. 4), there were no clear differences in these factors between the two dives. Identifying differences in the gelatinous zooplankton communities between the two water columns was therefore abandoned and, instead, the vertical distributions of different feeding types were simply graphed on a trial basis (Fig. 16). All observed gelatinous zooplankton taxa were assigned to three feeding types – namely "Crustacean & Larva Feeding", "Filter Feeding (Tunicata)" and "Gelatinous Feeding (Narcomedusae)", respectively, based on records in the literature (e.g. Madin 1974, Purcell 1991, 2003, Choy et al. 2017). "Crustacean & Larva Feeding" gelatinous zooplankton were most abundant at shallower depths and the number of individuals decreased with depth. No clear pattern vs depth was observed for "Filter Feeders" and "Gelatinous Feeders", though they were observed mostly below 350 m (HPD0081).

## DISCUSSION

### 1. Video data management

To ensure the reliability and traceability of image-based survey data, metadata management is of paramount importance. The present study paid particular attention to the "time accuracy" of the video records. When movie files are only used as references for when samples were taken, or for qualitative analyses such as for behavioral or taxonomic studies, temporal accuracy may not always be singularly

important. However, ROV investigations enable the extraction of precise information about each organism's local environment (e.g. depth, salinity, temperature, oxygen, etc.) at sub-second frequencies when electronic sensors are deployed. Such environmental data needs to be precisely linked to events/object appearance in the movie data to allow us to conduct accurate habitat mapping and discriminate between multiple individuals. For digital movie files, embedded "Timecode" is an optimal solution to retain accurate time information for each recorded event, because the accuracy is at "frame level" which can be to 34 msec or shorter. In the present study, a GPS-linked timecode inserter was not employed, so the local-time values superimposed on the lower resolution movie files were used as the exclusive reference time source (eg. local time on the CTD computer was incorrect). By including timecode information in the file name of each movie file/clip or frame grab, every single image can be traced back to the original source video.

**2. Video data analysis**

To extract as much data as possible, especially quantitative data, from archived ROV dives is a major task in data mining. As long as the ROV camera angles are not "fixed" and the descending speed of the ROV varies, analyses from video records are unable to be described as 100% quantitative. However, 100% quantitative ROV investigations require that surveys do not stop somewhere or track an object, even when a "rare species" is found. Because community analysis is impossible without baseline data, gathering taxonomic reference video clips for the species that inhabit the survey area is also necessary. Therefore, in cases where only one dive could be conducted at a single station, the investigation becomes a trade-off

between quantitative performance and qualitative performance, as in the present study. In this respect, when the analysis is being done, the analyst always has to identify possible biases in the observations. In the present study, the descending speed of the ROV varied, and zooming-tracking of an object happened many times when interesting objects appeared. In short, the survey was biased by the observational time per depth stratum. For the reasons described above, observation time was calculated by excluding the time spent tracking, zooming and stopping. Through this process, semi-quantitative analyses were possible.

## 3. Results from the ROV investigations

*Taxa Identification of Gelatinous Zooplankton Using ROV Video Records*

One difficulty in morphological identification based on ROV video records is that there is usually no strict, agreed-upon criterion. Shots of gelatinous zooplankton at the best angles always help confirm their key morphological characters for taxon identification (e.g. projections on the body surface, shape of the stomach pouches, etc.). In some species, these critical morphological characters (e.g. tentacle bulbs, internal canal structures, etc.) can be visible through their transparent bodies. However, often when gelatinous zooplankton pass by the ROV, they swim around or are disturbed by water turbulence from the ROV, and opportunities for extracting good shots for taxon identification from the ROV video records are few indeed. Hence, taxon identification from ROV videos depends greatly not only by what morphological characters can be observed by the analyst, but also how much experience or qualitative observational skills the analyst has and their taxonomic speciality, if they are a taxonomist. Hunt and Lindsay (1999) described the necessity

of subjective video analysis, because all observed organisms cannot be physically captured as specimens. To keep the analysis objective, more than two observers have to take part in the analysis, and of course, the published data should be 100% agreed upon by all observers, though the accuracy depends on the experience levels of the observers.

*Baseline Data from ROV Video Records*

Morphotaxon is a reasonable taxonomic unit when identification cannot be done to species level for all individuals, although it does not strictly allow evaluation of actual species diversity. A total of 81 morphotaxa (23 ctenophores, 24 siphonophores, 21 hydromedusae, 6 scyphozoans and 7 thaliaceans) of gelatinous macrozooplankton were observed in the present study, 29% (24 species) of taxa were identified to species level, and 24 % (20 taxa) to genus level. This indicates that approximately 50% of the observed morphotaxa were unable to be identified to a lower level than genus level through these ROV observations. However, if the approximately 50% of morphotaxa referred to above were excluded from the analysis, approximately 50% of the data would be lost. For the accumulation of baseline data, as much data as possible on what kind of, and how many, gelatinous zooplankton occurred there is quite important, because it enables estimation of the total number of gelatinous zooplankton. Therefore, the present study included all observed morphotaxa in the results.

## CONCLUSIONS

To ensure the reliability of management and of analysis, a protocol for mid-water ROV video records was described and established in the present study. For both data management and data analysis, accurate time data played a key role to maintain consistency of the source data and for abundance normalisation. A total of 81 morphotaxa of gelatinous zooplankton were identified, and their vertical distributions were recorded, although only 29% of the observed gelatinous zooplankton were identifiable at species level.

**REFERENCES**

Choy CA, Haddock SHD, Robison BH (2017) Deep pelagic food web structure as revealed by in situ feeding observations. Proc R Soc B 284: 20172116. http://dx.doi.org/10.1098/rspb.2017.2116

Fewkes JW (1886) Report on the Medusae collected by the U.S. Fish Commission Steamer 'Albatross' in the Region at the Gulf Stream in 1883-84. Rept US Fish Comm for 1884.

Hidaka-Umetsu M, Lindsay DJ, Yamamoto H (2015) Management and use of multiple video formats and resolutions in ROVs. JAMSTEC Rep Res Dev 20: 1–28. (in Japanese)

Hidaka-Umetsu M, Lindsay DJ (2018) First record of the mesopelagic narcomedusan genus *Solmissus* ingesting a fish, with notes on morphotype diversity in *S. incisa* (Fewkes, 1886). Plankton Benthos Res 13(2): 41-45.

Hunt JC, Lindsay DJ (1999) Methodology for creating an observational database of midwater fauna using submersibles: results from Sagami Bay, Japan. Plankton Biol Ecol 46(1): 75–87.

Japan Meteorological Agency (2018) 71, Kaikata Seamount; National Catalogue of the Active Volcanoes in Japan. Available at: http://www.data.jma.go.jp/svd/vois/data/tokyo/STOCK/souran_eng/volcanoes/071_kaikata_seamount.pdf (accessed on 20 November 2018)

Lindsay D, Umetsu M, Grossmann M, Miyake H, Yamamoto H (2015) Chapter 51, The gelatinous macroplankton community at the Hatoma Knoll hydrothermal vent. In: Subseafloor biosphere linked to global hydrothermal systems; TAIGA Concept (eds Ishibashi J., Okino K. and Sunamura M). ISBN 978-4-431-54864-5. Tokyo, Springer, pp. 639–666. DOI 10.1007/978-4-431-54865-2_51.

Madin LP (1974) Field observations on the feeding behavior of salps (Tunicata : Thaliacea). Mar Biol 25: 143–147.

Minemizu R, Kubota S, Hirano Y, Lindsay D (2015) A photographic guide to the jellyfishes of Japan. ISBN 978-4-582-54242-4. Tokyo, Heibonsha. (in Japanese)

Naka J (1989) Sea Bottom Observation around the KC Peak of the Kaikata

Seamount, Bonin Islands. JAMSTEC J Deep-Sea Res 5: 57-65.

Purcell JE (1991) Predation by *Aequorea victoria* on other species of potentially competing pelagic hydrozoans. Mar Ecol Prog Ser 72: 255–260.

Purcell JE (2003) Predation on zooplankton by large jellyfish, *Aurelia labiata*, *Cyanea capillata* and *Aequorea aequorea*, in Prince William Sound, Alaska. Mar Ecol Prog Ser 246: 137–152.

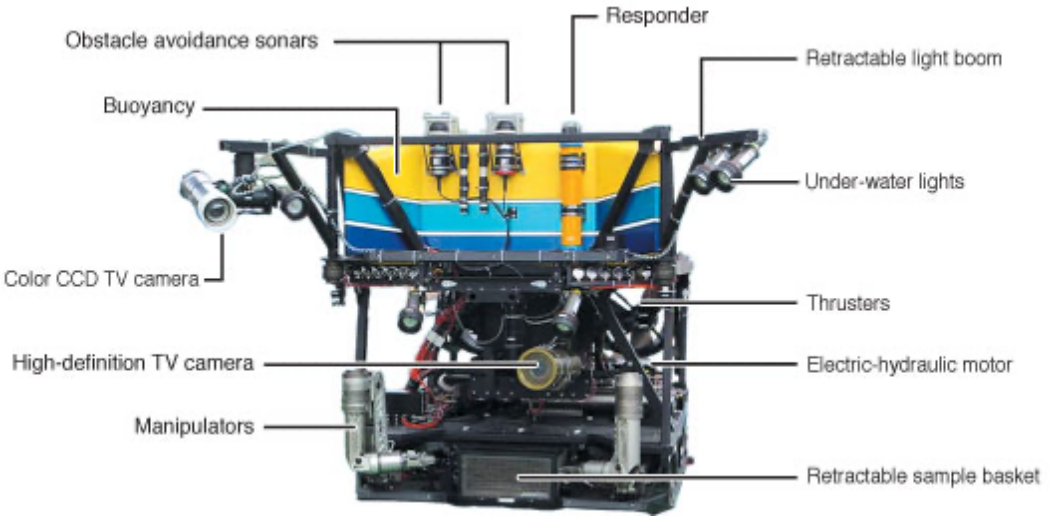


Fig. 2. Remotely-Operated Vehicle *Hyper-Dolphin* and its brief specifications.

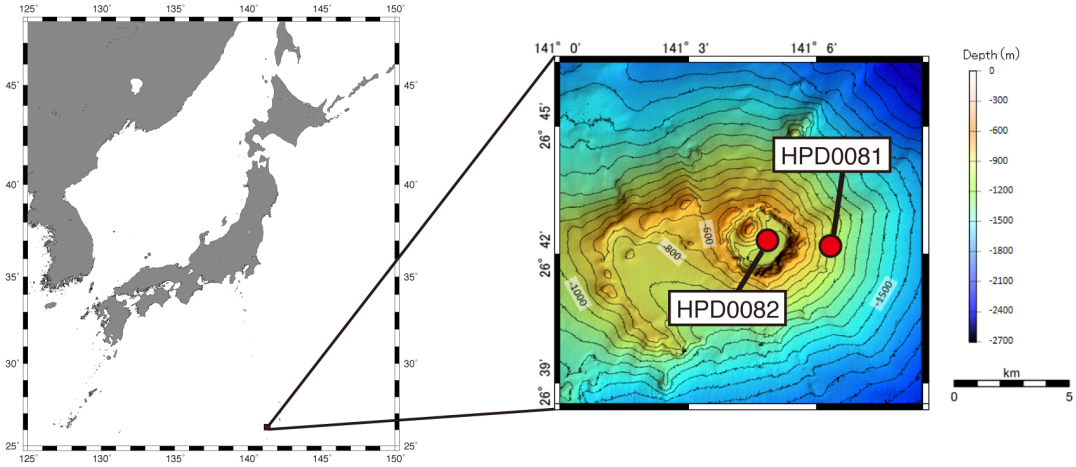


Fig. 3. Dive localities at the Kaikata Seamount.

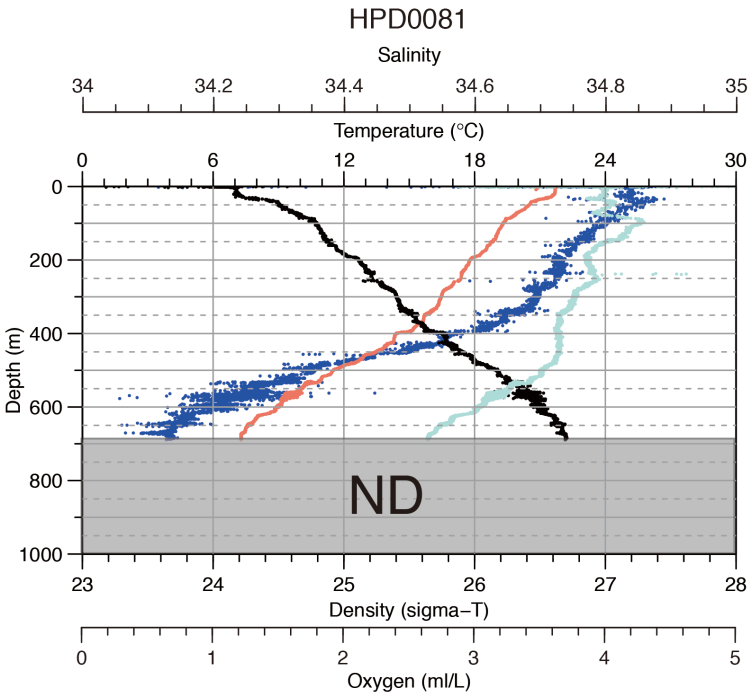
HPD0081
Salinity
34
34.2
34.4
34.6
34.8
35
Temperature (°C)
0
6
12
18
24
30
Depth (m)
0
200
400
600
800
1000
ND
23
24
25
26
27
28
Density (sigma−T)
0
1
2
3
4
5
Oxygen (ml/L)

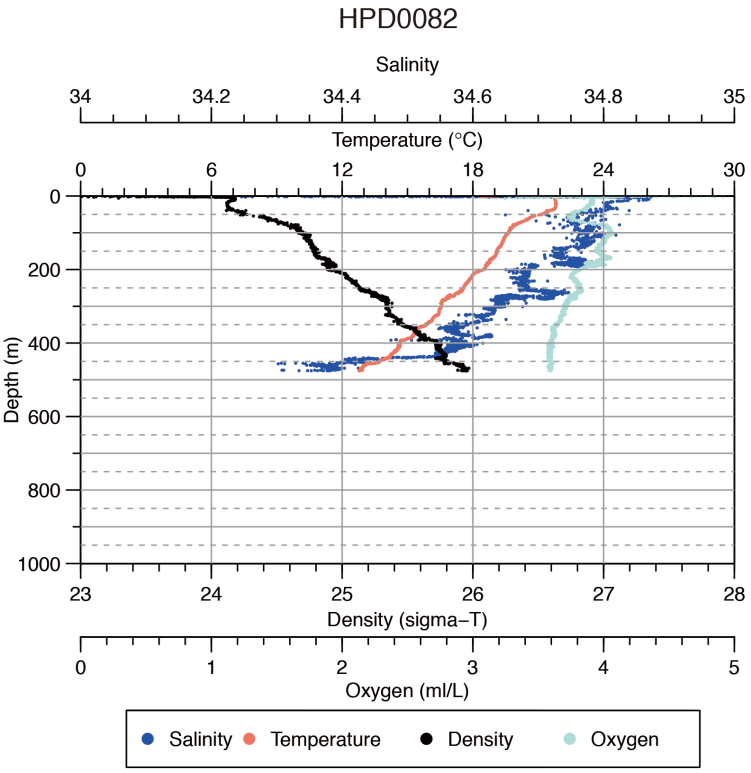
HPD0082
Salinity
34
34.2
34.4
34.6
34.8
35
Temperature (°C)
0
6
12
18
24
30
Depth (m)
0
200
400
600
800
1000
23
24
25
26
27
28
Density (sigma−T)
0
1
2
3
4
5
Oxygen (ml/L)
Salinity
Temperature
Density
Oxygen

Fig. 4. Vertical environmental profiles for dive HPD0081 (upper) and HPD0082 (below)

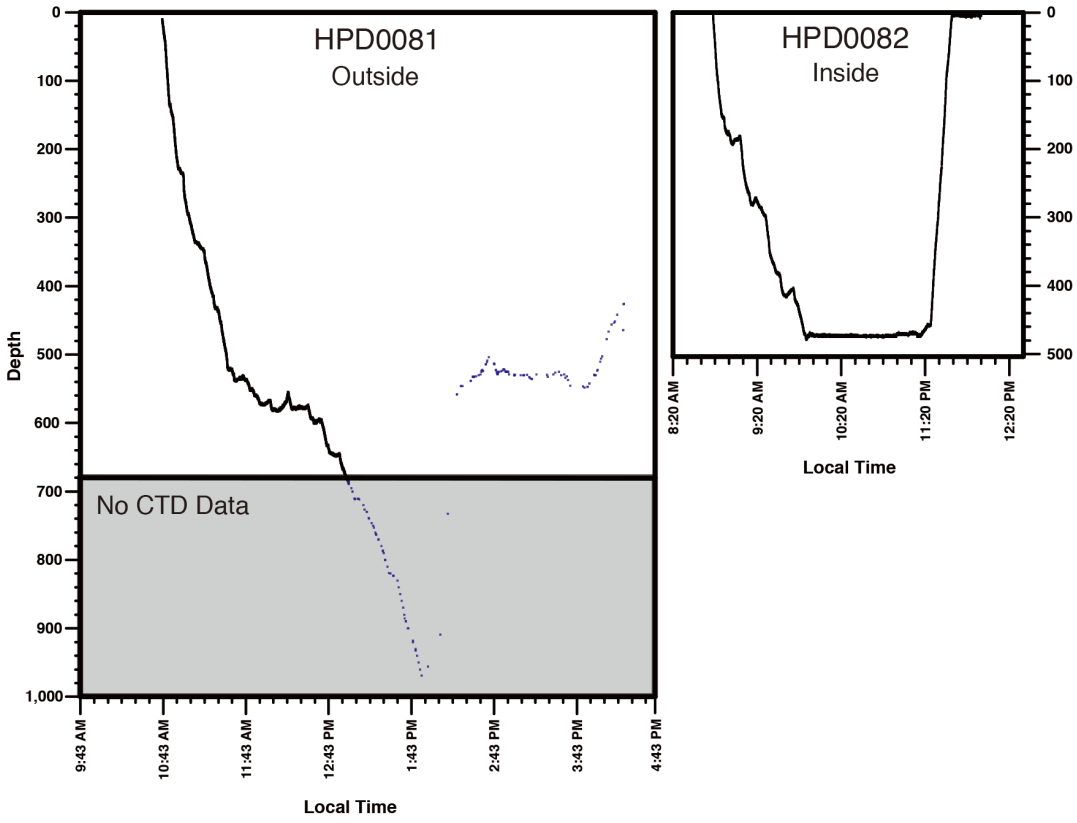


Fig. 5. Vertical profiles for dive HPD0081 (left) and HPD0082 (right). When no CTD data was available, depth and time were extracted from the video overlay values.

Fig. 6. High quality HDTV video with no overlay

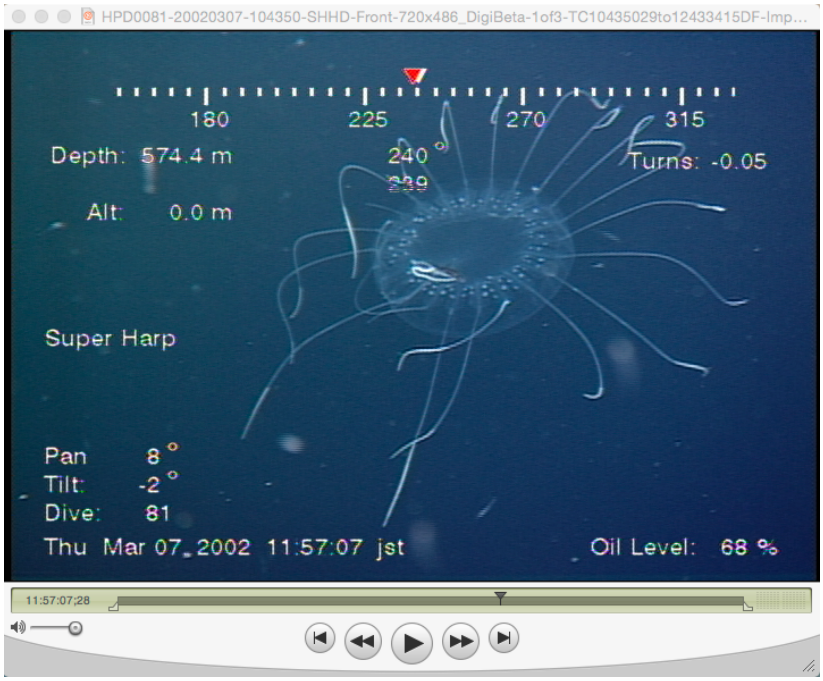


Fig. 7. NTSC video with overlay superimposed

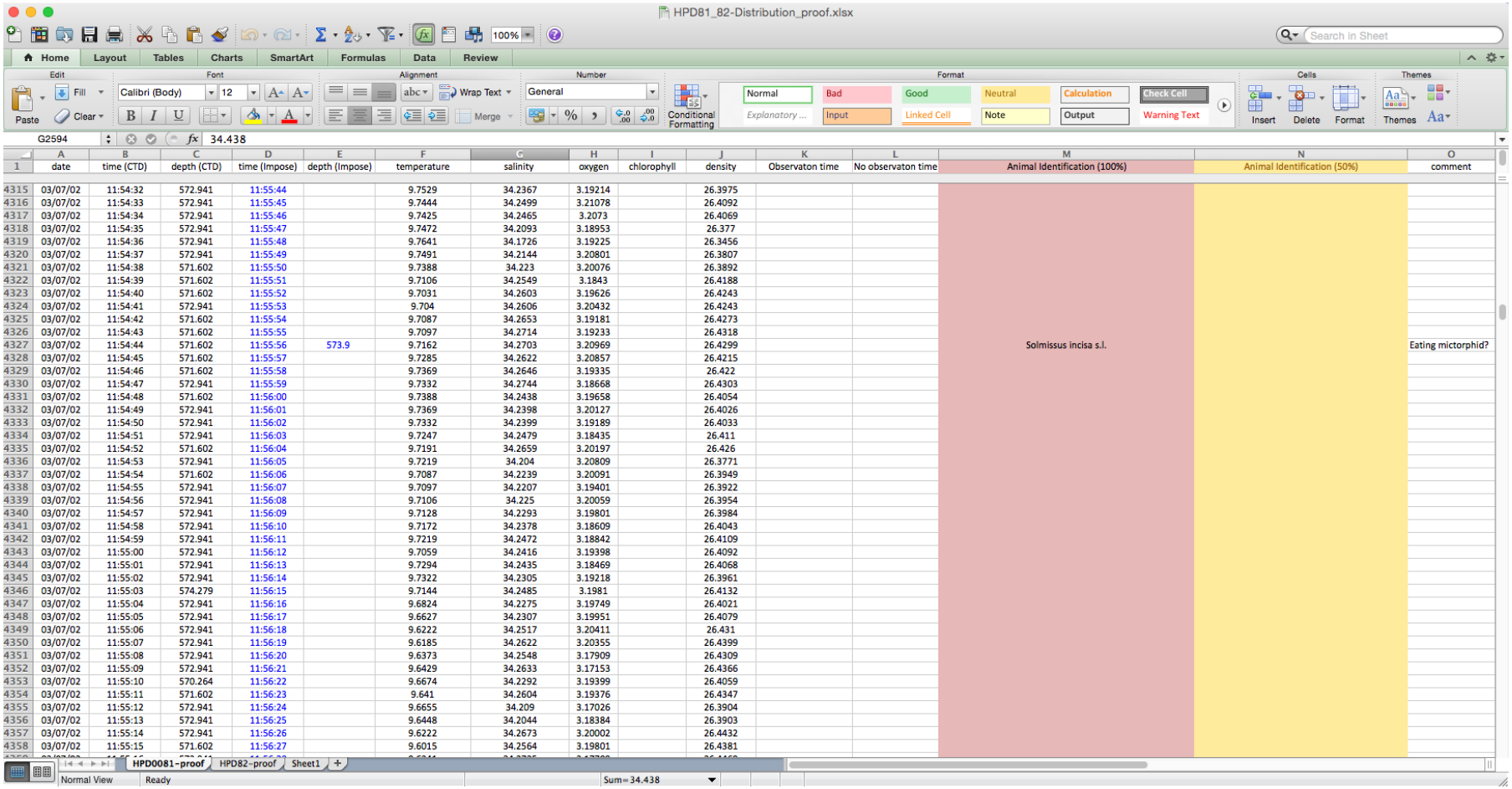


| | A | B | C | D | E | F | G | H | I | J | K | L | M | N | O |
|---|---|---|---|---|---|---|---|---|---|---|---|---|---|---|---|
| 1 | date | time (CTD) | depth (CTD) | time (Impose) | depth (Impose) | temperature | salinity | oxygen | chlorophyll | density | Observaton time | No observaton time | Animal Identification (100%) | Animal Identification (50%) | comment |
| 4315 | 03/07/02 | 11:54:32 | 572.941 | 11:55:44 | | 9.7529 | 34.2367 | 3.19214 | | 26.3975 | | | | | |
| 4316 | 03/07/02 | 11:54:33 | 572.941 | 11:55:45 | | 9.7444 | 34.2499 | 3.21078 | | 26.4092 | | | | | |
| 4317 | 03/07/02 | 11:54:34 | 572.941 | 11:55:46 | | 9.7425 | 34.2465 | 3.2073 | | 26.4069 | | | | | |
| 4318 | 03/07/02 | 11:54:35 | 572.941 | 11:55:47 | | 9.7472 | 34.2093 | 3.18953 | | 26.377 | | | | | |
| 4319 | 03/07/02 | 11:54:36 | 572.941 | 11:55:48 | | 9.7641 | 34.1726 | 3.19225 | | 26.3456 | | | | | |
| 4320 | 03/07/02 | 11:54:37 | 572.941 | 11:55:49 | | 9.7491 | 34.2144 | 3.20801 | | 26.3807 | | | | | |
| 4321 | 03/07/02 | 11:54:38 | 571.602 | 11:55:50 | | 9.7388 | 34.223 | 3.20076 | | 26.3892 | | | | | |
| 4322 | 03/07/02 | 11:54:39 | 571.602 | 11:55:51 | | 9.7106 | 34.2549 | 3.1843 | | 26.4188 | | | | | |
| 4323 | 03/07/02 | 11:54:40 | 571.602 | 11:55:52 | | 9.7031 | 34.2603 | 3.19626 | | 26.4243 | | | | | |
| 4324 | 03/07/02 | 11:54:41 | 572.941 | 11:55:53 | | 9.704 | 34.2606 | 3.20432 | | 26.4243 | | | | | |
| 4325 | 03/07/02 | 11:54:42 | 571.602 | 11:55:54 | | 9.7087 | 34.2653 | 3.19181 | | 26.4273 | | | | | |
| 4326 | 03/07/02 | 11:54:43 | 571.602 | 11:55:55 | | 9.7097 | 34.2714 | 3.19233 | | 26.4318 | | | | | |
| 4327 | 03/07/02 | 11:54:44 | 571.602 | 11:55:56 | 573.9 | 9.7162 | 34.2703 | 3.20969 | | 26.4299 | | | Solmissus incisa s.l. | | Eating mictorphid? |
| 4328 | 03/07/02 | 11:54:45 | 571.602 | 11:55:57 | | 9.7285 | 34.2622 | 3.20857 | | 26.4215 | | | | | |
| 4329 | 03/07/02 | 11:54:46 | 571.602 | 11:55:58 | | 9.7369 | 34.2646 | 3.19335 | | 26.422 | | | | | |
| 4330 | 03/07/02 | 11:54:47 | 572.941 | 11:55:59 | | 9.7332 | 34.2744 | 3.18668 | | 26.4303 | | | | | |
| 4331 | 03/07/02 | 11:54:48 | 571.602 | 11:56:00 | | 9.7388 | 34.2438 | 3.19658 | | 26.4054 | | | | | |
| 4332 | 03/07/02 | 11:54:49 | 572.941 | 11:56:01 | | 9.7369 | 34.2398 | 3.20127 | | 26.4026 | | | | | |
| 4333 | 03/07/02 | 11:54:50 | 572.941 | 11:56:02 | | 9.7332 | 34.2399 | 3.19189 | | 26.4033 | | | | | |
| 4334 | 03/07/02 | 11:54:51 | 572.941 | 11:56:03 | | 9.7247 | 34.2479 | 3.18435 | | 26.411 | | | | | |
| 4335 | 03/07/02 | 11:54:52 | 571.602 | 11:56:04 | | 9.7191 | 34.2659 | 3.20197 | | 26.426 | | | | | |
| 4336 | 03/07/02 | 11:54:53 | 572.941 | 11:56:05 | | 9.7219 | 34.204 | 3.20809 | | 26.3771 | | | | | |
| 4337 | 03/07/02 | 11:54:54 | 571.602 | 11:56:06 | | 9.7087 | 34.2239 | 3.20091 | | 26.3949 | | | | | |
| 4338 | 03/07/02 | 11:54:55 | 572.941 | 11:56:07 | | 9.7097 | 34.2207 | 3.19401 | | 26.3922 | | | | | |
| 4339 | 03/07/02 | 11:54:56 | 572.941 | 11:56:08 | | 9.7106 | 34.225 | 3.20059 | | 26.3954 | | | | | |
| 4340 | 03/07/02 | 11:54:57 | 572.941 | 11:56:09 | | 9.7128 | 34.2293 | 3.19801 | | 26.3984 | | | | | |
| 4341 | 03/07/02 | 11:54:58 | 572.941 | 11:56:10 | | 9.7172 | 34.2378 | 3.18609 | | 26.4043 | | | | | |
| 4342 | 03/07/02 | 11:54:59 | 572.941 | 11:56:11 | | 9.7219 | 34.2472 | 3.18842 | | 26.4109 | | | | | |
| 4343 | 03/07/02 | 11:55:00 | 572.941 | 11:56:12 | | 9.7059 | 34.2416 | 3.19398 | | 26.4092 | | | | | |
| 4344 | 03/07/02 | 11:55:01 | 572.941 | 11:56:13 | | 9.7294 | 34.2435 | 3.18469 | | 26.4068 | | | | | |
| 4345 | 03/07/02 | 11:55:02 | 572.941 | 11:56:14 | | 9.7322 | 34.2305 | 3.19218 | | 26.3961 | | | | | |
| 4346 | 03/07/02 | 11:55:03 | 574.279 | 11:56:15 | | 9.7144 | 34.2485 | 3.1981 | | 26.4132 | | | | | |
| 4347 | 03/07/02 | 11:55:04 | 572.941 | 11:56:16 | | 9.6824 | 34.2275 | 3.19749 | | 26.4021 | | | | | |
| 4348 | 03/07/02 | 11:55:05 | 572.941 | 11:56:17 | | 9.6627 | 34.2307 | 3.19951 | | 26.4079 | | | | | |
| 4349 | 03/07/02 | 11:55:06 | 572.941 | 11:56:18 | | 9.6222 | 34.2517 | 3.20411 | | 26.431 | | | | | |
| 4350 | 03/07/02 | 11:55:07 | 572.941 | 11:56:19 | | 9.6185 | 34.2622 | 3.20355 | | 26.4399 | | | | | |
| 4351 | 03/07/02 | 11:55:08 | 572.941 | 11:56:20 | | 9.6373 | 34.2548 | 3.17909 | | 26.4309 | | | | | |
| 4352 | 03/07/02 | 11:55:09 | 572.941 | 11:56:21 | | 9.6429 | 34.2633 | 3.17153 | | 26.4366 | | | | | |
| 4353 | 03/07/02 | 11:55:10 | 570.264 | 11:56:22 | | 9.6674 | 34.2292 | 3.19399 | | 26.4059 | | | | | |
| 4354 | 03/07/02 | 11:55:11 | 571.602 | 11:56:23 | | 9.641 | 34.2604 | 3.19376 | | 26.4347 | | | | | |
| 4355 | 03/07/02 | 11:55:12 | 572.941 | 11:56:24 | | 9.6655 | 34.209 | 3.17026 | | 26.3904 | | | | | |
| 4356 | 03/07/02 | 11:55:13 | 572.941 | 11:56:25 | | 9.6448 | 34.2044 | 3.18384 | | 26.3903 | | | | | |
| 4357 | 03/07/02 | 11:55:14 | 572.941 | 11:56:26 | | 9.6222 | 34.2673 | 3.20002 | | 26.4432 | | | | | |
| 4358 | 03/07/02 | 11:55:15 | 571.602 | 11:56:27 | | 9.6015 | 34.2564 | 3.19801 | | 26.4381 | | | | | |

Fig. 8. Example of metadata

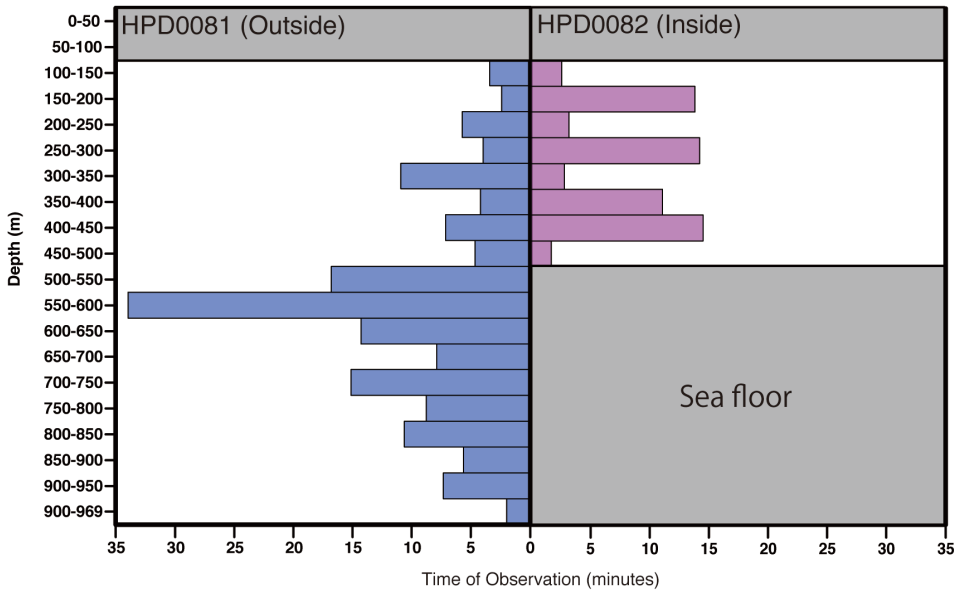


Fig. 9. Time of observation outside and inside Kaikata Seamount for each 50 m depth strata during descent.

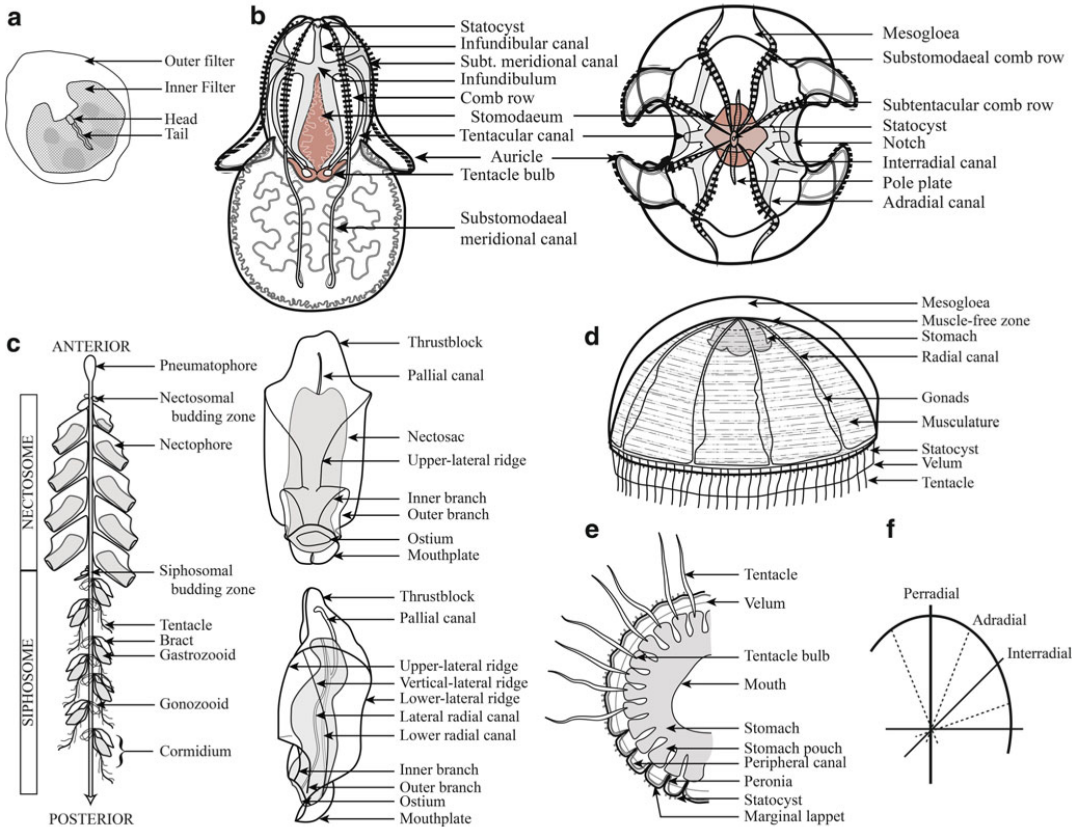


**Fig. 51.2** Terminology for (**a**) larvacean appendicularians, (**b**) lobate ctenophores, (**c**) physonect siphonophores, (**d**) trachymedusae, (**e**) narcomedusae, and (**f**) the main axes of radially symmetrical animals

Fig. 10. Terminology for Larvacean appendicularians (a), Lobate ctenophores (b), Physonect siphonophores (c), trachymedusae (hydromedusae) (d), narcomedusae (e), the main axes of radially symmetrical animals (f), from Lindsay et al. 2015 fig. 51.2.

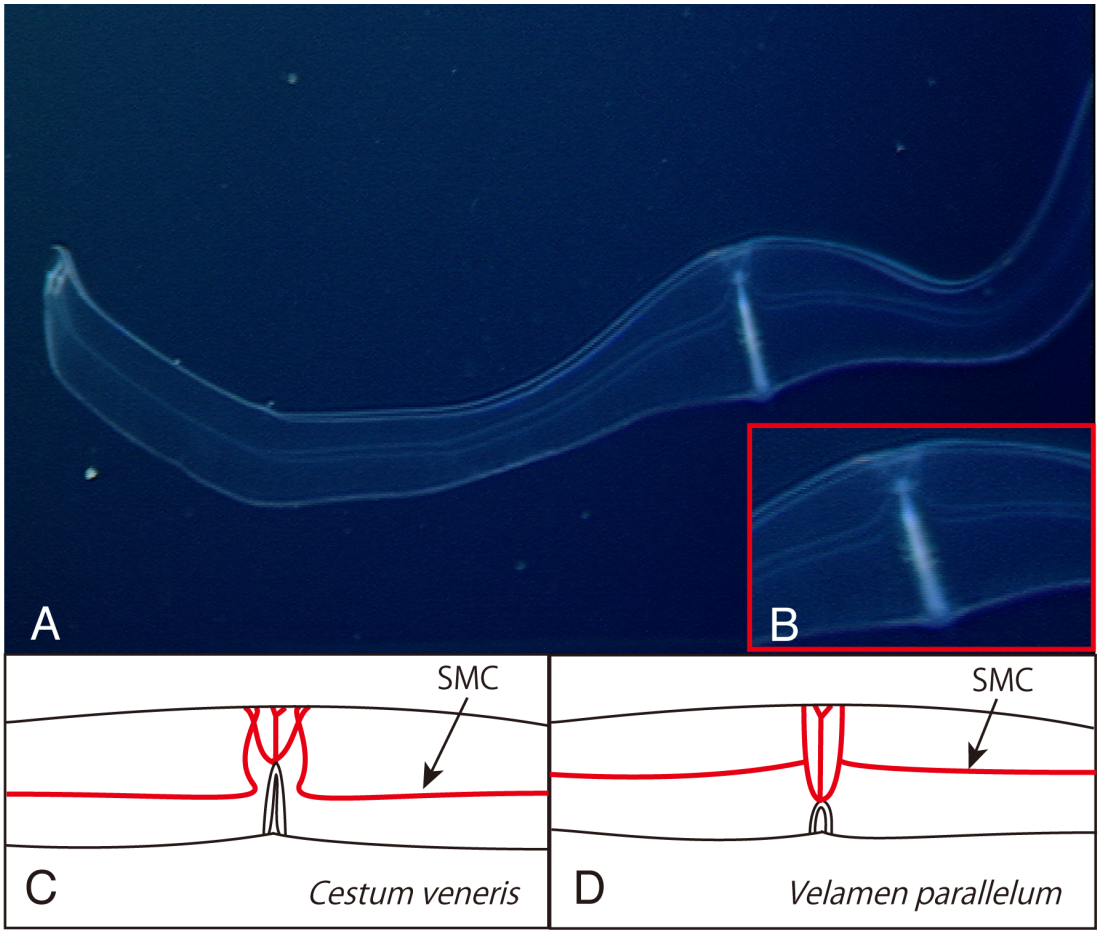


Fig. 11. A frame grab of *Cestum veneris,* this individual was observed at 335 m depth during dive HPD0081 (A, B). Diagrams of the canal structures of *C. veneris* (C) and *Velamen parallelum* (D). SMC: Subtentacular Meridional Canal

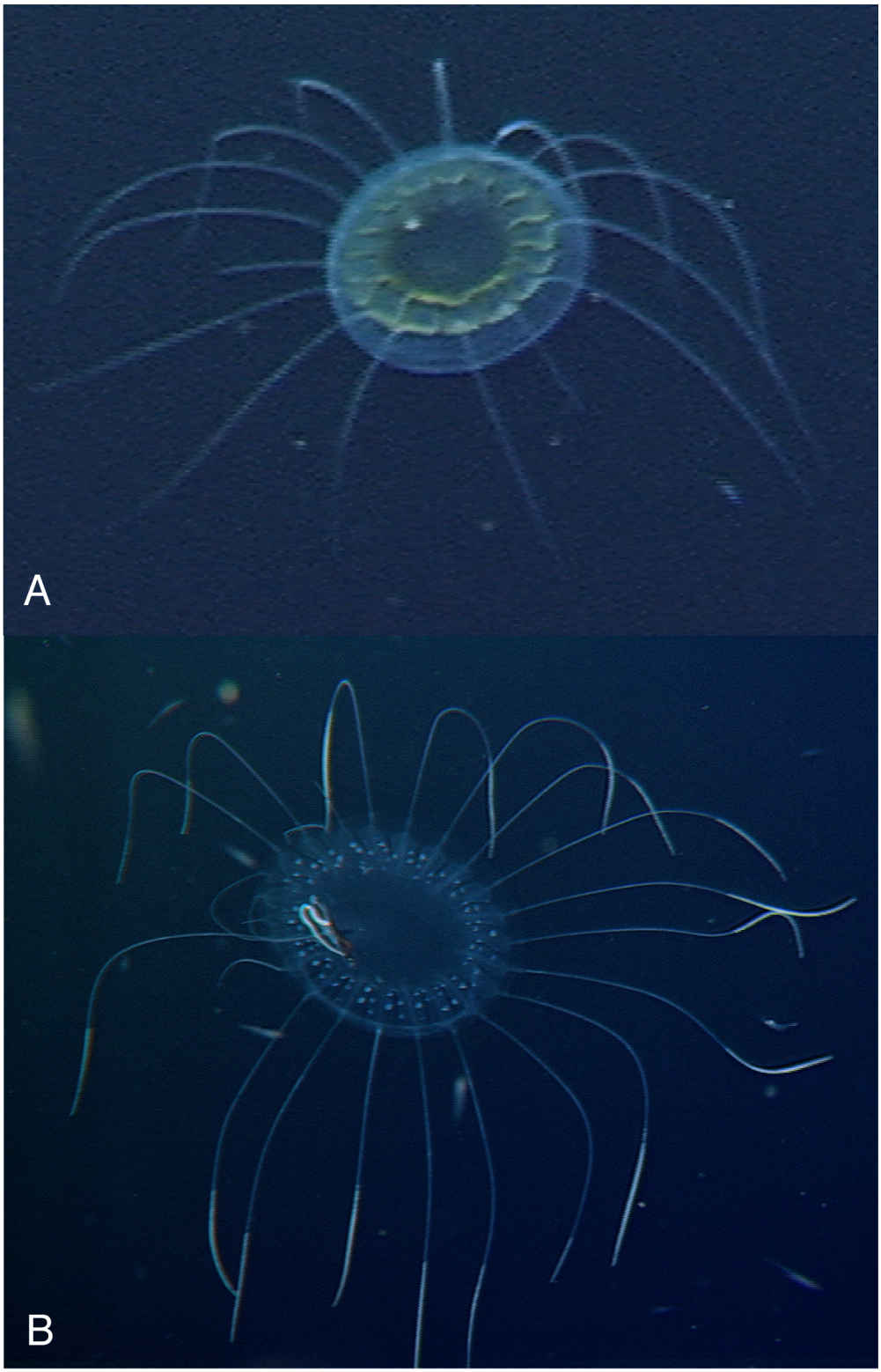


Fig. 12. A frame grab of *Solmissus marshalli,* this individual was observed at 228 m depth during dive HPD0081 (A). A frame grab of *Solmissus incisa* s.l.*,* this individual was observed at 573 m depth during dive HPD0081 (B).

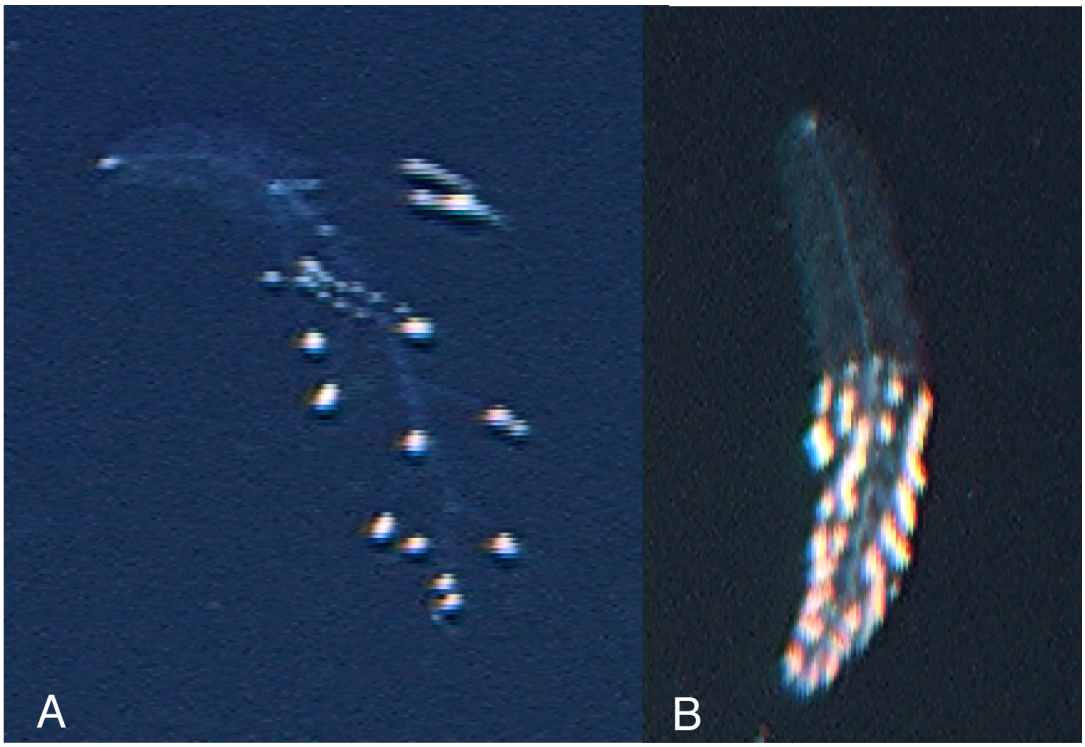


Fig. 13. A frame grab of *Forskalia asymmetrica* observed at 641 m depth during dive HPD0081 (A). A frame grab of *Forskalia formosa* observed at 711 m depth during dive HPD0081 (B).

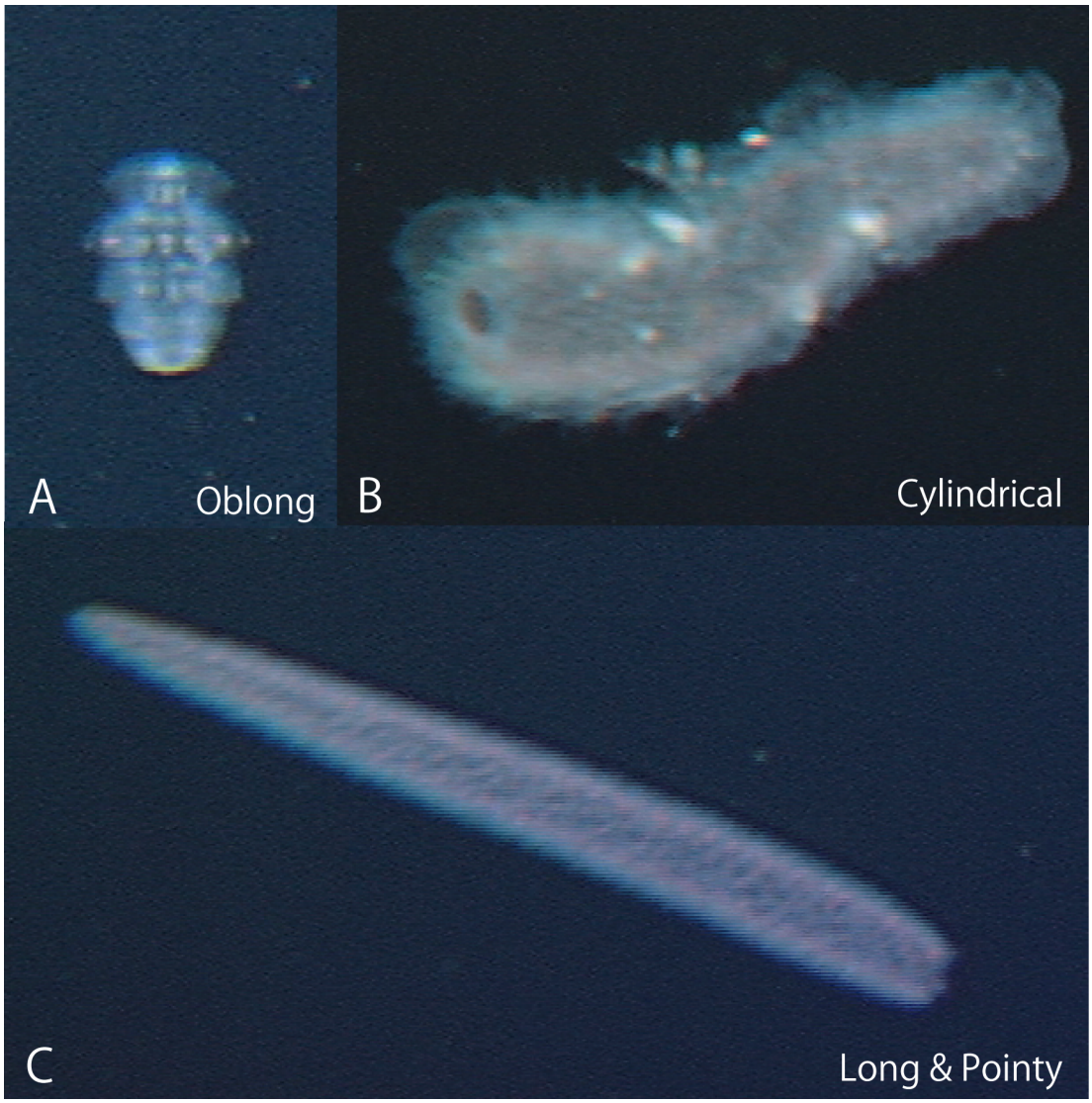


Fig. 14. A frame grab of the Pyrosomatidae "Oblong" morphological type observed at 582 m depth during dive HPD0081 (A). A frame grab of the Pyrosomatidae "Cylindrical" morphological type observed at 711 m depth during dive HPD0081 (B). A frame grab of the Pyrosomatidae "Long & Pointy" morphological type observed at 739 m depth during dive HPD0081 (C).

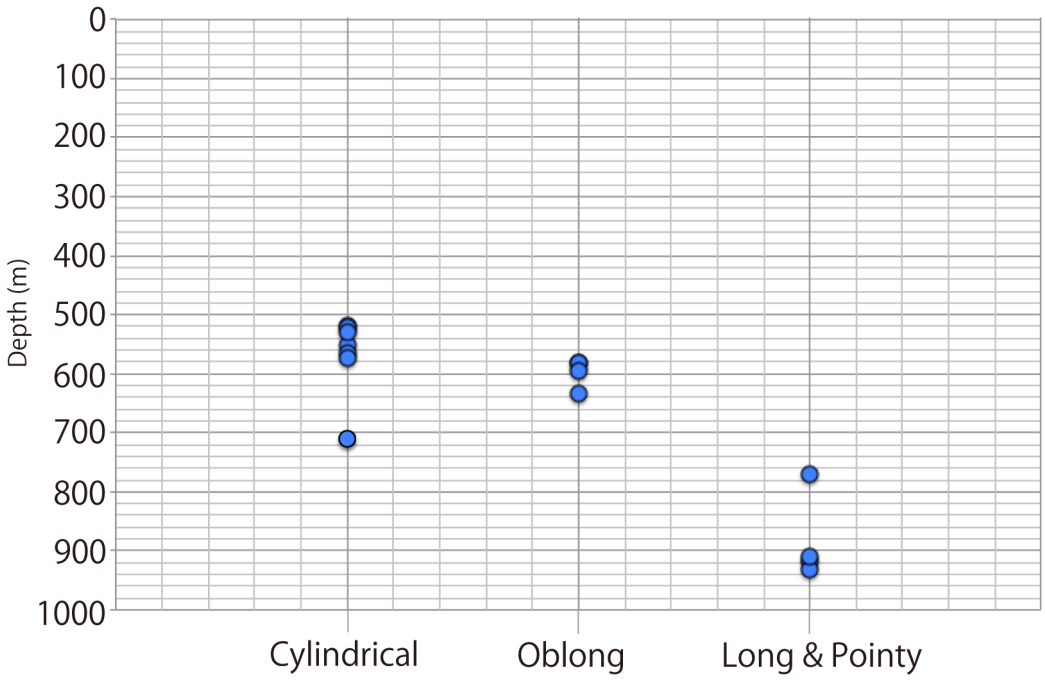


Fig. 15. The vertical distribution of Pyrosomatidae by colony morphology. *Morphotype "Cylindrical" includes four individuals of *Pyrosoma atlanticum* (521 m, 552 m, 711 m, 711 m).

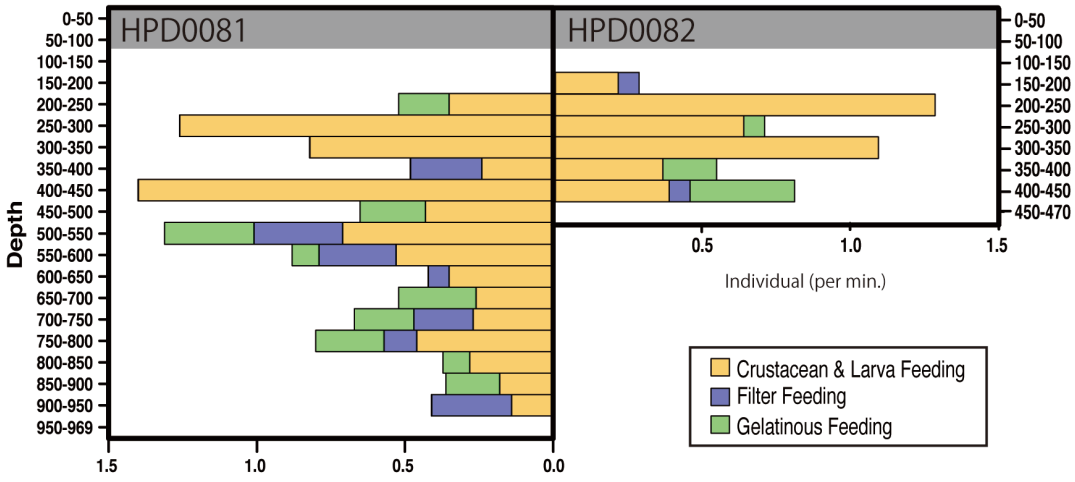


Fig. 16. Vertical distribution of gelatinous zooplankton sorted by feeding types. Orange: Crustacean- and larva-feeding, Blue: Filter-feeding, Green: Gelatinous zooplankton-feeding.

Table 1. All of the identified morphotaxa and observed depths

| Identified Morpho-taxa | HPD0081 | HPD0082 |
|---|---|---|
| Phylum Ctenophora | | |
| Class Tentaculata | | |
| Order Lobata | | |
| Undescribed Lobata sp. A "No auricles" | – | 465, 467 m |
| *Bathocyroe fosteri* Madin & Harbison, 1978 | 502–700 m | 471 m |
| *Bathocyroe* sp. not *fosteri* | 799 m | – |
| *Bathocyroe* spp. | 426–932 m | 379 m |
| *Eurhamphaea vexilligera* Gegenbaur, 1865 | 532 m | – |
| *Kiyohimea aurita* Komai & Tokioka, 1940 | 525–546 m | – |
| *Kiyohimea usagi* Matsumoto & Robison, 1992 | 559–594 m | – |
| *Kiyohimea* sp. | 582 m | – |
| Eurhamphaeidae sp. | – | 417 m |
| Ocyropsis sp. | 312 m | – |
| Lobata sp. "Boli" | 434 m | 463 m |
| Lobata spp. | 368–530 m | 406 m |
| Lobata s.l. | 414 m | 372 m |
| Order Thalassocalycida | | |
| *Thalassocalyce inconstans* Madin & Harbison, 1978 | – | 380, 433 m |
| *Thalassocalyce* spp. | 426, 530 m | 463–467 m |
| *Thalassocalyce* or Lobata sp. | – | 466–471 m |
| *Thalassocalyce* or Medusoid larva | 442 m | – |
| Order Cestida | | |
| *Cestum veneris* Lesueur, 1813 | 284, 335 m | 348 m |
| Cestidae spp. | 295–401 m | – |
| Order Cydippida | | |
| Mertensia sp. | 523 m | – |
| Cydippida sp. A "Little ruby" | 823 m | – |
| Cydippida sp. B | 819 m | – |
| Cydippida spp. | 530, 823 m | – |
| Phylum Cnidaria | | |
| Class Hydrozoa | | |
| Order Siphonophorae | | |
| *Agalma okenii* Eschscholtz, 1825 | 531 m | – |
| *Nanomia bijuga* (Delle Chiaje, 1844) | 229, 580 m | 368, 368 m |
| Agalmatidae spp. | 437, 456 m | – |
| *Stephanomia amphytridis* Lesueur & Petit, 1807 (Larvae) | 646 m | – |
| *Bargmannia amoena* Pugh, 1999 | 467, 514 m | 466 m |
| *Bargmannia elongata* Totton, 1954 | 529 m | – |
| *Bargmannia* spp. | 536, 593 m | 453 m |
| *Forskalia asymmetrica* Pugh, 2003 | 504–549 m | 469 m |
| *Forskalia formosa* Keferstein & Ehlers, 1860 | 499–711 m | 467 m |
| *Forskalia* spp. | 341–546 m | – |
| Physonectae spp. | 302–787 m | – |

| | | |
|---|---|---|
| *Vogtia* sp. | 470 m | – |
| Hippopodiidae sp. | – | 539 m |
| *Chuniphyes multidentata* Lens & van Riemsdijk, 1908 | 601 m | – |
| Clausophyidae sp. | 588 m | – |
| Diphyomorph spp. | 324, 564 m | 180–238 m |
| *Desmophyes* sp. | – | 300 m |
| *Rosacea* spp. | – | 187, 248 m |
| Prayinae spp. | – | 233, 270 m |
| Prayidae sp. A "*Nectadamas* like" | 579, 581 m | – |
| Prayidae sp. | 636 m | – |
| Calycophorae spp. | 464 m | 276–326 m |
| Siphonophore sp. A "Fireworks" | 522 m | – |
| Siphonophore spp. | 276–668 m | 261–467 m |
| Order Leptomedusae | | |
| Leptomedusae sp. | – | 185 m |
| Order Narcomedusae | | |
| *Aeginura grimaldii* Maas, 1904 | 890 m | – |
| *Solmundella bitentaculata* (Quoy & Gaimard, 1833) | 537–823 m | 267, 471 |
| *Bathykorus* sp. | 682 m | – |
| Aeginidae sp. | – | 471 m |
| *Pegantha* spp. | 526–562 m | – |
| Solmarisidae sp. | 727 m | 424 m |
| *Solmissus incisa* s.l. | 497–574 m | 469 m |
| *Solmissus marshalli* Agassiz & Mayer, 1902 | 278 m | 411 m |
| *Solmissus* spp. | 525–581 m | 278–431 m |
| Narcomedusae spp. | 514, 563 m | – |
| Order Trachymedusae | | |
| *Halicreas minimum* Fewkes, 1882 | 510 m | – |
| *Halicreas* sp. | 730 m | – |
| *Haliscera* sp. | – | 410 m |
| Halicreatidae spp. | 326, 582 m | 276 m |
| *Arctapodema* sp. | 534 m | – |
| *Rhopalonema* sp. | – | 277 m |
| *Colobonema sericeum* Vanhöffen, 1902 | 477–597 m | 406, 470 m |
| Rhopalonematidae spp. | 339 m | 467 m |
| Trachymedusae spp. | 227–530 m | – |
| Hydromedusa spp. | 346, 528 m | – |
| Class Scyphozoa | | |
| Order Coronatae | | |
| *Periphylla periphylla* (Péron & Lesueur, 1810) | 763 m | – |
| Periphyllidae sp. | 733 m | – |
| *Atolla* sp. | 747–762 m | – |
| *Nausithoe* sp. | 578 m | – |
| Order Semaeostomeae | | |
| *Poralia* sp. | 677 m | – |
| Medusa spp. | 513–885 m | 274, 275 m |
| Phylum Chordata | | |

| | | |
|---|---|---|
| Class Thaliacea | | |
| Order Doliolida | | |
| Doliolida spp. (Nurse) | 399 m | 184 m |
| Order Salpida | | |
| Salpinae spp. (Aggregate) | 528–581 m | – |
| Salpinae sp. (Solitary) | 581 m | – |
| Order Pyrosomatida | | |
| *Pyrosoma atlanticum* Péron, 1804 | 520–711 m | – |
| Pyrosomatidae spp. "Oblong" | 530–634 m | 426 m |
| Pyrosomatidae spp. "Cylindrical" | 518–574 m | – |
| Pyrosomatidae spp. "Long & Pointy" | 770–932 m | – |

# **CHAPTER 2:** Comparative ROV Surveys of the Gelatinous Macrozooplankton Communities Inside and Outside an Inactive Caldera: Kurose Hole


## ABSTRACT

Large numbers of the leptomedusa *Earleria bruuni* were observed inside a semi-closed deep-sea caldera during a comparative survey of the macrozooplankton fauna inside and outside the Kurose Hole, Izu-Ogasawara Islands, by the Remotely Operated Vehicle (ROV) *Dolphin-3K*, on 24 September 2000. The Kurose Hole is an inactive volcanic caldera of 790 m bottom depth, located within the Izu-Bonin island arc, south of Tokyo. Archived video and audio data from a dive by the Human Occupied Vehicle (HOV) *Shinkai 2000,* carried out three weeks after the ROV dives, were also analyzed. During all dives within the caldera, *E. bruuni* was present in large numbers and, during the HOV dive, two specimens for morphological analysis were obtained. Herein, we report *E. bruuni* from the Pacific Ocean for the first time. The vertical profiles of environmental factors and the vertical distributions of gelatinous macrozooplankton taxa such as salps, ctenophores, hydromedusae, siphonophores and scyphomedusae were extremely different inside and outside the caldera. Inside the caldera the water temperatures were warm and dissolved oxygen levels were high compared to outside. For each taxon, their distributions were characterized and compared between the inside and outside of the caldera, and with previous literature reports.

## INTRODUCTION

Scyphomedusae, hydrozoans (hydromedusae, siphonophores) and ctenophores are all known to exponentially increase their numbers when environmental conditions become favorable (e.g. Purcell 2005, Uye 2008, Abe et al. 2014). Therefore, to clarify the environmental preferences for each gelatinous zooplankton taxon it is important to quantitatively assess their populations in different environments. Water temperatures inside the caldera of the Kurose Hole are several degrees warmer than those outside (Iwabuchi et al. 1989), which suggests that the caldera should be an ideal study site to investigate the effects of different environmental conditions on biological communities at essentially the same biogeographic location. The Kurose Hole is a caldera that is about 5–7 km in diameter, with the depth of its rim at around 250 m at its deepest point and 114m at its shallowest point, and with the maximum depth of the caldera floor being just over 790 m depth (Iwabuchi et al. 1989, Yuasa et al. 1991), making it a highly closed environment inside the caldera. By comparing vertical distributions of gelatinous zooplankton inside and outside the caldera, chapter 2 attempts to contrast the gelatinous zooplankton communities of the external, cold and internal, warm water masses. Video data from ROV dives inside and outside the Kurose Hole, along with supplementary data from a crewed submersible dive within the caldera, were analyzed for the present study.

## MATERIALS AND METHODS

### 1. Data collection

Data were collected using the Remotely-Operated Vehicle (ROV) *Dolphin-3K* and the Human Occupied Vehicle (HOV) *Shinkai 2000* in the Kurose Hole (33°24'N, 139°41'E, Fig. 17), which is located in the Izu-Bonin Arc, due south of Tokyo (Yuasa et al. 1991). Two *Dolphin-3K* dives (3K488, 3K489) were performed inside and outside the Kurose Hole, respectively, on 24 September 2000 during the R/V *Natsushima* cruise NT00-10, as pre-dive safety surveys for subsequent *Shinkai 2000* dives. Although one dive inside and one dive outside the Kurose Hole caldera were planned for cruise NT00-11 of the R/V *Natsushima*, due to bad weather conditions only one dive was carried out. This was *Shinkai 2000* Dive 1227, inside the Kurose Hole on 17 October 2000. Observations were made and video recorded from the surface to the seafloor in order to analyze the community composition of the midwater gelatinous macrozooplankton.

## 2. Details of Survey Platforms

### *2.1. Dolphin-3K*

The *Dolphin-3K* was equipped with a Victor/JVC KY-F32 three chip CCD camera and six lights: three 400-SeaArc HMI/MSR forward-facing metal halide lamps and three 250-W SeaLine SL-120/250 halogen lamps (one in the rear, two in the front). Video footage was recorded on BCT-D124L Digital Betacam tapes, which were reviewed in their entirety, animals being identified wherever possible. Specimens were collected for positive identification using a single cannister suction sampler (3K488) or an 18-cannister suction sampler (3K489) and were transferred to shipboard aquaria for positive identification. Environmental parameters (pressure, temperature, conductivity, dissolved oxygen concentration) were measured using a

SeaBird SBE19 CTD with an SBE13 oxygen sensor attached to the vehicles, and depth, salinity and water density were calculated from these parameters. Physico-chemical parameters were correlated to the presence of a given animal by matching the time on the CTD dataset to the time on the video.

*2.2. Shinkai 2000*

The *Shinkai 2000* was equipped with a Victor GF-S1000 HU three chip, CCD camera specially modified for the vehicle. There were eight lights: five 250-W SeaLine SL-120/250 halogen lamps and three 400-W SeaArc HMI/MSR metal halide lamps. Video footage was recorded on BCT-D124L Digital Betacam tapes. Specimens were collected for positive identification using a 6-cannister suction sampler and a gate valve sampler (see Hunt et al. 1997). Physico-chemical data were collected and correlated with observations as above. During the midwater dive, comments by the observer (DJL) were recorded on the audio track of the tapes and the observational database that resulted from this dive therefore consisted of both video-recorded data and live observations made through the observation port of the vehicle.

## 3. Observational analysis

*3.1. Distribution and Community Comparison*

To compare the distribution and community composition of gelatinous macrozooplankton inside and outside the Kurose Hole, both *Dolphin-3K* dives 488 (3K488: inside, launched at 33°24.500'N, 139°40.500'E) and 489 (3K489: outside, launched at 33°29.500'N, 139°38.000'E) were analyzed in their entirety from the

surface to the seafloor. There was too much ambient sunlight to reliably observe translucent animals using the ROV video footage in the shallow strata and the upper 100 m were therefore excluded from the analyses. In addition to the ROV dives, *Shinkai 2000* Dive 1227 (2K1227: inside, launched at 33°24.500'N, 139°41.000'E) was reanalyzed and species reidentified by the original observer (DJL in October 2016). Animals were identified to the lowest taxonomic level possible using the most recent taxonomic and field guides to each group (Bouillon et al. 2006, Kitamura 2008, Kitamura et al. 2008 a, b, Miura 2008, Widmer et al. 2010, Lindsay et al. 2015, Minemizu et al. 2015). However, mesozooplankton such as copepods and larvaceans were unable to be analyzed quantitatively. For the ROV dives, where descent speed was relatively constant, the amount of time spent observing in each 20-m depth strata was calculated and animal abundances normalized (Fig. 18). The average observation time in each 20-m depth strata was 1 minute 15 seconds during dive 3K488 (range: 53–118 seconds, total observing time 42.75 minutes) and 1 minute 13 seconds during dive 3K489 (range: 51–102 seconds, total observing time 42.58 minutes). Data were graphed using the software packages "Aabel 3" (build 3.0.6, Gigawiz Ltd. Co.) and "ArcGIS" (Environmental Systems Research Institute, Inc.). Vertical profiles of environmental physicochemical parameters were made using the software package "R" (build 3.3.2, R Development Core Team 2008) (Fig. 19).

### *3.2 Morphological Observations of* Earleria bruuni *(Navas, 1969)*

Two specimens of *E. bruuni* were collected during *Shinkai 2000* Dive 1227 using the 6-cannister suction sampler (samples 2K1227SS5 and 2K1227SS6).

The specimens were transferred to a petri dish for taxonomic observations under a shipboard dissecting microscope (Nikon SMZ-U, 0.75-7.5×) outfitted with a video camera mounted on a C-0.45× Nikon TV lens and recorded in HDV format. Whenever magnification was changed, a ruler was placed beneath the petri dish and recorded for information on scale. Still images of 720 × 480 pixels were captured in TIFF format (.tif). All images were processed in "Adobe Photoshop CC (Ver. 2015)" using the noise reduction filter, auto tone, auto contrast, and auto color on the default values. Size measurements in this study are based on the footage of living specimens. After observation, one specimen was preserved by freezing (2K1227SS5b) and the other one was preserved in 5% buffered formalin-seawater solution (2K1227SS6a). Specimen 2K1227SS6a was re-observed for this study under two types of microscopes (Leica MZ16F with 2.0× lens, and OLYMPUS IX71 with 40.0× and 100.0× Lens). The frozen sample was sequenced according to the method of Collins et al. (2008).

## RESULTS

### 1. Environmental profiles

The caldera of the Kurose Hole was filled with warm water, with a minimum temperature of around 10˚C, during both the *Dolphin-3K* and *Shinkai 2000* dives. Higher water temperatures were observed in the surface layers during the *Dolphin-3K* dives when the main axis of the Kuroshio Current lay above the dive sites (Fig. 19). Extremely different vertical profiles of environmental parameters were apparent below 200m depth between the inside (3K488, 2K1227) and outside (3K489) of the Kurose Hole. Water density Sigma-T values were lower, while temperature, salinity

and oxygen concentrations were higher below the edge of the rim inside the caldera. A strong signal (low salinity, high oxygen) indicating the presence of North Pacific Intermediate Water was observed in the 400m-500m depth strata outside the Kurose Hole.

**2. Comparison of macrozooplankton community inside and outside the Kurose Hole**

Comparative taxon richness and abundances of gelatinous macrozooplankton are shown in Fig. 20, based on observations made during descent for *Dolphin-3K* dives 3K488 and 3K489. Inside the Kurose Hole, the total number of individuals observed was about two times higher than outside, although taxon richness was much lower and scyphomedusae were not observed. Siphonophores and ctenophores were dominant taxa outside, but not inside, the Kurose Hole. Even though total observation times were the same during both dives (43 minutes total each), the number of taxa divided by the number of individuals observed inside and outside the Kurose Hole were 0.14 and 0.60, respectively.

All gelatinous macrozooplankton occurrences are graphed in Figure 21, along with data from Dive 2K1227 inside the caldera. A total of 38 taxa were identified in the three dives: 10 ctenophores, 12 siphonophores, 10 hydromeduse, 2 scyphomedusae, 4 others. Most individuals were distributed below 300 m depth. Some taxa seemed to be associated with warm waters, some with cold waters, and others were indeterminate. Hydromedusae were the most dominant “warm-taxon”, with abundances of a leptomedusa with four round gonads and a dark red manubrium being extremely high between 519–777m depth. Two of the medusae were captured

and identified under the microscope as *Earleria bruuni* (Navas, 1969), which has been redescribed below. These medusae were limited to the near-bottom layer, inside the isothermic water mass in the Kurose Hole (Fig. 22). *Nanomia bijuga* (Delle Chiaje, 1844) was only observed inside the caldera (Fig. 21). *Colobonema sericeum* Vanhöffen, 1902 occurred in every dive, always between 483 m to 693 m depth. *Solmissus incisa* sensu lato and scyphomedusae species occurred only outside of the caldera. *Bathocyroe* spp. were only observed below 650 m depth outside the caldera. Two individuals of an undescribed Lobata taxon that lacks auricles were observed – one inside and the other outside the caldera, in different water masses. Salps were common in the warm water masses.

**3. Systematics**

Order LEPTOTHECATA Cornelius, 1992

Family MITROCOMIDAE Haeckel, 1879 (part); Torrey, 1909

Leptomedusae with basis of manubrium attached to subumbrella along continuation of radial canals, 4 or more simple radial canals, marginal tentacles hollow, marginal cirri present in some genera, gonads oval or linear, only radial canals, open statocysts, no ocelli.

Genus *Earleria* Collins, Ross, Genzano & Mianzan, 2006

*Earleria* Collins *et al.,* 2006: 125. Type species: *Earleria bruuni* (Navas, 1969). Mitrocomidae with four radial canals, with numerous open marginal statocysts, without ocelli and without marginal cirri.

*Earleria bruuni* (Navas, 1969)

(Fig. 23)

*Synonymy*

*Halistaura bruuni.* Navas 1969: 307-310.

*Foersteria bruuni*. Gili et al. 1998: 113-134.

*Foersteria bruuni*. Gili et al. 1999: 313-329.

*Earleria bruuni.* Collins et al. 2006: 125.

*Foersteria bruuni*. Lindsay & Miyake 2009: 424 [2K1227SS5b].

*Earleria bruuni.* Widmer et al. 2010: 56.

*Material Examined*

[2K1227SS5b: 032345] 2.5 cm diameter, mature female, inside Kurose Hole, Izu-Bonin Arc, Northwestern Pacific, 33°24.708'N, 139°40.482'E, 615 m depth, 12:27, 11.11°C, 33.41, 7.67 mL/L, 5% Formalin. [2K1227SS6a: 032359] 2.4 cm diameter, mature male, inside Kurose Hole, Izu-Bonin Arc, Northwestern Pacific, 33°24.708'N, 139°40.482'E, 532 m depth, 15:45, 11.16°C, 33.41, 7.66 mL/L, -80°C Frozen.

*Diagnosis (Emended)*

No peduncle, number of tentacles 40-89, with large cnidocysts in tentacle bulbs, gonads oval, laterally flattened, on distal half of radial canals, marginal statocysts open, one between each 2 successive tentacles.

*Description*

Umbrella flattened, mesoglea relatively thin, ex-umbrella transparent, sub-umbrella sub-hemispherical and relatively flat, transparent. No gastric peduncle. Base of manubrium quadratic. Short, small, quadratic manubrium dark red or brownish-colored. Quadrangular mouth with four flared lips. 4 radial canals, whitish, translucent, straight, of uniform width. Four gonads on distal half of each radial canal, not extending onto upper half and cream-colored, mature male (2K1227SS6a) gonads ovoid and laterally flattened, mature female (2K1227SS5b) gonads sausage-shaped, longer than mature male gonads, split by a median groove. Number of tentacles were 85 and 89, respectively. Nematocysts of two types – spherical nematocysts of mean diameter 2-3 µm (n=10) and oblong nematocysts of approximate dimensions 2µm x 4µm (n=10). Without marginal cirri. Numerous open marginal statocysts, 1 between each 2 marginal tentacle bases.

*Colour*

Manubrium dark red, tentacle bulbs red pigmented and tentacles white.

*Size*

Maximum size to at least 2.5 cm diameter

*Comparisons*

*Earleria bruuni* can be distinguished from other members of the genus by the combination of the following characters: flat umbrella, no peduncle, tentacle bulbs with cnidocysts and more than 40 tentacles.

*Distribution*

Bay of Bengal (Navas 1969), Kurose Hole (present material)

*Remarks*

*Earleria bruuni* was described from the Bay of Bengal by Navas (1969) as *Halistaura bruuni* Navas, 1969. The only other record in the literature occurred some 50 years later off Japan as *Foersteria bruuni* (Navas 1969), but was written in Japanese and gave no morphological description (Lindsay & Miyake 2009). The authors gave the species a Japanese name, "Kurose kurage", meaning "jellyfish from Kurose", based on one of the specimens from *Shinkai 2000* dive 1227 in their checklist of mid-water jellyfishes from Japanese waters (Lindsay & Miyake 2009). Navas (1969) reported a total of 13 individuals (5.5-15.0 mm diameter), which included 6 mature males and 4 mature females. Although only two specimens were captured in the present study, one was a mature male (2.4 cm diameter) and the other a mature female (2.5 cm diameter), both much larger than the specimens in the original description, and correspondingly having more tentacles. The number of tentacles in medusae of the genus *Earleria* are known to increase with growth (Widmer et al. 2010).

## DISCUSSION

### 1. Water mass and macro-zooplankton community

Several different distributional patterns were observed – *Nanomia bijuga* and salps were distributed over a wide depth range inside the caldera, *Bargmannia* spp.

were similar but slightly deeper, while *Earleria bruuni* were patchy in their occurrence and were restricted to the near-bottom layer. On the other hand, *Colobonema sericeum* occurred both inside and outside the caldera but in higher numbers and over a wider depth range inside. The diel vertical migrator *N. bijuga* has been reported from the epipelagic and mesopelagic zones in many places in the Pacific Ocean (Hunt & Lindsay 1999, Minemizu et al. 2015), including down to 300 m (9˚C) and 400 m (12˚C) in the warm Celebes and Sulu Seas, respectively (Grossmann et al. 2015). In the present study, *N. bijuga* was observed only inside the caldera between 271 m (11.4˚C) and 742 m (11.1˚C) but it has also been reported from depths down to 800–900 m (4.5˚C) in the Monterey Bay (Robison et al. 1998). The reason it was not observed outside the caldera may just be an artifact due to the high descent speed and low resolution of the ROV's camera compared to that of the human eye, since all occurrences during the present study were during the HOV survey. In contrast, the large, easily recognizable *Colobonema sericeum* was observed both inside (483–693 m, 11.2–11.1˚C) and outside (584–606 m, 5.5–4.9˚C) the caldera, with depth seemingly more important than temperature in determining its distribution and reinforcing its status as a cosmopolitan species, except in polar regions, the deep, warm Mediterranean (e.g. Larson et al. 1991, Minemizu et al. 2015) and possibly the Red Sea. It has been reported to occur between 500–600 m in the Celebes Sea at temperatures of 5.0–5.5˚C and in the deep, warm Sulu Sea between 300–400 m at temperatures of 12–13˚C (Grossmann et al. 2015). Small rhopalonematid medusae that resembled *C. sericeum* were observed inside the Kurose Hole caldera at 133 m and 302 m depth and, although specimens were not captured to allow positive identification, it may be that this species exhibits an

ontogenetic migration to depth as it matures. *Bathocyroe* spp. were only observed below 550 m depth outside the caldera, even though the volume of water observed inside the caldera by the *Shinkai 2000* was comparatively much greater than that observed by the ROV. *Solmissus incisa* sensu lato (including several different morphotypes of this species, see Lindsay et al. 2015) was similarly also only observed outside the caldera, even though it is easily recognizable to the naked eye even from a distance. The cold water-adapted deep-sea scyphomedusae *Atolla* spp. and *Periphylla periphylla* (Péron & Lesueur, 1810) (Lindsay et al. 2004) were only observed in the deeper layers outside the caldera. Consequently, the present study revealed that the gelatinous macrozooplankton community inside the closed, warmer environment of the caldera was considerably different to that outside with regards to both the community composition and the vertical distributions of the fauna.

Iwabuchi et al. (1989) suggested that rather than the Kurose Hole being filled by a warm water mass derived from influx and vertical mixing of Kuroshio current waters into the caldera, it was more likely, based on the salinity values inside the caldera being lower than the values of Kuroshio Water, that the internal water mass was formed through geothermal heating and subsequent vertical mixing. The low salinity values presumably derive from the pore waters of the subducted sediments from which the geothermally heated waters originate. The occurrence of macrozooplanktonic taxa in the deeper waters of the caldera is therefore considered not to be due to active transport to deeper depths within a surface- or subsurface-derived current of Kuroshio origin but rather due to movements by the animals themselves. This warm, lower salinity water mass seems to provide an “oasis” for the gelatinous macrozooplankton living inside.

**2. *Earleria bruuni***

*Earleria bruuni* occurred at a high population density, being observed between 519 m and 777 m depth, where salinity ranged from 34.38 to 34.40 and temperature was stable at 11.1˚C. They were limited to the near bottom layer, where isothermic water occurred inside the Kurose Hole caldera. Minimum depth distribution revealed by the *Shinkai 2000* dive was slightly shallower (519 m) than by the ROV *Dolphin-3K* (612 m) but as only one dive was carried out by each platform the difference in observed distributions could just as easily have been due to inherent patchiness as to the greater ease of detecting rare (low density) individuals through the greater volume scanned by the human eye. According to Navas (1969) and Navas & Vannucci (1991), *E. bruuni* were collected in the 125–1000 m depth strata with the most accurate depth record being for 125–250 m depth. In that strata salinity ranged from 34.7 to 35.0 and temperature from 12.2˚C to 17.35˚C (Navas 1969), being sandwiched between Bay of Bengal Surface Water (BBSW) and Bay of Bengal Sub Surface Water (BBSSW) in the maximum salinity layer and were never caught in the surface layer (Navas & Vannucci 1991). *E. bruuni* from the Kurose Hole and the Bay of Bengal were observed under similar water temperatures but different salinities and it can therefore be characterized as a warm water mass species. Although *E. bruuni* was not observed outside the caldera, based on the similar environmental factors to those associated with its occurrence in the Bay of Bengal, it should be able to occur. Their dark pigmented gut suggests that they are adapted to catch deep-living bioluminescent prey and we speculate that the *E. bruuni* report

from the Bay of Bengal was due to them being upwelled from the near-bottom layer to near the surface.

Most of the reports on the occurrence of congeners are from semi-closed environments such as canyons or fjords. *Earleria antoniae* (Gili, Bouillon, Pagès, Palanquea, Puig & Heussner, 1998) and *Earleria araiae* (Gili, Bouillon, Pagès, Palanquea & Puig, 1999) were reported from canyons in the Mediterranean Sea (Gili et al. 1998, Gili et al. 1999, Bouillon et al. 2000). *Earleria purpurea* (Foerster, 1923) were reported as one of the benthopelagic species present in fjords of British Columbia in the 50–450 m depth strata (Mackie 1985), and deeper than 200 m depth in Monterey Bay (Larson et al. 1992). *Earleria quadrata* (Hosia & Pagès, 2007) were reported from a fjord in Norway deeper than 500 m (Hosia & Pagès 2007). In this respect, it can be hypothesized that the genus *Earleria* favours deep, isolated water masses. An advantage of the steep-walled concave geography of the fjords and canyons they inhabit is that the particle concentration should increase with depth. Indeed, the cross-sectional area at the 700 m isobath in the Kurose Hole is 30 times smaller than at the caldera rim, and this would act to concentrate sinking particles and vertically migrating plankton, increasing ambient food concentrations.

In addition, the detailed life cycle of the congeneric species *Earleria corachloeae* has been revealed and their polyps were found on the head of the midwater shrimp *Pasiphaea pacifica* Rathbun, 1902 (Widmer et al. 2010). Correspondingly, *Pasiphaea* spp. were observed during all dives in the present study, some individuals were passing through the patch of *E. bruuni* inside the Kurose-Hole between 730 m and 777 m depth. In terms of reproduction, the topography of the

Kurose-Hole retains the water it contains and the organisms within it, presumably enhancing blooming of *E. bruuni* and providing favorable substrates for the polyps.

**3. Differences between ROV vs. HOV observations**

In order to clarify the distribution of gelatinous macrozooplankton, which are transparent and fragile animals, the advantages and disadvantages of various survey methods must be assessed. Direct observations, such as are possible with ROV or HOV dives, can provide accurate information on the distribution of gelatinous macrozooplankton and associations with other organisms, but the amount of data/volume of water sampled is not as high as with net sampling and not all specimens can be identified to species level. Furthermore, when community structure is surveyed through net sampling versus ROV observation, the sampled or observed species composition is different (Raskoff et al. 2010), because of individual sizes, fragility and/or transparency. Likewise, differences between ROV observations and HOV observations were found in the present study because a human's eyes have better resolution than that of a video camera. During *Shinkai 2000* dive 1227, more individuals were observed and more species level identifications were possible than with the *Dolphin-3K* dives. However, the technical restrictions imposed by the ROV actually leads to a more quantitative evaluation, since camera angle, imaged volume, etc. are restrained and recorded, unlike with the human eye. Consequently, it seems that HOV investigations by an experienced researcher are effective for biodiversity surveys, while ROV investigations may be more efficient for an environmental impact assessment (EIA), which requires a repeatable, uniform method. With the development of high-resolution imaging technology such as 4K and 8K video

camera systems, we can expect more detailed and quantitative investigation methods to be developed for gelatinous macrozooplankton surveys, finally bridging the gap between naked-eye and camera-based investigations.

## CONCLUSIONS

Comparative ROV dives revealed that semi-closed systems such as deep-sea calderas can have unique environmental factors and gelatinous macrozooplankton communities. In the Kurose Hole, Izu-Ogasawara Islands, extremely low taxon diversity was found inside the caldera, and large numbers of the leptomedusa *Earleria bruuni* were observed inside the caldera, being the predominant species. Blooming of *Earleria bruuni* was also observed during the additional HOV dive, which was performed three weeks later. Surprisingly, the current report of *E. bruuni* is the first in 50 years, even though the medusa was extremely abundant in the Kurose Hole. Two major causes for this phenomenon may be, firstly, the isolated habitat formed inside the caldera with an isothermic warm water mass when compared to outside the caldera may be a highly suitable habitat for the medusa, and, secondly, the steep, concave topography could concentrate sinking particles and vertically migrating plankton, thereby increasing ambient food concentrations and leading to the observed blooming of *E. bruuni*.

## REFERENCES

Abe Y, Yamaguchi A, Matsuno K, Kono T, Imai I (2014) Short-term changes in the population structure of hydromedusa *Aglantha digitale* during the spring

phytoplankton bloom in the Oyashio region. Bull Fac Fish Hokkaido Univ 64(3): 71–81.

Bouillon J, Pagès F, Gili JM, Palanques A, Puig P, Heussner S (2000) Deep-water Hydromedusae from the Lacaze-Duthiers submarine canyon (Banyuls, northwestern Mediterranean) and description of two new genera, *Guillea* and *Parateclaia*. Sci Mar 64(S1): 87–95.

Bouillon J, Gravili C, Pagès F, Gili JM, Boero F (2006) An introduction to Hydrozoa. ISBN 2-85653-580-1. Muséum national d'Histoire naturelle, Paris.

Collins AG, Bentlage B, Lindner A, Lindsay D, Haddock SHD, Jarms G, Norenburg JL, Jankowski T, Cartwright P (2008) Phylogenetics of Trachylina (Cnidaria: Hydrozoa) with new insights on the evolution of some problematical taxa. J Mar Biol Assoc UK 88(8): 1673–1685.

Collins JSH, Ross AJ, Genzano G, Mianzan H (2006) *Earleria* gen. nov. & *Gabriella* gen. nov., replacement names for *Foersteria* Arai & Brinckmann-Voss, 1980 (Cnidaria, Hydrozoa, Mitrocomidae) and *Foersteria* Wehner, 1988 (Crustacea, Decapoda, Prosopidae), junior homonyms of *Foersteria* Szépligeti, 1896 (Insecta, Hymenoptera, Braconidae). Bulletin of the Mizunami Fossil Museum 33: 125–126.

Gili JM, Bouillon J, Pagès F, Palanques A, Puig P, Heussner S (1998) Origin and biogeography of the deep-water Mediterranean Hydromedusae including the

description of two new species collected in submarine canyons of Northwestern Mediterranean. Sci Mar 62: 113–134.

Gili JM, Bouillon J, Pagès F, Palanques A, Puig P. (1999) Submarine canyons as habitats of prolific plankton populations: three new deep-sea Hydroidomedusae in the western Mediterranean. Zool J Linn Soc 125: 313–329.

Grossmann MM, Nishikawa J, Lindsay DJ (2015) Diversity and community structure of pelagic cnidarians in the Celebes and Sulu Seas, southeast Asian tropical marginal seas. Deep-Sea Res I 100: 54–63. doi:10.1016/j.dsr.2015.02.005.

Hosia A, Pagès F (2007) Unexpected new species of deep-water Hydroidomedusae from Korsfjorden, Norway. Mar Biol 151: 177–184.

Hunt JC, Hashimoto J, Fujiwara Y, Lindsay DJ, Fujikura K, Tsuchida S, Yamamoto T (1997) The development, implementation, and establishment of a meso-pelagic and bentho-pelagic biological survey program using submersibles in the seas around Japan. JAMSTEC J Deep Sea Res 13: 675–685.

Hunt JC, Lindsay DJ (1999) Methodology for creating an observational database of midwater fauna using submersibles: results from Sagami Bay, Japan. Plankton Biol Ecol 46(1): 75–87.

Iwabuchi Y, Ashi J, Fujioka K (1989) Geological and geomorphological survey of the Kurose Hole, north of the Hachijo Island. JAMSTEC J Deep Sea Res 5: 37–41. (in Japanese)

Kitamura M (2008) Chapter 30, Urochordata. In: Deep-sea life – biological observations using research submersibles (eds Fujikura K, Okutani T, Maruyama T). ISBN 978-4-486-01787-5. Kanagawa, Tokai University Press, pp. 351–355. (in Japanese)

Kitamura M, Miyake H, Lindsay DJ (2008a) Chapter 24, Cnidaria. In: Deep-sea life – biological observations using research submersibles (eds Fujikura K, Okutani T, Maruyama T). ISBN 978-4-486-01787-5. Kanagawa, Tokai University Press, pp. 295–320. (in Japanese)

Kitamura M, Miyake H, Lindsay DJ, Horita T (2008b) Chapter 25, Ctenophora. In: Deep-sea life – biological observations using research submersibles (eds Fujikura K, Okutani T, Maruyama T). ISBN 978-4-486-01787-5. Kanagawa, Tokai University Press, pp. 321–328. (in Japanese)

Larson R J, Mills CE, Harbison GR (1991) Western Atlantic midwater hydrozoan and scyphozoan medusae: *in situ* studies using manned submersibles. Hydrobiologia 216/217: 311–317.

Larson RJ, Matsumoto GI, Madin LP, Lewis LM (1992) Deep-sea benthic and benthopelagic medusae: recent observations from submersibles and a remotely operated vehicle. Bull Mar Sci 51(3): 277–286.

Lindsay DJ, Furushima Y, Miyake H, Kitamura M, Hunt JC (2004) The scyphomedusan fauna of the Japan Trench: preliminary results from a remotely-operated vehicle. Hydrobiologia 530/531: 537–547.

Lindsay DJ, Miyake H (2009) A checklist of midwater cnidarians and ctenophores from Japanese waters: species sampled during submersible surveys from 1993–2008 with notes on their taxonomy. Kaiyo Monthly 41: 417–438. (in Japanese)

Lindsay D, Umetsu M, Grossmann M, Miyake H, Yamamoto H (2015) Chapter 51, The gelatinous macroplankton community at the Hatoma Knoll hydrothermal vent. In: Subseafloor biosphere linked to global hydrothermal systems; TAIGA Concept (eds Ishibashi J., Okino K. and Sunamura M). ISBN 978-4-431-54864-5. Tokyo, Springer, pp. 639–666. DOI 10.1007/978-4-431-54865-2_51.

Mackie GO (1985) Midwater plankton of British Columbia studied by submersible PISCES IV. J Plankton Res 7: 753–777.

Minemizu R, Kubota S, Hirano Y, Lindsay D (2015) A photographic guide to the jellyfishes of Japan. ISBN 978-4-582-54242-4. Heibonsha, Tokyo 358 pp. (in Japanese)

Miura T (2008) Chapter 27, Annelida. In: Deep-sea life – biological observations using research submersibles (eds Fujikura K, Okutani T, Maruyama T). ISBN 978-4-486-01787-5. Kanagawa, Tokai University Press, pp. 343–344. (in Japanese)

Navas D (1969) *Halistaura bruuni* sp. nov. (Leptomedusae, Mitrocomidae) with notes on its distribution and ecology. Mar Biol 2: 307–310.

Navas D, Vannucci M (1991) The hydromedusae and water masses of the Indian Ocean. Bol Inst Oceanogr 39(1): 25–60.

Purcell JE (2005) Climate effects on formation of jellyfish and ctenophore blooms: a review. J Mar Biol Assoc U K 85: 461–476.

Raskoff KA, Hopcroft RR, Kosobokova KN, Purcell J, Youngbluth M (2010) Jellies under ice: ROV observations from the Arctic 2005 Hidden Ocean expedition. Deep-Sea Res II 57: 111–126.

R Development Core Team (2008) R: A language and environment for statistical computing. R Foundation for Statistical Computing, Vienna, Austria. ISBN 3-900051-07-0. URL http://www.R-project.org.

Robison BH, Reisenbichler KR, Sherlock RE, Silguero JMB, Chavez FP (1998) Seasonal abundance of the siphonophore, *Nanomia bijuga*, in Monterey Bay. Deep-Sea Res II 45: 1741–1751.

Uye S-I (2008) Blooms of the giant jellyfish *Nemopilema nomurai*: a threat to the fisheries sustainability of the East Asian Marginal Seas. Plankton Benthos Res 3: 125–131.

Widmer CL, Cailliet G, Geller J (2010) The life cycle of *Earleria corachloeae* n. sp. (Cnidaria: Hydrozoa) with epibiotic hydroids on mid-water shrimp. Mar Biol 157: 49–58.

Yuasa M, Murakami F, Saito E, Watanabe K (1991) Submarine topography of seamounts on the volcanic front of the Izu-Ogasawara (Bonin) Arc. Bull Geol Surv Japan 42(12): 703–743.

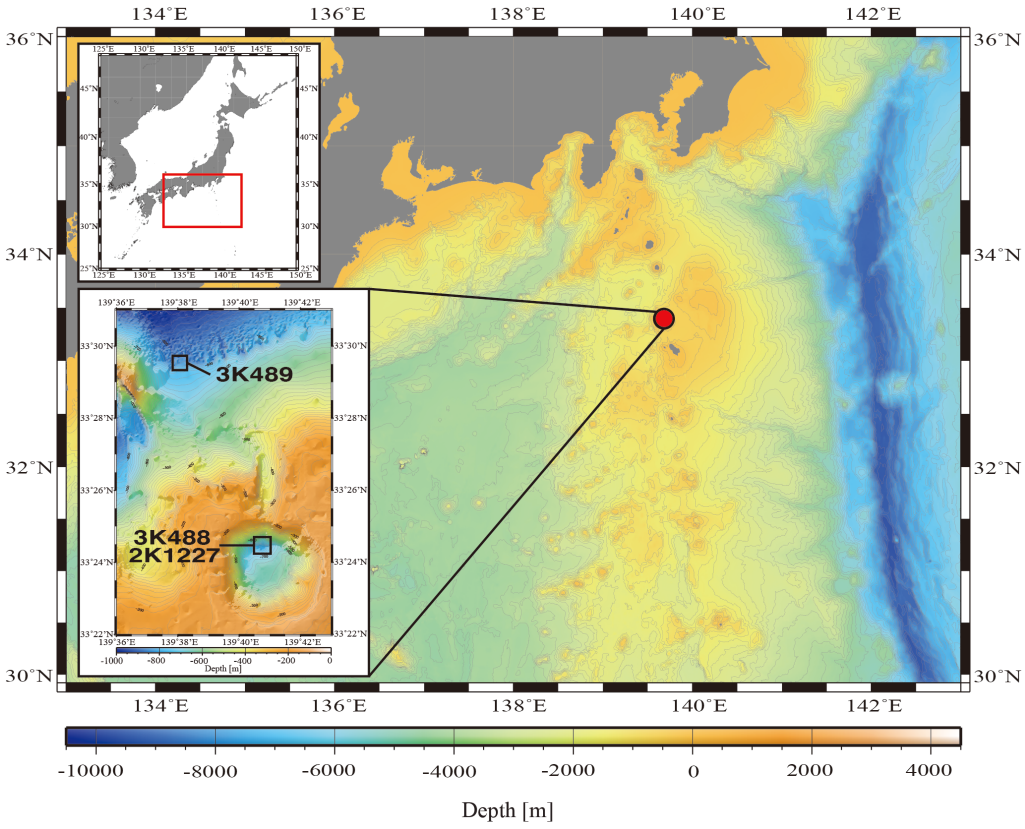


Fig. 17. Map showing the dive locations

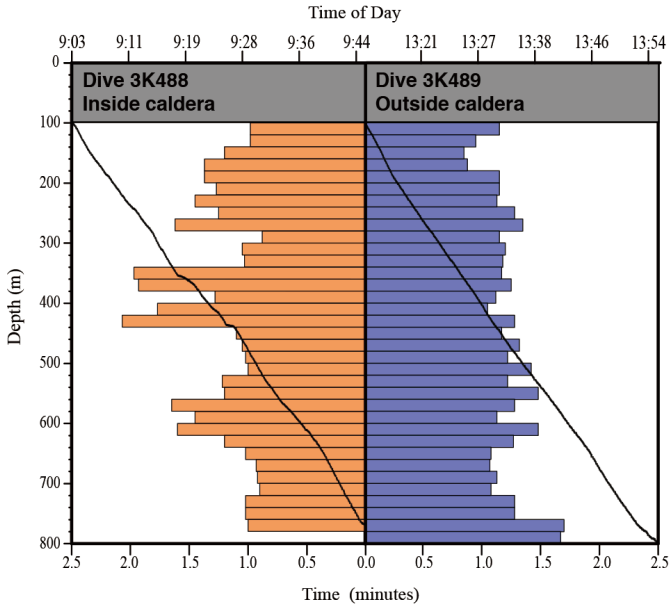


Fig. 18. Time spent observing inside and outside the Kurose Hole. Black lines show *Dolphin-3K* time vs depth dive profiles. Bar graphs show time spent observing for every 20 m depth stratum.

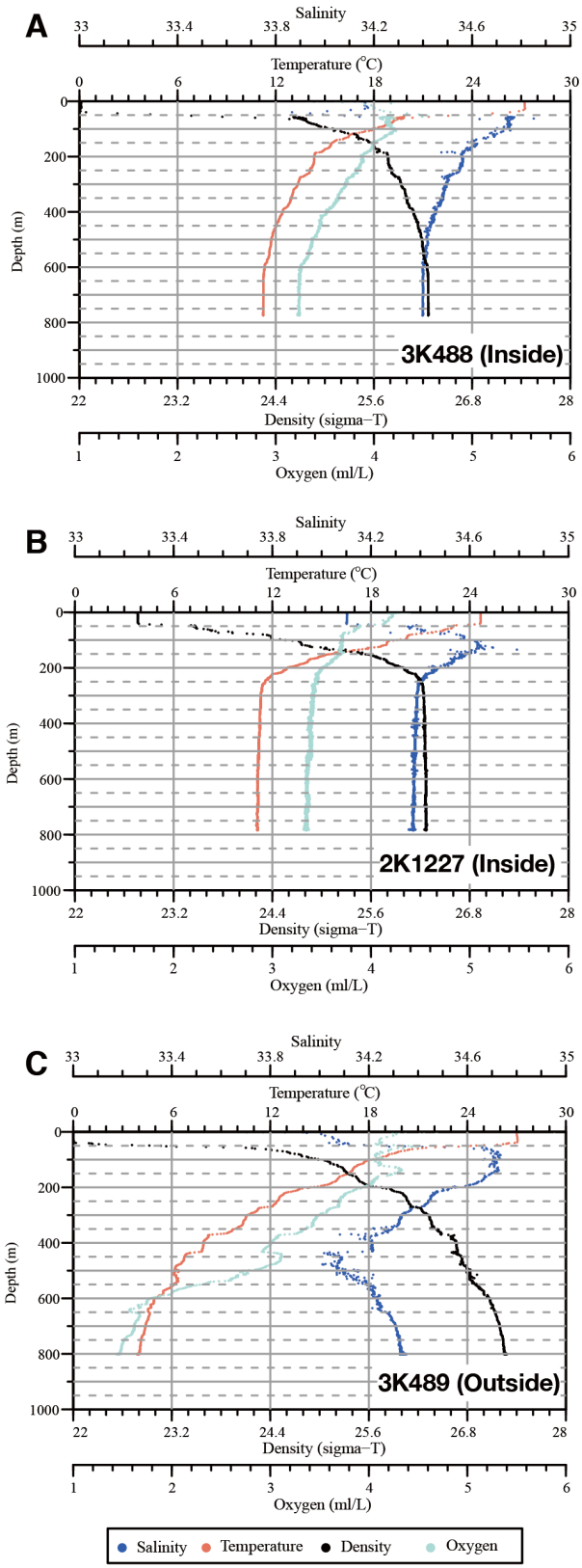


Fig. 19. Vertical profiles of temperature, salinity, oxygen and density vs depth. (A) 3K488; (B) 2K1227; (C) 3K489.

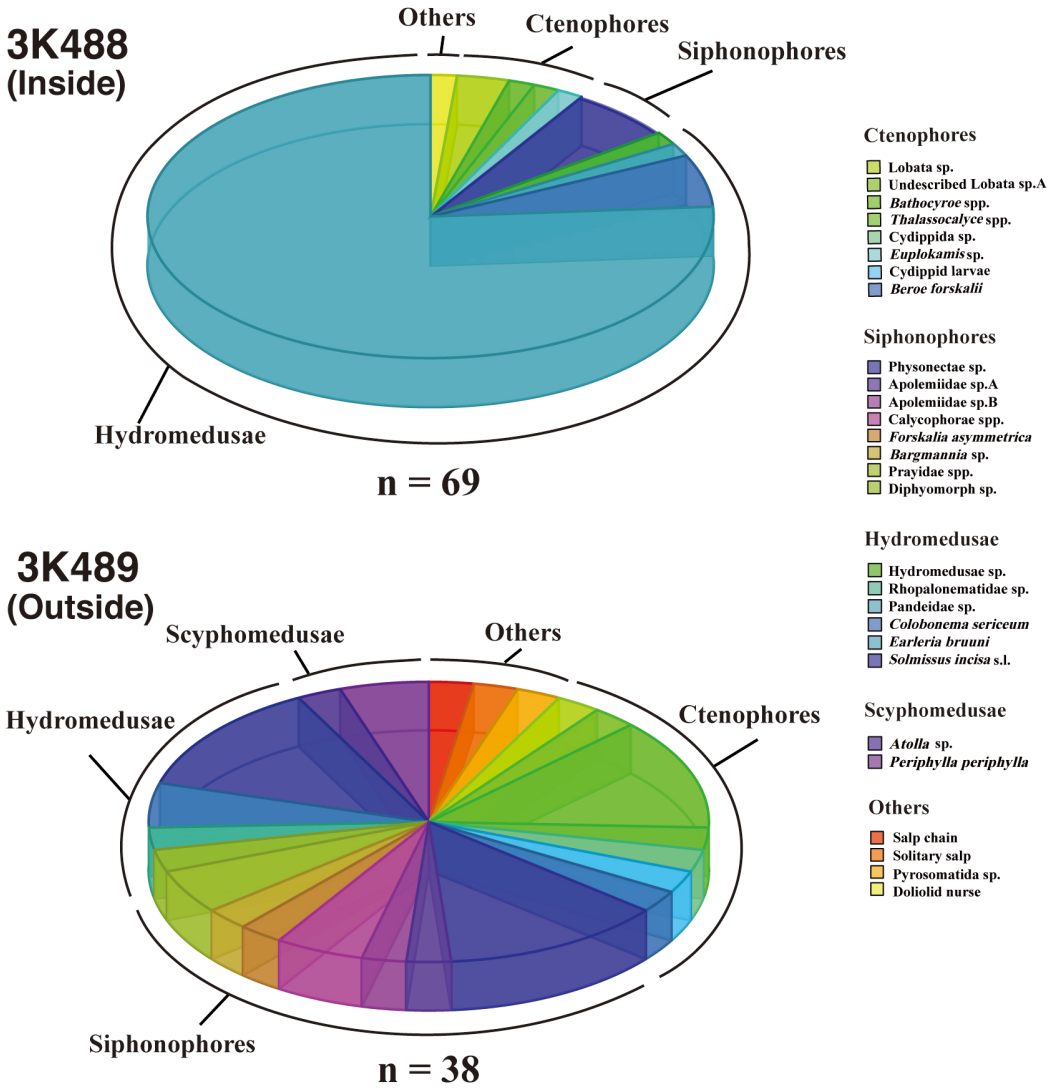


Fig. 20. Pie graphs comparing taxon richness and evenness of macrozooplankton between dives inside (3K488) and outside (3K489) the Kurose Hole.

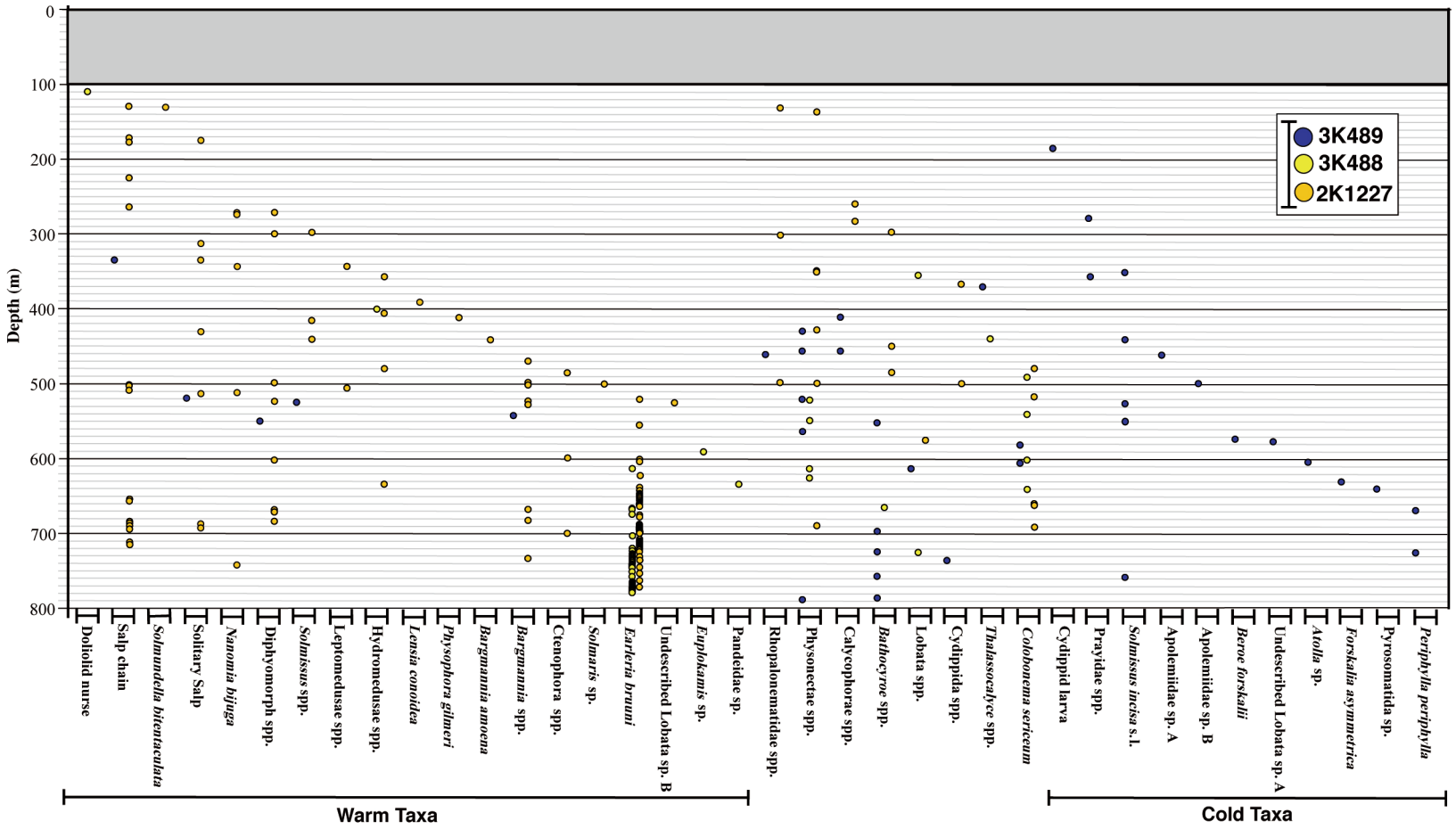


Fig. 21. Taxon occurrence records vs depth for the two *Dolphin-3K* dives (3K488, 3K489) and the *Shinkai 2000* dive (2K1227).

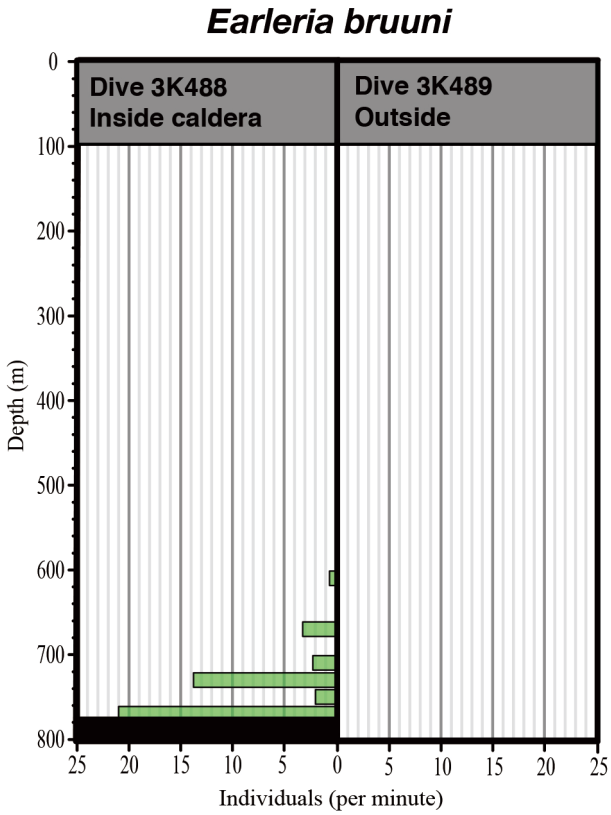


Fig. 22. Comparative vertical distribution of *Earleria bruuni* inside and outside the Kurose Hole.

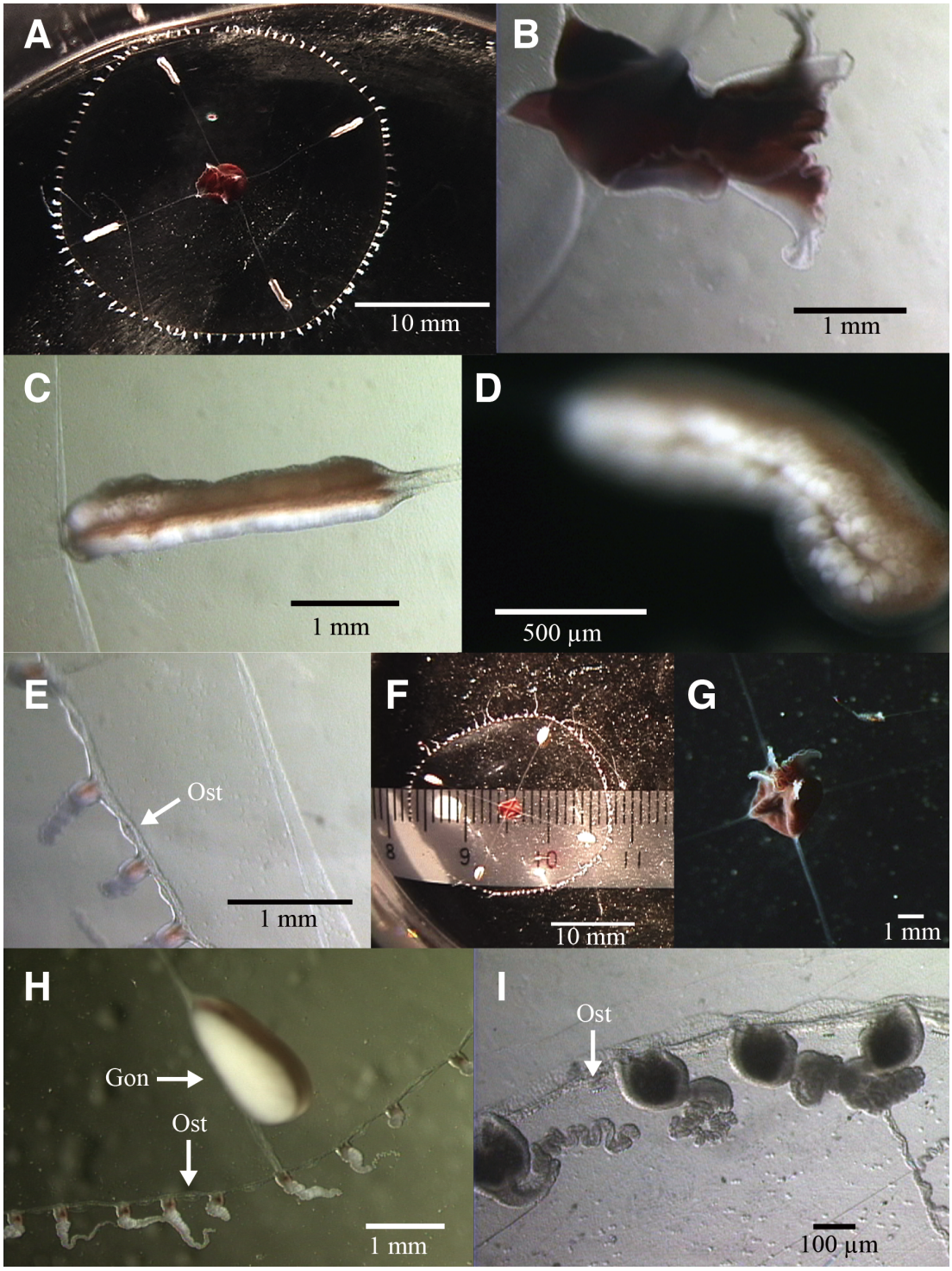


Fig. 23. *Earleria bruuni* (Navas, 1969). A-E: 2K1227SS5b. (A) aboral view of mature female; (B) close-up of manubrium; (C–D) close-up of gonads; (E) close-up of umbrella margin. F–I: 2K1227SS6a. (F) aboral view of mature male; (G) oral view of manubrium; (H) close-up of gonad and umbrella margin; (I) close-up of umbrella margin and tentacles. Ost, Open statocyst. Gon, Gonad.

# **CHAPTER 3:** Comparative ROV Surveys of the Gelatinous Macrozooplankton Communities Inside and Outside an Active Caldera: Sumisu Caldera


## ABSTRACT

ROV dive surveys were carried out inside and outside the Sumisu Caldera, located in the Izu-Bonin Arc. The caldera is hydrothermally active and nourishes a unique chemosynthetic ecosystem, which includes *Bathymodiolus* mussel beds and vestimentiferan tubeworms. Sixty-one gelatinous zooplankton morphotaxa were observed (21 ctenophores, 16 siphonophores, 10 hydromedusae, 4 scyphozoans and 10 thaliaceans), and notes on their taxonomy and fine-scale distributional data are presented. The vertical distribution patterns of gelatinous zooplankton clearly differed inside and outside the caldera: three gelatinous zooplankton morphotaxa, the ctenophores Lobata sp. "Boli" and undescribed Lobata "No auricles", and the hydromedusa *Earleria bruuni*, were highly abundant inside, but not outside, of the caldera. Thaliaceans and *Solmissus incisa* s.l. (Narcomedusae) were distributed over a wider vertical range inside the caldera than outside. The utility of ROV video records for investigating midwater gelatinous zooplankton taxonomy and ecology is discussed, and the efficacy of ROV investigations for this type of research is shown.


## INTRODUCTION

Several scientific reports focusing on the interactions between pelagic zooplankton and hydrothermal vents refer to the occurrence of gelatinous

zooplankton, such as medusae, at high abundances around vents (e.g. Berg & Van Dover 1987, Burd & Thomson 1994, Vinogradov et al. 2003). Burd & Thomson (2000) focused on this, investigating the abundance and biomass of medusae based on net sampling data. They concluded that "medusae percent biomass and abundance were greater in the region of deep-water (>1000 m depth) scattering layers at the Endeavour vent field than in the surrounding northeast Pacific, where deep zooplankton scattering layers were not present and total standing stock was lower". This suggests that gelatinous zooplankton is one category of biota that would likely be affected by deep-sea mineral mining if the hydrothermal vent ecosystems were disturbed. Lindsay et al. (2015) supposed that gelatinous zooplankton could be influential consumers at hydrothermal vents. They therefore produced a synopsis of the gelatinous zooplankton fauna at the Hatoma Knoll hydrothermal vent site, based on ROV video footage, and this became the first taxonomic guide to this fauna to be based on characters visible in video images. Following the same concept, the present study provides detailed comparative vertical distribution data, obtained from ROV video footage, and taxonomic treatments of the gelatinous zooplankton above an active vent site and at an off-vent site, inside and outside a deep-sea caldera.

## MATERIALS AND METHODS

Two mid-water dive surveys using the Remotely-Operated Vehicle (ROV*) Hyper-Dolphin* were carried out during cruise KY02-03 (doi.org/10.17596/0000166) of the R/V Kaiyo (from 18 February–13 March 2002) at the Sumisu Caldera (31° 27' N, 140° 03' E). This hydrothermally active, semi-closed caldera is located within the

Izu-Bonin arc and has a diameter of 10 km, with the deepest point of its rim being at about 490 m depth (Iwabuchi 1999, Japan Coast Guard 2017) (Fig. 24).

The first dive (HPD0083) to compare the gelatinous zooplankton community was conducted outside the caldera (launched at 31°29'03" N, 140° 09' 20"E) from 10:43 on 9 March 2002, while the second dive (HPD0084) was conducted inside (launched at 31°28'18" N, 140° 04' 01"E) from 8:48 on 10 March 2002. Video footage, recorded during the descent from the surface to the seafloor, was analyzed quantitatively. The upper 100-m depth stratum was omitted from the analysis because there was too much ambient light to detect translucent gelatinous zooplankton with consistent accuracy. The observation times for each 50-m depth stratum were calculated and are shown in Table 2. The average observation time within each 50-m stratum was 8 minutes 45 seconds during dive HPD0083 (range: 3 minutes 18 seconds – 20 minutes 30 seconds, total observation time 140 minutes 6 seconds) and 6 minutes 26 seconds during dive HPD0084 (range: 2 minutes 23 seconds – 20 minutes 30 seconds, total observation time 109 minutes 23 seconds).

The ROV *Hyper-Dolphin* was equipped with an HDTV (High-Definition TeleVision) camera integrating an ultra-sensitive super HARP (High gain Avalanche Rushing Photo-conductor) tube. Camera sensitivity was F 1.8 at 2 lux, gain was variable at 4-200 times, the signal to noise ratio was 43 dB, and resolution was 800 TV lines. The zoom lens had a minimum focal length of 5.5 mm and a 5× zooming ratio. There were five 400-W SeaArc HMI/MSR metal halide lamps. Two were situated on the port swing arm, and one on the starboard swing arm. These arms were usually opened such that the lights optimized the field of view of the high definition camera when zoomed out and centered in the direction of ROV transit, but were

sometimes moved to optimize lighting when making observations (i.e., pan-tilting or zooming the HD camera) of individual organisms in situ. The remaining two lights were forward-pointing and fixed to the frame of the vehicle. Video footage was recorded continuously and simultaneously on BCT-124HDL HDCAM tapes via a native digital signal at 1080i and 29.97 frames sec-1 and was also down-converted to an analogue composite NTSC signal and recorded with depth/time overlay on Sony BCT-D124L Digital BetaCam tapes. After the cruise, these video tapes were played back on a Sony HDW-M2100 or DVW-A510 video deck and the video was digitized (Apple ProRes 4:2:2 codec, QuickTime Movie container [.mov]) using an AJA Ki Pro unit. The original timecode embedded in the HDTV files was replaced using qtChange2.26 (videotoolshed.com) to match the time shown in the video overlay on the digitized NTSC movie files to frame-level accuracy. The movie files were then analyzed using QuickTime Player Pro 7.6.6 with reference to the embedded time-stamp.

Physico-chemical data were collected using a SeaBird SBE19 CTD (Conductivity, Temperature, and Depth profiling system) and an SBE13 dissolved oxygen sensor attached to the vehicle on both dives. The vertical profiles are plotted in Figure 25. CTD and dissolved oxygen were correlated to the presence of animals by matching the depth information recorded by the CTD to the depth information on the video text overlay. Physico-chemical parameters associated with each morphotaxon occurrence are presented in the following order: temperature, salinity, dissolved oxygen concentration.

Gelatinous zooplankton were identified to the lowest taxonomic level during descent through the water column, although appendicularians were excluded from

the analysis because it was hard to distinguish whether living individuals were inside the feeding filters or not, therefore making them unable to be counted quantitatively. For the identifications, the following recent taxonomic works, field guides, and original descriptions were used: Madin & Harbison (1978), Chihara & Murano (1997), Nishikawa (1997), Wrobel & Mills (1998), Pugh (1999, 2003, 2005), Bouillon et al. (2006), Kitamura (2008), Kitamura et al. (2008 a, b), Lindsay & Miyake (2009), Horita et al. (2011), Lindsay et al. (2015), Minemizu et al. (2015), Licandro et al. (2017 a, b), Licandro & Lindsay (2017). The terminology used in the results is primarily that of Lindsay et al. (2015). Voucher images of each morphotaxon are available as supplementary material at http://www.jamstec.go.jp/datadoi/doi/10.17596/0001982.html. Individual morphotaxon occurrences were binned into 50-m depth strata to investigate the vertical distribution of each morphotaxon. Animal abundances were normalized through dividing by the time spent observing in each stratum after first subtracting time spent with the camera zoomed in or where its field of view was blocked by instruments, etc.

## RESULTS

### 1. Environmental profiles

The surface mixed layer was observed to extend throughout the upper 250 m during both dives HPD0083 and HPD0084 (Fig. 25). As depth increased, temperature and salinity decreased fairly rapidly to 600 m depth. Below 600 m depth, extremely different vertical profiles of environmental parameters were observed between the outside (HPD0083) and inside (HPD0084) of the Sumisu Caldera. A

salinity minimum, indicating the presence of North Pacific Intermediate Water (Reid 1965), was observed in the 600-800 m depth strata outside the Sumisu Caldera, while temperature and oxygen levels continued to decrease with increasing depth. On the other hand, the Sumisu Caldera was filled with warmer water with a minimum temperature of around 10˚C, relatively high oxygen and no salinity minimum. Below 600 m depth, density values were mostly stable, indicating a high degree of mixing right to the bottom of the caldera.

**2. Gelatinous zooplankton**

A total of 61 gelatinous zooplankton taxa were identified during dives HPD0083 and HPD0084: 21 ctenophores, 16 siphonophores, 10 hydromedusae, 4 scyphozoans and 10 thaliacean taxa. The vertical distributions for each taxonomic group per 50 m-thick depth stratum are graphed in Fig. 26, and Figs. 28-30. Details of their distributions, the characters that allowed their identification from video sequences, and interpretive comments appear below. The number of observed taxa outside and inside the Sumisu Caldera were 39 (n = 201) vs. 41 (n = 215), while the total time of observation was 140 vs. 109 min, respectively.

*2.1. Ctenophora*

Twenty-one ctenophore taxa were observed, with 11 taxa identifiable to genus level (described genera) or lower, and with 13 of the 21 taxa definitely belonging to separate, distinct species. Ctenophora was one of the most dominant taxa both outside and inside the Sumisu Caldera (16 and 14 taxa observed, respectively). Lobate ctenophores were abundant in the subsurface layer outside the

caldera, but a bimodal distribution was observed inside the caldera with maximum abundance peaks at 350–400 m and 750–800 m depth. They were observed over a wide depth range, while most "cydippid" ctenophores were distributed below 500 m depth both inside and outside the caldera (Fig. 26). The genus *Bathocyroe* and the morphotype "Undescribed Lobata [No auricles]" were abundant inside the caldera.

**Undescribed Lobata "No auricles"** (Fig. 27A, B) — A total of 7 individuals of this morphotype were observed only inside the Sumisu Caldera between 826 m–864 m depth (10.0–10.1°C, 34.29–34.31, 2.8 ml $L^{-1}$). The body shape superficially resembled the genus *Bolinopsis* but they lacked auricles, which lobate ctenophores usually have. Substomodeal comb rows did not extend onto the oral lobes. In the present study, only one morphotype was observed, despite several morphotypes of lobate ctenophores lacking auricles having been reported in the literature (Fig. 25.20 in Kitamura et al. 2008 b, Fig. 51.10 in Lindsay et al. 2015, Plate 75A in Mills & Haddock 2007, Fig. 1D in Podar et al. 2001).

***Bathocyroe fosteri* Madin & Harbison, 1978** — *Bathocyroe fosteri* occurred both outside and inside the Sumisu Caldera, at 716 m (7.4°C, 34.28, 2.2 ml $L^{-1}$) and at 687 m and 688 m depths (10.5 & 10.5°C, 34.35 & 34.31, 2.9 & 2.9 ml $L^{-1}$), respectively. *Bathocyroe fosteri* possessed extremely short comb rows in comparison with the total body length and fairly large, wide auricles; body with a pair of broad oral lobes slightly compressed in tentacular plane; body colour transparent, except for red-pigmented stomodaeum; eight short comb rows of equal length extending to level of

tentacle bulbs; two pairs of white tentacle bulbs facing each other near aboral end of stomodaeum.

*Remarks*: the extremely short comb rows and broad auricles enable this species to be easily distinguished from its congeners.

***Bathocyroe longigula* Horita, Akiyama & Kubota, 2011** (Fig. 27 C, D) — *Bathocyroe longigula* was observed inside the Sumisu Caldera at 622 m and at 686 m depth (10.7 & 10.5°C, 34.38 & 34.38, 2.9 & 2.9 ml $L^{-1}$). *Bathocyroe longigula* had an extremely long, stomodaeum extending to almost half the length of its oral lobes; stomodaeum clearly observed as long, white line in present video records.

*Remarks*: Tiny, irregularly-shaped dark-orange spots have been reported to be scattered along the meridional canals, but were unable to be observed in the present video footage due to lighting and resolution constraints. This is only the second record of *B. longigula* in the literature, although an individual we consider assignable to this species was reported at 428 m depth in Sagami Bay by Kitamura et al. (2008 b; see Fig. 25.13). This species was described from southwestern Japan in coastal waters at the surface (14.5°C), so this is the lowest temperature and deepest record for the species.

***Bathocyroe* sp. Non *fosteri*** — Two individuals of this ctenophore morphotype were observed inside the Sumisu Caldera at 662 m and 686 m depth (10.6 & 10.5°C, 34.31 & 34.36, 2.9 & 2.9 ml $L^{-1}$). *Bathocyroe* sp. Not *B. fosteri* were clearly distinguishable from *B. fosteri* by having comb rows extending to the level of the base of the oral lobes.

*Remarks*: The ctenophores are possibly *B. longigula* but the comparative length of the stomodaeum could not be ascertained.

***Bathocyroe* spp.** — Three individuals were observed between 585–756 m depth (6.5–10.9°C, 34.27–34.32, 2.0–3.0 ml $L^{-1}$) outside the Sumisu Caldera, five individuals were observed between 577–753 m depth (10.4–11.4°C, 34.32–34.36, 2.8–3.1 ml $L^{-1}$) inside. Most of the individuals were identified by the position of the tentacle bulbs at the aboral end of the stomodaeum and/or by the "frog kick" lobe-flapping behavior, the undulating form of which is particular to the genus *Bathocyroe*.

*Remarks*: *Bathocyroe* spp. includes several indeterminable species of *Bathocyroe*.

**Lobata sp. "Boli"** — Three individuals of Lobata sp. "Boli" were observed between 231–338 m depth (17.1–18.7°C, 34.71–34.80, 3.6–4.1 ml $L^{-1}$) above the outside of the caldera, eleven individuals between 577–753 m depth (15.6–16.6°C, 34.59–34.64, 3.5–3.6 ml $L^{-1}$) above the inside of the caldera. Lobata sp. "Boli" is a proxy name for one morphotype of lobate ctenophore. Lobata sp. "Boli" possessed an elliptical body shape; oral lobes were as large as half body length; body colour transparent; comb row lengths superficially equal, but substomodaeal comb rows slightly longer than subtentacular comb rows; mouth placed halfway along length of oral lobes, with tentacle bulbs present. Video quality did not allow observations of the auricles or canal structures.

*Remarks*: They might be immature *Bolinopsis*.

***Bolinopsis* sp.** — Only one individual of *Bolinopsis* sp. was observed at 284m (18.3°C, 34.77, 3.8 ml $L^{-1}$) above the outside of the caldera. The ctenophore possessed an ovoid body shape; statocyst deeply sunken; substomodaeal comb rows extending to end of oral lobes, auricles extending to almost same level as tip of mouth; subtentacular comb rows ratio 4/7 to total body length.

*Remarks*: Three congeners are known from Japanese waters, *Bolinopsis infundibulum* (O.F. Müller, 1776), *Bolinopsis mikado* (Moser, 1907) and *Bolinopsis rubripunctata* Tokioka, 1964. The observed individual was obviously distinguishable from *B. infundibulum* because of the differences in the length of the comb rows, but was difficult to attribute to, or distinguish from, *B. mikado* or *B. rubripunctata.* Furthermore, *Bolinopsis mikado* sensu Komai, 1918 resembles *Bolinopsis vitrea* (L. Agassiz, 1860) in the extreme (e.g., see illustrations from the São Sebastião Channel (Brazil) in Oliveira & Migotto 2006), not only in the general body structure but also with regard to the colour of the canals. These two species are possibly synonymous (personal observations), so it is also possible that *B. vitrea* occurs in Japanese waters.

***Eurhamphaea vexilligera*** Gegenbaur, 1856 — Three individuals of *E. vexilligera* were observed between 218–604 m depth (18.7–10.0°C, 34.80–34.31, 4.1–2.8 ml $L^{-1}$) outside the caldera. *Eurhamphaea vexilligera* possessed a fairly flattened body shape in the tentacular axis, aboral ends pointed and projected with two flexible filaments; round oral lobes arising at level of mouth, being small and only around 1/3 of total body length; auricles relatively short, their widths entirely equal, changing position only slowly; aboral sense organ extremely deeply sunken between the two pointy aboral projections.

*Remarks*: although reddish-pigmented spots along the meridional canals are an important character to identify this species, the present video did not allow visualization of the pigmentation. All individuals were identified by the body shape and presence of aboral filaments. To this date, although four other congeners have been described, they are all thought to be synonyms or to be *species inquirenda* (Mills 2017, and personal observations).

***Kiyohimea* sp.** — Only one *Kiyohimea* sp. was observed, at 572 m depth (11.5°C, 34.35, 3.1 ml $L^{-1}$) inside the Sumisu Caldera. *Kiyohimea* sp. possessed a strongly compressed body in the tentacular axis, as with *E. vexilligera*, and also possessed two triangular aboral processes, but lacked aboral filaments; the aboral sense organ was situated at the bottom of the depression between the aboral projections; subtentacular comb rows began at top of aboral projections and continued onto auricles, substomodaeal comb rows began slightly above level of statocyst and extended aborally beyond level of mouth.

*Remarks*: The genus *Kiyohimea* includes two species, *Kiyohimea usagi* Matsumoto & Robison, 1992 and *Kiyohimea aurita* Komai & Tokioka, 1940. At this time, these two congeners are distinguished by the presence or absence of oral tentacles; *K. usagi* possesses tentacles but *K. aurita* only possesses a vestigium. However, except for this character, these two species are extremely similar. It is possible that these species were described as two different species but in reality they are the same species at a different state of development. The life history of this species should be investigated in the future, paying close attention to its development.

***Ocyropsis* sp.** — Three individuals of *Ocyropsis* sp. were observed between 241–295 m depth (18.6–18.2°C, 34.79–34.73, 4.1–3.8 ml $L^{-1}$) above the outside of the caldera. *Ocyropsis* sp. possessed a laterally compressed body in the tentacular axis with a rounded aboral end, with the body shape looking like a rounded rectangle when viewed from the stomodaeal plane, since it had a slightly flattened aboral end; stout body structure and large lobes produced a vigorous flapping motion; auricles were long; four of the eight comb rows ran nearly parallel and almost faced the other four comb rows across the tentacular axis; substomodaeal comb rows were longer than subtentacular comb rows.

**Lobata spp.** — Three other individuals of Lobata spp. were observed above the outside of the caldera between 112–352 m depth (18.8–16.7°C, 34.81–34.69, 4.1–3.6 ml $L^{-1}$), six individuals of Lobata spp. were observed inside the caldera between 634–871 m depth (10.7–10.0°C, 34.31–34.34, 2.9–2.8 ml $L^{-1}$). Apart from possessing two oral lobes, nothing more was able to be ascertained about their morphology due to the quality of the video. Lobata spp. obviously included more than one species.

***Cestum veneris* Lesueur, 1813** — One individual of *C. veneris* was observed at 167 m depth (18.7°C, 34.81, 4.1 ml $L^{-1}$) above the outside of the caldera. *Cestum veneris* possessed a fairly flattened, ribbon-like body shape, without any lobes and/or auricles, that was strongly compressed in the tentacular plane and extended in the stomodaeal plane; four subtentacular meridional canals arose from the stomodaeum, then curved immediately outward and ran along the mid-line of the body.

Remarks: Family Cestidae includes only two species, belonging to two different genera: *C. veneris* and *Velamen parallelum* (Fol, 1869). These two species are distinguished by characteristics of the comb rows, meridional canal structure, form of the gonads, and body size. *Velamen parallelum* possesses four subtentacular meridional canals that arise directly, without curving, at the midpoint of the body to run parallel to the body edge.

**Cestidae sp.** — Four individuals of Cestidae sp. were observed between 161–326 m depth (18.7–17.4°C, 34.80–34.71, 4.1–3.7 ml $L^{-1}$) above the outside of the caldera, and one individual was observed at 312 m (17.0°C, 34.69, 3.7 ml $L^{-1}$) above the inside of the caldera. The most representative character of the family is a ribbon-like, long and flat body shape without lobes and/or auricles with a basically transparent body colour.

*Remarks*: Occasionally, cestid ctenophores superficially seem like the leptocephalus larva stage of Anguilliformes (i.e. eels), especially when they curl themselves up. When ribbon-like, transparent, gelatinous animals are observed, one should carefully investigate whether or not they have a head, or whether there are gastrovascular structures in the midline of the body.

**"Cydippid larvae"** — "Cydippid larvae" occurred both inside and outside the Sumisu Caldera at 613 m (9.6°C, 34.32, 2.7 ml $L^{-1}$) outside the caldera and at 548 m (12.1°C, 34.39, 3.2 ml $L^{-1}$) inside the caldera. "Cydippid larvae" possessed a transparent ovoid body, with eight short comb rows and two tentacles that were

positioned at the midpoint of the stomodaeum and near the external surface of the body.

*Remarks*: presumably the larval stage of lobate, cestid or thalassocalycid ctenophores.

**Cydippida sp. "Little ruby"** — One individual of Cydippida sp. "Little ruby" was observed at 756 m (6.48°C, 34.28, 2.0 ml $L^{-1}$) outside the Sumisu Caldera. Cydippida sp. "Little ruby" was ovoid in body shape, being slightly compressed in the substomodaeal plane; cardinal red-colored body and dark red-pigmented stomodaeum; tentacle bulbs long; fine tentacles with numerous simple side branches, superficially emerging from the aboral end, however the opening of the tentacle sheath was wide and extensive, so the tentacles can seem to emerge at any level; eight comb rows extended nearly the entire body length.

*Remarks*: Cydippida sp. "Little ruby" is clearly an undescribed species. The canal structure has yet to be observed in detail (Fig. 25.9 in Kitamura et al. 2008 b).

***Bathyctena* sp. "Sagami"** — One individual of *Bathyctena* sp. "Sagami" was observed at 707 m depth (10.40°C, 34.37, 2.9 ml $L^{-1}$) inside the Sumisu Caldera. *Bathyctena* sp. "Sagami" possessed a spherical body shape; body colour transparent, dark reddish-brown pigmented stomodaeum with side branches called diverticula arising from the paragastric canals and extending onto the stomodaeum; short, white tentacle bulbs were large and angled in an "L" shape, placed mid-length along the body; comb row lengths equal, extending 70-80% of total body length.

*Remarks*: *Bathyctena* sp. “Sagami” is often observed with its tentacles retracted (Hidaka, unpublished data). When sighted in situ during ROV dives, the two large tentacle bulbs are very reflective and appear as two bright white, round spots, leading to its other nickname "two spots". The first report of *Bathyctena* sp. “Sagami” was between 500 to 1000 m in depth in Sagami Bay, which is located halfway along the Pacific coast of Japan (Lindsay & Hunt 2005). Lindsay & Miyake (2007) gave a preliminary morphological description, with more detailed descriptions of the species given in Japanese in 2009 (Lindsay & Miyake 2009), under the Japanese common name "Sagami-shinkai-fuusenkurage" meaning "bathyctenid cydippid from Sagami", and by Lindsay in 2015 (Minemizu et al. 2015).

**Mertensiidae sp. “Wadako”** — One individual of Mertensiidae sp. “Wadako” was observed at 533 m (12.19°C, 34.43, 3.2 ml $L^{-1}$) outside the Sumisu Caldera. Mertensiidae sp. “Wadako” possessed an extremely compressed body in the substomodaeal plane with two keel-like projections at the aboral end, and a slightly extended mouth; transparent body; statocyst not sunken; substomodaeal comb rows extended from tip of aboral end of keels to edge of mouth; subtentacular comb rows extended from aboral end near statocyst to edge of mouth; two tentacle bulbs of boomerang shape, curved concavely towards mouth; tentacle sheath opening at same level as base of keels; tentacles arose from stomodaeal side of tentacle bulbs, emerging aborally with sausage-shaped, coiled tentilla.

*Remarks*: Kitamura et al. (2008 b) gave a short description of the morphotype Mertensiidae sp. “Wadako”, as "Mertensia sp." (Fig. 25.6 in Kitamura et al. 2008 b). Since then, Lindsay & Miyake (2009) gave a slightly more detailed description in

Japanese as "Mertensiidae sp. B", based on two collected specimens. In the article, they also gave it the Japanese common name "Wadako-kurage" meaning " Japanese traditional kite-shaped jellyfish". This morphotype has been observed in Sagami and Suruga Bays (Kitamura et al. 2008 b), and outside the Sumisu Caldera (present study).

***Hormiphora palmata* Chun, 1898** — Two individuals of *H. palmata* were observed at 624 m and 661 m (9.32 & 8.67°C, 34.31 & 34.28, 2.7 & 2.5 ml L-1) outside the Sumisu Caldera. *Hormiphora palmata* possessed a teardrop-shaped body, with an extending mouth and a slightly flattened aboral end; body colour transparent; eight comb rows of equal length, extending 2/3-4/5 total body length from aboral end, with the comb rows evenly spaced; tentacle bulbs long and narrow, placed quite close and parallel to the stomodaeum; broad tentacle sheaths ran toward aboral end in a gentle curve, opening at approximately 1/6 body length from aboral end; white tentacles with numerous thread-like tentilla arising slightly aboral to the midpoint of the tentacle bulbs.

*Remarks*: *Hormiphora palmata* is a common cydippid ctenophore, usually found in open-ocean, surface waters. However, the present study is the deepest-yet observation record for the species, at 661 m depth.

According to the original description of the species (Chun 1898), immature individuals possess palm-shaped tentilla on their tentacles, and these are so large that they are unable to be retracted into the tentacle sheaths. However, the present morphotype has been reported to only have simple, thread-like tentilla, even at a body length of only 8 mm (Minemizu et al. 2015). Developmental studies on H.

palmata should be carried in the future. *Hormiphora japonica* Moser, 1907 is a synonym.

**Cydippida sp. "White tear drop"** — Two individuals of Cydippida sp. "White tear drop" were observed at 588 m and 618 m (10.64 & 9.62°C, 34.27 & 34.32, 2.9 & 2.8 ml $L^{-1}$) outside Sumisu Caldera, and one individual was observed at 696m (10.45°C, 34.37, 2.9 ml $L^{-1}$) inside the caldera. This cydippid morphotype has a white-coloured, elongated teardrop-shaped body; tentacle sheaths open near the aboral end, or there is an extensive groove between adjacent subtentacular comb rows that make it seem so; tentacles possess simple, thread-like tentilla.

*Remarks*: Cydippida sp. "White tear drop" appears to belong to the Pleurobrachiidae or perhaps an undescribed family (personal observations).

**Cydippida spp.** — Two individuals assignable only to Cydippida spp. were observed at 555 m and 866 m (11.3 & 10.5°C, 34.39 & 34.30, 3.0 & 1.6 ml $L^{-1}$) outside the caldera, and two individuals were observed at 320 m and 786 m (16.9 & 10.2°C, 34.61 & 34.35, 3.6 & 2.8 ml $L^{-1}$) inside the caldera. These individuals were ovoid in shape, possessed two extended tentacles with tentacle bases not being near the external surface, and had 8 comb rows.

**Ctenophore spp.** — One individual, identifiable only to Phylum, was observed at 413 m (15.45°C, 34.56, 3.5 ml $L^{-1}$) inside the Sumisu Caldera. Ovoid body and bright comb rows were visible.

*2.2. Cnidaria*

A total of 30 morphotaxa of Cnidarians were observed at the Sumisu Caldera. Siphonophores were sparsely distributed throughout all depth strata both inside and outside the caldera (Fig. 28-29). Hydromedusae were infrequent, except for two remarkable species – the very abundant hydromedusa Earleria bruuni (Navas, 1969) inside the caldera, and the frequently observed deep-sea narcomedusa Solmissus incisa sensu lato, respectively (Fig. 28, Fig. 29. Scyphomedusae were only observed below 580 m depth.

2.2.1 Siphonophores

A total of 16 siphonophore morphotaxa were observed, with 10 morphotaxa identifiable to genus level (described genera) or lower, and with 9 of the 16 morphotaxa definitely belonging to separate, distinct species. The number of observed siphonophoran morphotaxa outside and inside the caldera was 9 vs. 11, respectively. There were no significant patterns (Fig. 28).

***Agalma elegans* (pro parte M. Sars, 1846)** — One individual of *A. elegans* was observed at 288 m (18.2°C, 34.76, 3.8 ml $L^{-1}$) above the outside of the Sumisu Caldera. *Agalma elegans* possessed an evenly-elongated colony shape with a linearly arranged stem, and with the siphosome being much longer, but the same width, as the nectosome; the pneumatophore had a long stalk, causing it to almost always be oriented vertically; adjacent gastrozooids were very widely spaced and were the only zooids that were visibly pigmented.

*Remarks*: The widely spaced gastrozooids and the siphosome being equal to or more slender than the nectosome are critical characters to distinguish it from *Agalma okeni* Eschscholtz, 1825. Most of the original description of *A. elegans*, apart from the structure of the tentilla, was based on the morphology of *Nanomia cara* Agassiz, 1865 (Sars 1846).

***Erenna* sp. —** One individual of *Erenna* sp. was observed at 705 m depth (10.4°C, 34.33, 2.8 ml $L^{-1}$) inside the Sumisu Caldera. *Erenna* sp. possessed a thick nectosome, had conspicuous nematocyst patches on the ostia of the nectophores and tips of the bracts, and the distance between adjacent gastrozooids was short.
*Remarks*: The macromorphology of this individual closely resembled *Erenna insidiator* Pugh & Haddock, 2016, although the diagnostic characters for the species were not readily evident in the video footage.

***Bargmannia amoena* Pugh, 1999 —** One individual of *B. amoena* was observed at 486 m depth (13.6°C, 34.48, 3.4 ml $L^{-1}$) outside the Sumisu Caldera, while two individuals were observed at 580m and 581m depth (11.2 & 11.2°C, 34.40 & 34.39, 3.0 & 3.0 ml $L^{-1}$) inside the caldera. *Bargmannia amoena* possessed a longitudinally extended and laterally flattened nectosome with distinctive, elongated nectophores (up to 32); the siphosome was thinner and cormidia indistinct compared to *Bargmannia elongata* Totton, 1954 (see p. 161 of Minemizu et al. 2015 for comparison of macromorphologies); whitish gastrozooids were positioned sparsely but in a regular manner on the stem.
*Remarks*: The flaccidity of the siphosome contrasts with that of *B. elongata.*

***Bargmannia* sp. —** Only one individual of *Bargmannia* sp. was observed, at 540 m depth (12.1°C, 34.42, 3.2 ml $L^{-1}$) outside the Sumisu Caldera. *Bargmannia* sp. possessed a longitudinally extended and laterally flattened nectosome and had distinctive elongated nectophores.

*Remarks*: The characteristic sinusoidal swimming behavior allowed easy identification to genus level.

***Physophora gilmeri* Pugh, 2005** — Two individuals of *P. gilmeri* were observed inside the Sumisu Caldera at 274 m and 390 m depth (17.7 & 15.7°C, 34.8 & 34.6, 3.8 & 3.5 ml $L^{-1}$). *Physophora gilmeri* possessed an elongated dome-shaped nectosome with a long and narrow pneumatophore; siphosome not elongated but rather in a corm just below the nectosome; palpons long and well-developed, encircling the colony in a manner reminiscent of a grass skirt, palpon tips pigmented bright orange, remainder of palpon coloured pale milky-white; bracts too transparent to discern.

*Remarks*: Two species in the genus *Physophora* have been described – *P. gilmeri* and *Physophora hydrostatica* Forsskål, 1775. If they are mature, it is easy to distinguish them by the different shape and colour of their pneumatophores, and coloration of palpons, etc. (for detailed comparisons see Pugh 2005). When viewed laterally, the nectophores of *P. hydrostatica* have a translucent circle corresponding to the cross section of the T-shaped nectosac, while *P. gilmeri*, which has a Y-shaped nectosac, does not have this translucent circle.

***Forskalia asymmetrica* Pugh, 2003 —** One individual of *F. asymmetrica* was observed at 602 m depth (10.1°C, 34.34, 2.8 ml $L^{-1}$) outside the Sumisu Caldera, two individuals were observed at 495 m and 582 m depth (14.1 & 11.2°C, 34.52 & 34.40, 3.4 & 3.0 ml $L^{-1}$) inside the caldera. *Forskalia asymmetrica* possessed a cylindrical, rather than tapering, nectosome, due to having low variation in the size of the nectophores; the siphosome dissociates and changes shape easily; spirally-coiled siphosome shorter than half entire colony length; nectophores flattened in the upper-lower plane; gastrozooids positioned a long distance from the siphosome stem, large in size, and relatively few in number.

***Forskalia formosa* Keferstein & Ehlers, 1860 —** One individual of *F. formosa* was observed inside the Sumisu Caldera at 638 m depth (10.7°C, 34.31, 2.9 ml $L^{-1}$). *Forskalia formosa* possessed an elongated, tapering nectosome; the pneumatophore extended considerably anterior to the main body of the nectosome; fir tree-shaped siphosome tapering posteriorly, thickness of the anterior end of the siphosome much wider than the width of nectosome when relaxed; spirally-coiled siphosome longer than half entire colony length; nectophores flattened in the upper-lower plane; gastrozooids positioned a long way from the siphosomal stem, the gastrozooids medium in size and number.

***Forskalia* spp. —** Two individuals of *Forskalia* spp. were observed at 570 m (11.1°C, 34.38, 3.0 ml $L^{-1}$) outside the caldera. *Forskalia* spp. possessed a spirally-coiled nectosome and siphosome, with the nectophores arranged multiserially and the colony shape resembling a spindly pinecone. Nectophores laterally flattened in

the upper-lower plane; siphosome fir tree-shaped; gastrozooids positioned a long way from the siphosomal stem, reddish or orange-coloured tentacles arose from the gastrozooids.

*Remarks*: Family Forskaliidae only includes the genus *Forskalia*, which is the only siphonophore to possess a spiral nectosome with nectophores arranged multiserially. In some cases, a *Physophora* species can superficially resemble *Forskalia* spp. but the genus *Physophora* possesses a corm-like siphosome with large palpons radiating out just below the nectosome. Spinning swimming behavior is often observed in *Forskalia*.

**Physonectae spp. (non-Forskaliidae, non-Physophoridae)** — Twelve individuals assignable only to the morphotaxon Physonectae due to poor video quality were observed outside the Sumisu Caldera between 260 m–824 m depth (18.4–5.4°C, 34.77–34.30, 3.9–1.7 ml $L^{-1}$) and five were observed inside between 328 m–627 m depth (16.6–10.7°C, 34.61–34.37, 3.6–2.9 ml $L^{-1}$). Physonectae were identified by the presence of a gas-filled apical organ called a "pneumatophore" and an array of swimming bells called "nectophores" beneath the pneumatophore.

*Remarks*: During ROV observations, a pneumatophore usually appears as a bright white spot or bubble, attached to the anterior pole of the nectosome. Some physonect siphonophore species retract the pneumatophore into an apical hollow in the nectosome.

***Clausophyes* sp.** — One individual of *Clausophyes* sp. was observed at 802 m (10.2°C, 34.36, 2.8 ml $L^{-1}$) inside the Sumisu Caldera. *Clausophyes* sp. possessed

two non-ridged nectophores that were heteromorphic and linearly opposed, and with the anterior nectophore tapering apically to a point; siphosome held within hydroecial flaps of posterior nectophore and therefore curving along lower line of posterior nectophore.

**Clausophyidae sp. (non-*Crystallophyes*, non-*Heteropyramis*)** — Two individuals of Clausophyidae sp. were observed at 630 & 666 m (9.1 & 8.5°C, 34.30 & 34.33, 2.6 & 2.5 ml $L^{-1}$) outside the Sumisu Caldera, one was observed at 813 m (10.2°C, 34.34, 2.8 ml $L^{-1}$) inside the caldera. These calycophoran, diphyomorph siphonophores had two nectophores that were heteromorphic and linearly opposed. The attachment point of the stem was considerably anterior to the ostium of the anterior nectophore and the attitude of the colony was angled obliquely to vertically. Remarks: Taxonomically, Clausophyidae also includes siphonophores with a single nectophore but all clausophyids we observed had two.

**Diphyomorph sp.** — One individual assignable to either the Clausophyidae or Diphyidae and recorded here as "Diphyomorph sp." was observed at 244 m (18.3°C, 34.77, 3.9 ml $L^{-1}$) above the inside of the caldera. Diphyomorphs typically possess two dissimilar, linearly-adjoined nectophores.

*Remarks*: Diphyomorph spp. observed in deep waters by ROVs are more likely to be Clausophyids than other diphyomorphs due to the larger colony sizes of members of this family.

***Sphaeronectes* sp. —** One individual of *Sphaeronectes* sp. was observed at 357 m (16.7°C, 34.69, 3.5 ml $L^{-1}$) outside the caldera. It possessed a single sub-spherical nectophore.

Remarks: *Sphaeronectes* spp. within the Sphaeronectidae are the only siphonophores to possess a single sub-spherical nectophore, with other single nectophore species having a streamlined, rocket-shaped nectophore. The Prayid subfamily Amphicaryoninae also looks spherical but has two nectophores, with one cradled by the other.

**Prayinae sp.** — One individual of Prayinae sp. was observed at 564 m (11.3°C, 34.39, 3.0 ml $L^{-1}$) outside the Sumisu Caldera. It possessed a pair of opposed, rounded nectophores, similar in size to each other.

*Remarks*: The form and branching pattern of the nectophoral mantle canals and presence/absence of a somatocyst-like caecal extension are important characters needed to identify Prayine genera but these were not apparent in the present video. This individual probably did not belong to the genus *Stephanophyes* because, exceptionally within the Prayinae, this genus often has more than two opposing nectophores.

**Calycophorae sp. (non-Hippopodidae) —** One individual of Calycophorae sp. was observed at 200 m (18.63°C, 34.80, 4.0 ml $L^{-1}$) above the inside of the caldera. The bright white spot indicative of an anterior pneumatophore was absent and one or two nectophores were present.

*Remarks*: When a siphonophoran colony has only one or two nectophores and no pneumatophore present, but it is impossible to tell whether there is only one nectophore (Sphaeronectidae, Nectopyramidinae, *Enneagonum*, *Heteropyramis*, *Muggiaea*, *Clausophyes laetmata* Pugh & Pages, 1993*, Diphyes chamissonis* Huxley, 1859) or whether the nectophores are opposed (Prayomorph) or linearly adjoined (Diphyomorph) it was treated as Calycophorae sp.

**Siphonophorae spp. (non-Physaliidae, non-Rhodaliidae)** — Seven colonies identifiable only as Siphonophorae were observed outside the Sumisu Caldera between 271–756 m depth (18.3–6.4°C, 34.77–34.28, 3.8–2.0 ml $L^{-1}$) and two inside at 380 m and 432 m (15.8 & 15.1°C, 34.64 & 34.36, 3.5 & 3.5 ml $L^{-1}$). The term Siphonophorae spp. refers to an elongated cnidarian colony where it is impossible to determine whether a pneumatophore or nectophores were present or not. This morphotaxon can include any kind of siphonophore except the cystonect Physaliidae (e.g., Portuguese man o' war; *Physalia physalis* (Linnaeus, 1758)) and the physonect Rhodaliidae (benthic siphonophores with a corm-like siphosome).

2.2.3. Hydromedusae

A total of 10 morphotaxa of Hydromedusae were observed (Fig. 28, Fig. 29), with 5 morphotaxa identifiable to genus level (described genera) or lower, and with 7 of the 10 morphotaxa definitely belonging to separate, distinct species. The number of observed hydromedusan morphotaxa outside and inside the caldera was 6 vs. 7, respectively. The leptomedusa *Earleria bruuni* was highly abundant inside the caldera. Narcomedusae differ from other hydromedusae in primarily preying on

gelatinous prey and, because they therefore belong to a different functional group, their distribution has been graphed separately (Fig. 29). *Solmissus incisa* sensu lato were relatively abundant both inside and outside the caldera and their population peak was in the 600–650 m depth strata (Fig. 29).

***Pandea conica* (Quoy & Gaimard, 1827)** — One individual of *P. conica* was observed at 245 m (18.63°C, 34.80, 4.0 ml $L^{-1}$) above the inside of the caldera. *Pandea conica* possessed a vertically-elongated, transparent exumbrella; frilled lips and well-developed gonads on the slender manubrium, manubrium length half the bell height; filiform tentacles with wide bulbs, numbering less than 40.

*Remarks*: We were not able to count the tentacles accurately, so the possibility exists that it might be *Pandea cybeles* Alvariño, 1988, which has 40 tentacles compared to the 20 of *P. conica*. However, according to a description of *P. conica* from Japan (by Shin Kubota in Minemizu et al. 2015), the number of tentacles can be up to 44.

***Earleria bruuni* (Navas, 1969)** — Twenty-three individuals of *E. bruuni* were observed only inside the Sumisu Caldera between 714–769 m (10.4–10.2°C, 34.36–34.34, 2.8 ml $L^{-1}$). *Earleria bruuni* possessed a fairly flattened umbrella with a small, dark red or brownish-pigmented manubrium; four cream-coloured, ellipsoidal gonads on the distal half of each radial canal, not extending onto the upper half; tentacles crowded and numerous so that it seems like the outer edge of the bell is white.

*Remarks*: *Earleria bruuni* was not observed even once outside the caldera, even though it was the most dominant species observed inside the Sumisu Caldera.

Hidaka-Umetsu & Lindsay (2017) discussed the possibility that medusae of the genus *Earleria* favour semi-closed submarine topography.

**Geryoniidae sp.** — One individual of Geryoniidae sp. was observed at 245 m (18.7°C, 34.79, 4.0 ml $L^{-1}$) above the outside of the caldera. Geryoniidae sp. possessed a hemispherical, transparent bell; a long, conical, gelatinous peduncle that protruded below the margin of the bell, and 4–6 long marginal tentacles. *Remarks*: Geryoniidae includes only two species, *Geryonia proboscidalis* (Forsskål, 1775) and *Liriope tetraphylla* (Chamisso & Eysenhardt, 1821). They are easily distinguished by the number of radial canals and tentacles, and the shape of the gonads. *Geryonia proboscidalis* usually has 6 radial canals, 6 flat heart-shaped gonads on the radial canals, and 6 long tentacles alternating with 6 small tentacles. *Liriope tetraphylla* usually has 4 radial canals, 4 flat leaf-shaped gonads on the radial canals, and 4 long tentacles alternating with 4 small tentacles. We could not accurately count the number of tentacles in the present video.

***Halicreas minimum* Fewkes, 1882** — Two individuals of *H. minimum* were observed at 701 m and 878 m (7.5 & 5.1°C, 34.28 & 34.29, 2.2 & 1.6 ml $L^{-1}$) outside the Sumisu Caldera, while one individual was observed at 661 m (10.6°C, 34.32, 2.9 ml $L^{-1}$) inside the caldera. *Halicreas minimum* possessed a vertically-compressed, hemispherical bell with a prominent gelatinous projection arising from the apex; body transparent, except for whitish to orange radial canals and tentacles; 8 broad radial canals containing whitish gonads; 8 clusters of gelatinous papillae on the exumbrella overlying the radial canals, difficult to observe from a distance. Tentacles

numbered in the hundreds and were prominent, being near transparent in the proximal half and intense white or reddish-coloured in the stiff, needle-like distal half.

*Remarks*: when viewed laterally, the radial canals lie in the same plane and are therefore visible as a bright white horizontal line, while the mass of tentacles, when contracted, form a thicker white band. The combination of two white parallel lines/bands of similar length formed by the radial canals and tentacles, the apical projection, and the angularity of the dorsal margins of the exumbrella allow us to easily identify this species *in situ*. Currently, *H. minimum* is considered the only valid species in the genus.

***Colobonema sericeum* Vanhöffen, 1902** — Four individuals of *C. sericeum* were observed between 468–644 m (14.2–8.7°C, 34.51–34.29, 3.4–2.5 ml $L^{-1}$) outside the caldera, and two individuals were observed at 581 and 663 m depth (11.2 & 10.6°C, 34.39 & 34.32, 3.0 & 2.9 ml $L^{-1}$) inside the caldera. *Colobonema sericeum* possessed a transparent, hemispherical exumbrella and conical subumbrella; well-developed velum; eight narrow radial canals, linear gonads attached to canals along most of their length; long, white stomach without peduncle; tentacles numbered up to 32, tentacle colour near-transparent proximally, becoming whiter distally, and with distal portions frequently curled up when stationary and in fishing position. Tentacles were often jettisoned when the medusae were stimulated.

*Remarks*: Tentacle colour sometimes appears to be blue during *in situ* ROV observations.

**Rhopalonematidae spp.** — One individual assignable only to Rhopalonematidae sp. was observed at 819 m depth (5.5°C, 34.30, 1.6 ml $L^{-1}$) outside, while the other was observed at 428 m depth (15.2°C, 34.58, 3.5 ml $L^{-1}$) inside the Sumisu Caldera. These individuals had transparent, hemispherical exumbrellas, eight radial canals and lacked gastric peduncles. The gonads on the radial canals were near the manubrium in the individual from 819 m depth.

*Remarks*: The morphology of the individual from 819 m depth suggests it may have been *Arctapodema* sp., especially since it jettisoned many fine tentacles when escaping – a behavior most commonly observed in *Arctapodema* spp.

**Trachymedusae sp.** — One hydromedusa assignable only to Trachymedusae sp. was observed at 615 m depth (10.8°C, 34.35, 3.0 ml $L^{-1}$) inside the Sumisu Caldera. Trachymedusae sp. possessed a hemispherical exumbrella; a number of thick white tentacles, and swam rapidly with vigorous pulses. The tentacles seemed to be whiter distally, suggesting that it may have belonged to the family Halicreatidae (*Halicreas*?).

***Solmissus incisa*** sensu lato — Five individuals of *S. incisa* s.l. were observed between 578–614 m (11.1–9.6°C, 34.37–34.32, 3.0–2.7 ml $L^{-1}$) outside the caldera, and seven individuals were observed between 448–688 m (14.7–10.5°C, 34.58–34.35, 3.4–2.9 ml $L^{-1}$) inside the caldera.

*Remarks*: At least two morphotypes of *Solmissus incisa* s.l. occurred. One morphotype was nicknamed "white socks" (see Hidaka-Umetsu & Lindsay 2018),

and this morphotype seems to correspond to *S. incisa* form B in Toyokawa et al. 1998. The other morphotype possessed a convex hemispherical bell and 24 triangular stomach pouches with perradial tentacles. The tips of the tentacles were curled and this morphotype does not seem to correspond to either form A or form B of *S. incisa* in Toyokawa et al. (1998), nor the morphotype reported by Lindsay et al. (2015).

**Narcomedusa spp.** — Three hydromedusae, assignable only to Narcomedusa spp., were observed between 600–660 m (10.1–8.7°C, 34.31–34.30, 2.8–2.5 ml $L^{-1}$) outside the Sumisu Caldera. Narcomedusa spp. possessed a flat, disk-like bell with tentacles arising from partway up the exumbrella, and lacked oral arms.
*Remarks*: Narcomedusa spp. resembled *Solmissus*.

**Hydromedusa spp.** — Three medusae, assignable only to Hydromedusa spp., were observed between 284–585 m (18.2–10.8°C, 34.77–34.34, 3.8–3.0 ml $L^{-1}$) outside the caldera, and two individuals were observed at 225 and 619 m (18.6 & 10.8°C, 34.80 & 34.38, 4.0 & 3.0 ml $L^{-1}$) inside the caldera. Hydromedusa spp. possessed a transparent, hemispherical bell, had numerous short tentacles, and lacked oral arms.
*Remarks*: Hydromedusa spp. probably includes several species.

### 2.2.4 Scyphomedusae

A total of 4 morphotaxa of Scyphomedusae were observed (Fig. 28). All of the Scyphomedusae occurred deeper than 583 m depth. The most abundant scyphomedusa *Periphylla periphylla* (Péron & Lesueur, 1810) was only observed outside the Sumisu Caldera.

**Ulmaridae gen. et sp. nov.** — One individual of Ulmaridae gen. et sp. nov. was observed at 813 m (10.2°C, 34.30, 2.8 ml $L^{-1}$) inside the Sumisu Caldera. Ulmaridae gen. et sp. nov. possessed a hemispherical umbrella with the bell margin cleft into 8 broad lobes (lappets); thick, transparent mesoglea; reddish to brown-coloured stomach and oral arms; base of stomach cross-shaped when viewed directly from above; a total of 16 canals arose from the base of the stomach; dozens of subumbrellar tentacles.

*Remarks*: This undescribed species was also observed at 843 m depth (10.1°C, 34.34, 2.8 ml $L^{-1}$) during the same dive inside the caldera (HPD0084), but it was not treated in the semi-quantitative analysis because it was filmed during the ascent. Because of absorption of red light by seawater the stomach and oral arms can appear brown or even grey when the medusa is observed from a distance.

***Periphylla periphylla* (Péron & Lesueur, 1810)** — Five individuals of *P. periphylla* were observed between 704–751 m (7.5–6.7°C, 34.29–34.23, 2.2–2.0 ml $L^{-1}$) outside the Sumisu Caldera. *Periphylla periphylla* possessed a steep conical or dome-shaped bell that was usually higher than wide; body colour transparent or brownish, conical stomach pigmented in cardinal red; whitish U- or J-shaped gonads in 4 pairs, near the base of the stomach; solid marginal tentacles arising from clefts between the lappets.

*Remarks*: *Periphylla periphylla* is considered a cosmopolitan species, being absent only in the Arctic Ocean and the Sea of Japan (Minemizu et al. 2015). The genus *Periphylla* is currently considered monotypic, although evidence exists that there may be more than one species (Lindsay 2005, Minemizu et al. 2015).

***Atolla* sp.** — One individual of *Atolla* sp. was observed at 694 m depth (7.9°C, 34.23, 2.3 ml $L^{-1}$) outside the Sumisu Caldera. *Atolla* sp. possessed a flat exumbrella with an obvious coronal furrow; brownish-coloured body with whitish tentacles; tentacles numbered more than 8 and it was also dragging a single, extremely long, hypertrophied tentacle.

*Remarks*: Based on the colour of the individual, it was not *Atolla vanhoffeni* Russell, 1957, which possesses a transparent bell.

**Coronatae sp. (Not Atollidae, Not Paraphyllinidae, Not Periphyllidae)** — One individual of Coronatae sp. was observed at 583 m depth (11.2°C, 34.39, 3.0 ml $L^{-1}$) inside the Sumisu Caldera. Coronatae sp. possessed a coronal furrow on the exumbrella; transparent body colour; more than 6 tentacles; tips of tentacles with terminal knob.

*Remarks*: This individual seems to belong either to the genus *Nausithoe* or *Atorella*.

*2.3. Thaliacea*

A total of ten morphotaxa of thaliaceans were observed, with 2 morphotaxa identifiable to genus level (described genera) or lower, and with 4 of the 10 morphotaxa definitely belonging to separate, distinct species. The number of observed thaliacean morphotaxa outside and inside the caldera was 6 vs. 7, respectively. While *Cyclosalpa* or salps belonging to the subfamily Cyclosalpinae were abundant in the upper subsurface layers (Fig. 30), salps belonging to the subfamily Salpinae were abundant at rather deeper depths both inside (HPD0083) and outside the Sumisu Caldera (HPD0084).

**Doliolid nurse** — A doliolid nurse colony was observed at 147 m depth (18.8°C, 34.81, 4.1 ml $L^{-1}$) above the inside of the caldera. One transparent, simple, barrel-shaped zooid pulled behind it a long, fuzzy tail-like structure, presumably zooids attached to its dorsal spur.

*Remarks*: Doliolid nurses can seem like siphonophores sometimes when observed in the video record. However, the siphosomes of siphonophores invariably possess obvious clusters of cormidia on their stems, visible as alternating white-clear areas, so that they can be distinguished from doliolids. The escape responses of siphonophores and doliolid nurses also differ, with nurses jetting back in the direction of the dorsal spur to form a V-shape.

***Cyclosalpa* sp. solitary zooid** — One solitary zooid of *Cyclosalpa* sp. was observed at 181 m depth (18.7°C, 34.77, 4.0 ml $L^{-1}$) above the inside of the caldera. *Cyclosalpa* sp. solitary zooid possessed a single transparent test with a straight gut overlying the gill bar, which lay obliquely in the middle of the tunic; more than five light organs were arranged on both sides of the tunic; it bore a coiled stolon ventrally.

***Cyclosalpa* spp. aggregate zooids** — Five chains of "*Cyclosalpa* spp. aggregate zooids" were observed between 103–241 m (18.8–18.7°C, 34.81–34.80, 4.1–4.0 ml $L^{-1}$) above the outside of the caldera, three were observed between 172–313 m (18.7–17.0°C, 34.76–34.64, 4.0–3.7 ml $L^{-1}$) above the inside of the caldera. Chain morphology was wheel-like or when composed of only a couple of zooids was chain-like, with zooids being conjoined tenaciously with a short peduncle. Each zooid

possessed two tail-like projections arising from the posterior part of the tunic and a ringed yellow gut lay at the base of the projections.

*Remarks*: *Cyclosalpa* spp. aggregate zooids were likely either *Cyclosalpa bakeri* Ritter, 1905 or *Cyclosalpa foxtoni* Van Soest, 1974. However, to identify the species it is necessary to observe the shape of the dorsal tubercle, which was not visible in the present video record.

**Cyclosalpinae spp. solitary zooid** — An individual of Cyclosalpinae sp. was observed at 176 m depth (18.8°C, 34.81, 4.1 ml $L^{-1}$) above the outside of the caldera, and one at 637 m depth (10.7°C, 34.31, 2.9 ml $L^{-1}$) inside the caldera. Cyclosalpinae sp. solitary zooid possessed a single transparent test, with a straight gut overlying the gill bar, which lay obliquely in the middle of the tunic. The individual observed outside the caldera (HPD0083) bore a coiled stolon ventrally, while the shape of the gut was not determinable in the video of the second individual.

**Salpinae cf. *Salpa* spp. aggregate zooids** — Two chains of *Salpa* spp. aggregate zooids were observed at 549 m and 608 m depth (12.0 & 10.9°C, 34.41 & 34.38, 3.2 & 3.0 ml $L^{-1}$) inside the caldera. Salpinae cf. *Salpa* spp. aggregate zooids formed linear chains; each blastozooid had pointy projections on both anterior and posterior ends.

**Salpinae sp. solitary zooid** — One individual of Salpinae sp. was observed at 478 m depth (13.8°C, 34.53, 3.3 ml $L^{-1}$) inside the caldera. "Salpinae sp. solitary zooid" possessed a single transparent test and had a spherical gut.

**Salpinae spp. aggregate zooids** — Nine chains of Salpinae spp. zooids were observed between 502–621 m (13.8–9.3°C, 34.50–34.32, 3.3–2.7 ml $L^{-1}$) outside the caldera, while eight were observed between 269–631 m (18.1–10.5°C, 34.75–34.37, 3.8–2.9 ml $L^{-1}$) inside the caldera. "Salpinae spp. aggregate" chains were straight chains and the zooid guts were spherical, appearing as bright white spots.

**Salpida sp. solitary zooid** — One individual of Salpida sp. was observed at 478 m depth (13.8°C, 34.53, 3.3 ml $L^{-1}$) outside the caldera. "Salpida sp. solitary zooid" possessed a transparent barrel-shaped tunic and had a gill bar that lay obliquely in the middle of the tunic.

***Pyrosoma atlanticum* Péron, 1804** — One colony of *P. atlanticum* was observed at 705 m depth (7.5°C, 34.28, 2.2 ml $L^{-1}$) outside the caldera. *Pyrosoma atlanticum* was a long, finger-shaped colony that had a pinkish colour. No spines/projections occurred around the open end of the colony and the width to length ratio of the colony was less than 0.16.

*Remarks*: size up to 60 cm.

**Pyrosomatidae spp.** — One colony of Pyrosomatidae spp. was observed at 705 m depth (7.5°C, 34.29, 2.2 ml $L^{-1}$) outside the caldera and three were observed between 497–801 m (14.0–10.2°C, 34.50–34.36, 3.4–2.8 ml $L^{-1}$) inside the caldera. Pyrosomatidae spp. colonies were long and cylindrical, colored pinkish, and some colonies could be seen to be tapered into a tip.

## DISCUSSION

### 1. Taxonomic identification based on ROV video records

Identifications of morphotaxa or morphospecies from ROV video records for ecological investigations are usually based on only a few morphological characters, due to priority being given to gathering quantitative data, and observation time per individual is often short. Hence, traditional identification methods, such as the use of hierarchical taxonomic keys, do not always work well. In particular, microscopic analyses are all but impossible. In this respect, in order to assess the pelagic fauna occurring above deep-sea mineral deposits for Environmental Impact Assessments using ROVs, the establishment of a field guide based on morphological characters visible with the naked eye or a lower resolution video camera is a pressing need. In expectation of this future demand, the present study described the morphological and behavioral characters for each taxon that we were able to observe in the ROV video record. As a result, a total of 61 gelatinous zooplankton morphotaxa: 21 ctenophore morphotaxa; 16 siphonophore morphotaxa; 10 hydromedusan morphotaxa; 4 scyphomedusan morphotaxa; 10 thaliacean morphotaxa were observed and recognized. Some of these morphotaxa were higher taxa, based on classical taxonomy, while some morphotaxa were described here independently of the existing, flawed higher taxonomy (e.g., "little ruby" cydippid).

The morphological characters that allow us to identify each morphotaxon in the video record are usually not one, but rather a combination of possession and/or absence of several morphological features. For instance, two genera of lobate ctenophores, *Eurhamphaea* and *Kiyohimea*, both possess two triangular projections on their aboral ends and this character is exceptional among the presently-described

lobate morphotaxa. *Eurhamphaea* also possesses one flexible filament on the distal extreme of each of these projections, while *Kiyohimea* lacks these filaments. On the basis of these two morphological characters alone, combined with the presence of "lobes", we can easily identify these two genera. Although taxonomic identification based on ROV images is not always easy, adopting practical morphological characters for taxon identifications is imperative for conducting ecosystem-level community characterizations into the future. Furthermore, we recommend that care should be taken when preparing taxonomic papers, such as new species descriptions, to include macromorphological characters allowing distinctions between morphotaxa to be made based on video and/or image data alone.

In his description of *Physophora gilmeri*, Pugh described comparative characteristic differences between the new species and *Physophora hydrostatica* in his discussion in a meticulous manner (Pugh 2005). For instance, he described and compared the colours and shapes of the pneumatophores, and colours and shapes of the palpons, etc. Thanks to the comparisons given in the discussion, we were able to clearly distinguish these congeners in the present video records. In another of Pugh's papers, he published photographs of the colonies of each species of the physonect siphonophore *Bargmannia*, along with their descriptions (Pugh 1999). With net-collected samples, siphonophore colonies are invariably broken into pieces and, therefore, most species descriptions of siphonophores have focused on the morphology of different zooid types, with morphological information at the whole colony level rarely being included. However, in accordance with developments concerning *in situ* survey methodologies, more and more image-based investigations are expected to be carried out. Therefore, concrete descriptions of the major

macromorphological characters that are observable from a distance and can serve to distinguish between morphotaxa observed *in situ*, are invaluable.

Amon et. al. (2007a, b) anticipated this need and created an atlas of benthic and benthopelagic megafauna based on the videos and still images recorded by ROVs and Autonomous Underwater Vehicles (AUVs) at the Clarion-Clipperton Zone (CCZ). There are *in situ* photographs and short descriptions of the species for a wide number of morphotaxa. In Japanese waters, there are two seminal papers that include taxonomic notes for identifying gelatinous zooplankton morphotaxa *in situ*. Toyokawa (1998) gave notes on a total of 14 morphotaxa of cnidarians and ctenophores using the human-occupied submersible vehicle *Shinkai 2000*, while Lindsay et al. (2015) described a total of 28 cnidarian, ctenophoran and appendicularian morphotaxa based on the video record from the ROV *Hyper-Dolphin*. The present study adds to this legacy.

**2. High gelatinous zooplankton concentrations in deep-sea calderas: ecological comparison**

In the present study, the numbers of gelatinous zooplankton morphotaxa observed outside and inside the caldera were 39 (n = 106) vs. 41 (n = 124) respectively, while the total time of observation was 140 vs. 109 min. Despite the observation time inside the caldera being 30 minutes shorter than outside, the number of observed morphotaxa was approximately equal to or higher, and the number of observed individuals was higher, inside the caldera. In particular, large numbers of three gelatinous zooplankton morphotaxa, Lobata sp. "Boli" (ctenophore), undescribed Lobata "No auricles" (ctenophore) and *Earleria bruuni* (Leptomedusae),

were observed inside the Sumisu Caldera. "Boli" occurred both inside and outside the caldera, but was most highly abundant inside the caldera in the 300–450 m depth stratum, which is somewhat deeper than the caldera rim (about 200 to 450 m depth). In contrast, "No auricles" was abundant just above the caldera floor in the depth range from 826 to 864 m. The distribution of *E. bruuni* was extremely concentrated with most individuals observed at 700–750 m depth. In Chapter 2, another similar ROV survey was conducted at a hydrothermally inactive deep-sea caldera (Kurose Hole), 218 km north of Sumisu Caldera, on 24 September 2000, and also reported high population densities of *E. bruuni* only inside the caldera. In that study, however, high concentrations of lobate ctenophores were not observed. In that previous study, the number of gelatinous zooplankton taxa observed outside and inside the caldera were 23 (n = 38) vs. 10 (n = 69) respectively, while the total time of observations was about 43 min both outside and inside. Similarly in both studies, the calderas were filled with an isothermic warm water-mass at a temperature of more than 10˚C. Kurose Hole possesses a shallow rim (107 m depth), while the rim of the Sumisu Caldera possesses channels at around 200-450 m depth. The most different feature between the calderas is the existence (Sumisu) or not (Kurose) of an active hydrothermal vent with associated chemosynthetic ecosystems.

Taking into account the two studies described above (this study and Chapter 2), three different hypotheses can be proposed as to why gelatinous zooplankton were present at high concentrations inside but not outside these deep-sea calderas. Firstly, blooming of *E. bruuni* was not a seasonal event (September at Kurose Hole, March at Sumisu Caldera), and it may be a 'normal' phenomenon in these two deep-sea calderas. As suggested in Chapter 2, *E. bruuni* seems to favor deep isolated water

masses, though the occurrence of *E. bruuni* was not restricted to near the caldera floor in the present study. In Chapter 2, it is hypothesized that steep-walled concave topography, such as calderas and deep-sea canyons, should concentrate food resources (i.e. sinking particles and vertically migrating plankton) with depth, hence blooming of *E. bruuni* was in the near-bottom layer where food should be most concentrated. In the Sumisu Caldera, this species was found in large numbers at the depth of active venting and therefore, presumably, where food concentrations (e.g., vent larvae, organic flocs, etc.) should be greatest.

Secondly, individuals belonging to the taxa Lobata sp. "Boli" were highly abundant just below the depth of the rim of the Sumisu Caldera, but were also observed outside the caldera at shallower depths. This animal was not observed just north of this area at the Kurose Hole on 24 September 2000 (Chapter 2). This difference may be due to "Boli" blooming seasonally and being trapped by the caldera, leading to higher local concentrations.

Thirdly, large numbers of an undescribed Lobata morphotaxa "No auricles" were only observed inside the hydrothermally-active Sumisu Caldera near the bottom. A similar morphotype of Lobata was observed around the Hatoma Knoll hydrothermal vent by Lindsay et al. (2015). This suggests that this morphotaxa may be favorably disposed to near-vent environments. The Sumisu Caldera contains chemosynthetic biological communities, including vestimentiferan tubeworms, mussels, sponges, and so on (Nishijima et al. 2010), thus these ctenophores could possibly consume the presumably abundant eggs and/or larvae of these invertebrates or be feeding directly on vent bacterial flocs sinking into the caldera basin.

Burd & Thomson (1994, 2000, 2015) examined the relationships between hydrothermal vents and zooplankton abundance, biomass, and productivity. According to their results, productivity over the total water column is highest in the regions surrounding hydrothermal vent sites. Not only gelatinous zooplankton, but also other taxa (e.g., copepods, amphipods, chaetognaths), have enhanced biomass throughout the entire water column above hydrothermal venting sites and shallow populations can exist at deeper depths (Burd & Thomson 1994, 2000, 2015). Burd & Thomson (2000) emphasized the relative importance of medusae above hydrothermal vents, however, their research was mainly based on net-sampled specimens, and the biomass and abundances of extremely fragile gelatinous zooplankton would still be underestimated. Deep-sea calderas are semi-closed environments. This indicates that the influence of high chemosynthetic primary productivity should be more potent than at other vent sites and that they may also act as a topological "trap" entraining plankton within their environs.

**3. Hypothetical food-web in a hydrothermally-active caldera**

The narcomedusa *Solmissus incisa* s.l. is a well-known predator of gelatinous zooplankton (e.g. Raskoff 2002, Choy et al. 2017). During the present study, we also observed two *S. incisa* s.l. that had ingested a salp chain and a narcomedusa, respectively (details described in Hidaka-Umetsu & Lindsay 2018).

The abundant filter-feeding thaliaceans that occurred in the area (Fig. 30) could be important prey for co-occurring *S. incisa* s.l.. Indeed, when these filter feeders were abundant and distributed over a wide depth range inside the caldera (Fig. 30), *S.*

*incisa* s.l. was also widely distributed and abundant (Fig. 29), compared to outside the caldera. It is entirely plausible that heightened productivity from both upwelling and chemosynthetic sources, combined with the concentration of sinking particles constrained by the funnel-like topology of calderas and entrainment of ascending particles from hydrothermal vents through turbulent mixing (Chapter 2), could stimulate sustained blooming of both filter-feeding thaliaceans and their predators around active submarine calderas, thereby also acting as hotspots for other predators of gelatinous zooplankton, including fish and other taxa.

## CONCLUSIONS

Remotely-Operated Vehicle (ROV) investigations allow direct *in situ* observations of zooplankton in their natural state and also make investigation of topologically challenging areas for plankton-net surveys, such as closed calderas and canyons, possible. The present study provided information about the detailed distribution of abundant gelatinous zooplankton in a hydrothermally active deep-sea caldera, giving notes on morphological characters able to be identified in the video record and outlining methodological treatment of these data. Some information allowing us to discuss the possible ecology of submarine calderas was also acquired. ROVs can be a powerful tool for the investigation of gelatinous macrozooplankton and, given the high abundances of these gelatinous organisms at the studied sites, should be an integral part of any baseline studies for environmental impact assessments of areas where deep-sea mining is proposed and, indeed, for the entirety of the vast global pelagic zone.

**REFERENCES**

Amon DJ, Ziegler AF, Drazen JC, Grischenko AV, Leitner AB, Lindsay DJ, Voight JR, Wicksten MK, Young CM, Smith CR (2017a) Megafauna of the UKSRL exploration contract area and eastern Clarion-Clipperton Zone in the Pacific Ocean: Annelida, Arthropoda, Bryozoa, Chordata, Ctenophora, Mollusca. Biodiv Data J 5:e14598. doi: 10.3897/BDJ.5.e14598.

Amon DJ, Ziegler AF, Kremenetskaia A, Mah CL, Mooi R, O'Hara T, Pawson DL, Roux M, Smith CR (2017b) Megafauna of the UKSRL exploration contract area and eastern Clarion-Clipperton Zone in the Pacific Ocean: Echinodermata. Biodiv Data J 5: e11794. doi: 10.3897/BDJ.5.e11794.

Berg CJ, Van Dover CL (1987) Benthopelagic macrozooplankton communities at and near deep-sea hydrothermal vents in the eastern Pacific Ocean and the Gulf of California. Deep-Sea Res Part A 34(3): 379-401.

Bouillon J, Gravili C, Pagès F, Gili J M, Boero F (2006). An introduction to Hydrozoa. ISBN 2-85653-580-1. Muséum national d'Histoire naturelle, Paris, 591 pp.

Burd BJ, Thomson RE, Jamieson GS (1992) Composition of a deep scattering layer overlying a mid-ocean ridge hydrothermal plume. Mar Biol 113: 517–526.

Burd BJ, Thomson RE (1994) Hydrothermal venting at Endeavour Ridge: effect on

zooplankton biomass throughout the water column. Deep-Sea Res Part I 41(9): 1407–1423.

Burd BJ, Thomson RE (2000) Distribution and relative importance of jellyfish in a region of hydrothermal venting. Deep-Sea Res Part I 47: 1703–1721.

Burd BJ, Thomson RE (2015) The importance of hydrothermal venting to water-column secondary production in the northeast Pacific. Deep-Sea Res Part II 121: 85–94.

Choy CA, Haddock SHD, Robison BH (2017) Deep pelagic food web structure as revealed by in situ feeding observations. Proc R Soc B 284: 20172116. http://dx.doi.org/10.1098/rspb.2017.2116

Chun C (1898) Die ctenophoren der Plankton-Expedition. Ergebnisse der Plankton-Expedition der Humboldt-Stifung. 2. K.a.:1-32.

Hidaka-Umetsu M, Lindsay DJ (2017) Comparative ROV surveys reveal jellyfish blooming in a deep-sea caldera: the first report of *Earleria bruuni* from the Pacific Ocean. J Mar Biol Ass UK, 1-11. doi:10.1017/S0025315417001540.

Hidaka-Umetsu M, Lindsay DJ (2018) First record of the mesopelagic narcomedusan genus *Solmissus* ingesting a fish, with notes on morphotype diversity in *S. incisa* (Fewkes, 1886). Plankton Benthos Res 13(2): 41-45.

Horita T, Akiyama H, Kubota S (2011) *Bathocyroe longigula* spec. nov., an undescribed ctenophore (Lobata: Bathocyroidae) from the epipelagic fauna of Japanese coastal waters. Zool Med Leiden 85(15): 877–886.

Iwabuchi Y (1999) Sumisu Caldera. JAMSTEC J Deep Sea Res 15: 83–94.

Japan Coast Guard (2018) Marine Volcano Database (in Japanese). Available at: http://www1.kaiho.mlit.go.jp/GIJUTSUKOKUSAI/kaiikiDB/kaiyo15-2.htm (accessed on 11 April 2018)

Kitamura M (2008) Chapter 30, Urochordata. In: Deep-sea Life – Biological observations using research submersibles. (eds Fujikura K, Okutani T, Maruyama T) ISBN 978-4-486-01787-5. Tokai University Press, Kanagawa, pp. 351–355. (in Japanese)

Kitamura M, Miyake H, Lindsay DJ (2008) Chapter 24, Cnidaria. In: Deep-sea Life – Biological observations using research submersibles. (eds Fujikura K, Okutani T, Maruyama T) ISBN 978-4-486-01787-5. Tokai University Press, Kanagawa, pp. 295–320. (in Japanese)

Kitamura M, Miyake H, Lindsay DJ, Horita T (2008) Chapter 25, Ctenophora. In: Deep-sea Life – Biological observations using research submersibles. (eds Fujikura

K, Okutani T, Maruyama T) ISBN 978-4-486-01787-5. Tokai University Press, Kanagawa, pp. 321–328. (in Japanese)

Licandro P, Carré C, Lindsay DJ (2017) Cnidaria: Colonial Hydrozoa (Siphonophorae). In: Marine Plankton: A Practical Guide to Ecology, Methodology, and Taxonomy. (eds Castellani C, Edwards M) ISBN 978-0-19-923326-7. Oxford University Press, Great Claredon Street, Oxford, pp. 232–250.

Licandro P, Fischer A, Lindsay DJ (2017) Cnidaria: Scyphozoa and Non-colonial Hydrozoa. In: Marine Plankton: A Practical Guide to Ecology, Methodology, and Taxonomy. (eds Castellani C, Edwards M) ISBN 978-0-19-923326-7. Oxford University Press, Great Claredon Street, Oxford, pp. 198–231.

Licandro P, Lindsay DJ (2017) Ctenophora. In: Marine Plankton: A Practical Guide to Ecology, Methodology, and Taxonomy. (eds Castellani C, Edwards M) ISBN 978-0-19-923326-7. Oxford University Press, Great Claredon Street, Oxford, pp. 251–263.

Lindsay DJ (2005) Planktonic communities below 2000 m depth. Bull Plankton Soc Japan 52(2): 113–118. (in Japanese)

Lindsay DJ, Hunt JC (2005) Biodiversity in midwater cnidarians and ctenophores: submersible-based results from deep-water bays in the Japan Sea and north-western Pacific. J Mar Biol Ass UK 85: 503–517.

Lindsay DJ, Miyake H (2007) A novel benthopelagic ctenophore from 7,217 m depth in the Ryukyu Trench, Japan, with notes on the taxonomy of deep-sea cydippids. Plankton Benthos Res 2(2): 98–102.

Lindsay DJ, Miyake H (2009) A checklist of midwater cnidarians and ctenophores from Japanese waters: species sampled during submersible surveys from 1993–2008 with notes on their taxonomy. Kaiyo Monthly 41(8): 417–438. (in Japanese)

Lindsay D, Umetsu M, Grossmann M, Miyake H, Yamamoto H (2015) Chapter 51, The gelatinous macroplankton community at the Hatoma Knoll hydrothermal vent. In: Subseafloor biosphere linked to hydrothermal systems: TAIGA Concept (eds Ishibashi J, Okino K, Sunamura M). ISBN 978-4-431-54864-5, Springer, Tokyo, pp. 639–666. DOI 10.1007/978-4-431-54865-2_51.

Madin LP, Harbison GR (1978) *Bathocyroe fosteri* gen. nov., sp. nov.: a mesopelagic ctenophore observed and collected from a submersible. J Mar Biol Ass UK 58: 559–564.

Mills CE (2017) Phylum Ctenophora: List of all valid species names. Available at: https://faculty.washington.edu/cemills/Ctenolist.html (accessed on 26 October 2017)

Mills CE, Haddock SHD (2007) Ctenophores. In: Light and Smith's Manual: Intertidal Invertebrates of the Central California Coast. Fourth Edition (ed Carlton JT). University of California Press, Berkeley, pp. 189-199.

Minemizu R, Kubota S, Hirano Y, Lindsay D (2015) A Photographic Guide to the Jellyfishes of Japan. Heibonsha, Tokyo 358 pp. (in Japanese)

Nishijima M, Lindsay DJ, Hata J, Nakamura A, Kasai H, Ise Y, Fisher C, Fujiwara Y, Kawato M, Maruyama T (2010) Association of Thioautotrophic Bacteria with Deep-sea Sponges. Mar Biotech 12: 253–260.

Nishikawa J (1997) Class Thaliacea. In: An Illustrated Guide to Marine Plankton in Japan. (eds Chihara M, Murano M) Tokai University Press, Tomigaya, Shibuya-ku, Tokyo, pp. 1351-1392. (in Japanese)

Oliveira OMP, Migotto AE (2006) Pelagic ctenophores from the São Sebastião Channel, southeastern Brazil. Zootaxa 1183:1–26.

Podar M, Haddock SHD, Sogin ML, Harbison GR (2001) A molecular phylogenetic framework for the phylum Ctenophora using 18S rRNA genes. Mol Phylogenetics Evol 2(2): 218–230.

Pugh PR (1999) A review of the genus *Bargmannia* Totton, 1954 (Siphonophorae, Physonectae, Pyrostephidae). Bull Nat Hist Mus Lond 65(1): 51–72.

Pugh PR (2003) A revision of the family Forskaliidae (Siphonophora, Physonectae). J Nat Hist 37:1281–1327.

Pugh PR (2005) A new species of *Physophora* (Siphonophora: Physonectae: Physophoridae) from the North Atlantic, with comments on related species. Syst Biodiversity 2(3): 251-270.

Raskoff KA (2002) Foraging, prey capture, and gut contents of the mesopelagic narcomedusa *Solmissus* spp. (Cnidaria: Hydrozoa) Mar Biol 141: 1099–1107.

Reid JL (1965) Intermediate waters of the Pacific Ocean. The Johns Hopkins Oceanographic Studies Number 2. Johns Hopkins Press, Baltimore, 85 pp.

Sars M (1846) Fauna littoralis Norvegiae oder Beschreibung und Abbildungen neuer oder wenig bekannten Seethiere, nebst Beobachtungen über die Organisation, Lebensweise und Entwickelung derselben. Heft I Johann Dahl, Christiania, Denmark, 94 pp

Toyokawa M, Toda T, Kikuchi T, Nishida S (1998) Cnidarians and ctenophores observed from the manned submersible *Shinkai 2000* in the midwater of Sagami Bay, Pacific coast of Japan. Plank Biol Ecol 45: 61–74.

Vinogradov GM, Vereshchaka AL, Aleinik DL (2003) Zooplankton distribution over

hydrothermal fields of the Mid-Atlantic Ridge. Oceanology 43(5): 656–669.

Wrobel D, Mills C (1998) Pacific Coast Pelagic Invertebrates: A Guide to the Common Gelatinous Animals. Sea Challengers and the Monterey Bay Aquarium, Monterey, California, 108 pp.

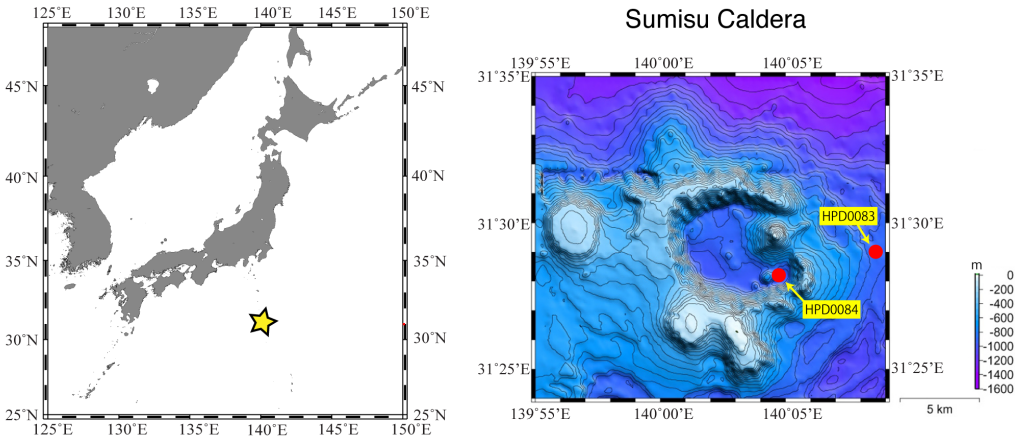


Fig. 24. Dive locations.

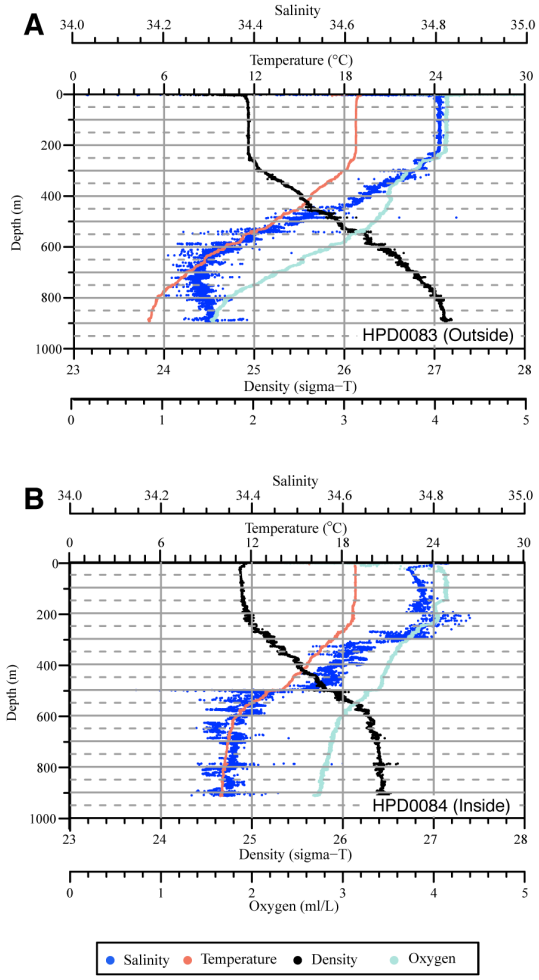


Fig. 25. Vertical profiles of temperature, salinity, oxygen and density vs depth. (A) HPD0083, (B) HPD0084.

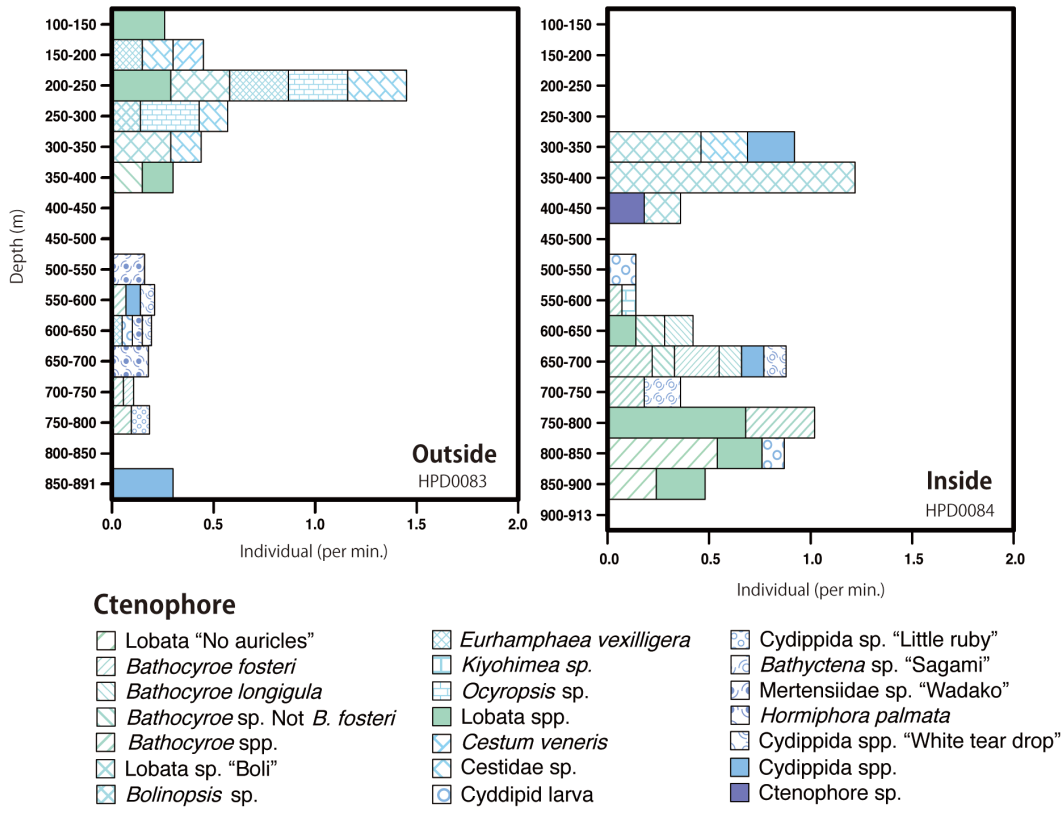


Fig. 26. Comparative vertical distribution of ctenophores for each 50-m depth stratum outside and inside the Sumisu Caldera.

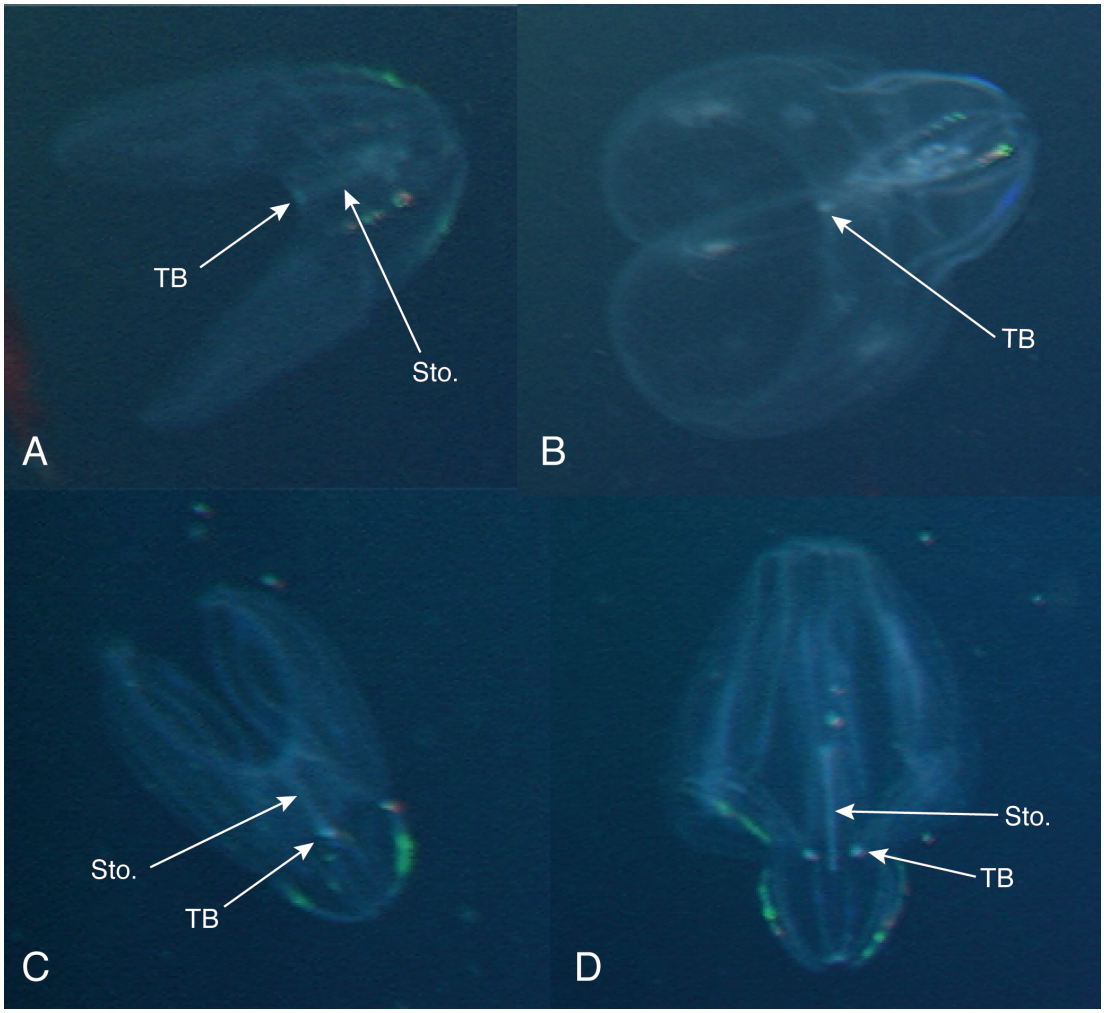


Fig. 27. Frame grabs of two lobate ctenophores Undescribed Lobata "No auricles" (A, B) and *Bathocyroe longigula* (C, D). Tb: tentacle bulb, Sto: Stomodaeum.

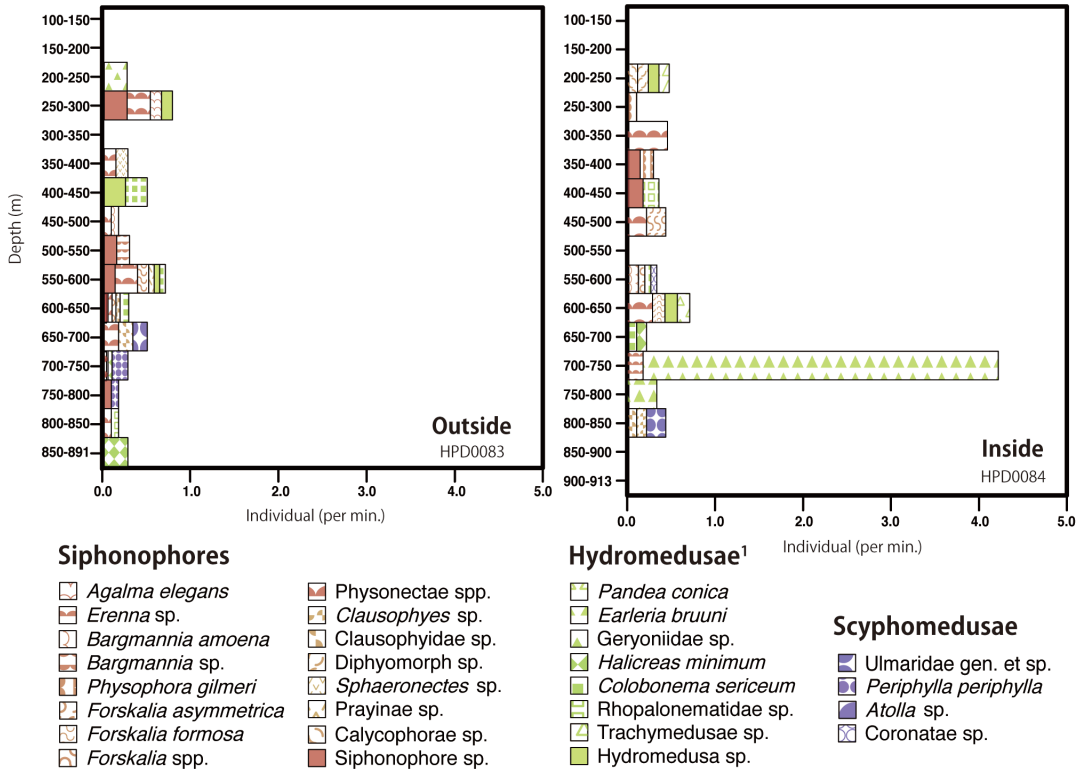


Fig. 28. Comparative vertical distribution of cnidarian jellyfishes for each 50-m depth stratum outside and inside the Sumisu caldera, excluding Narcomedusae.

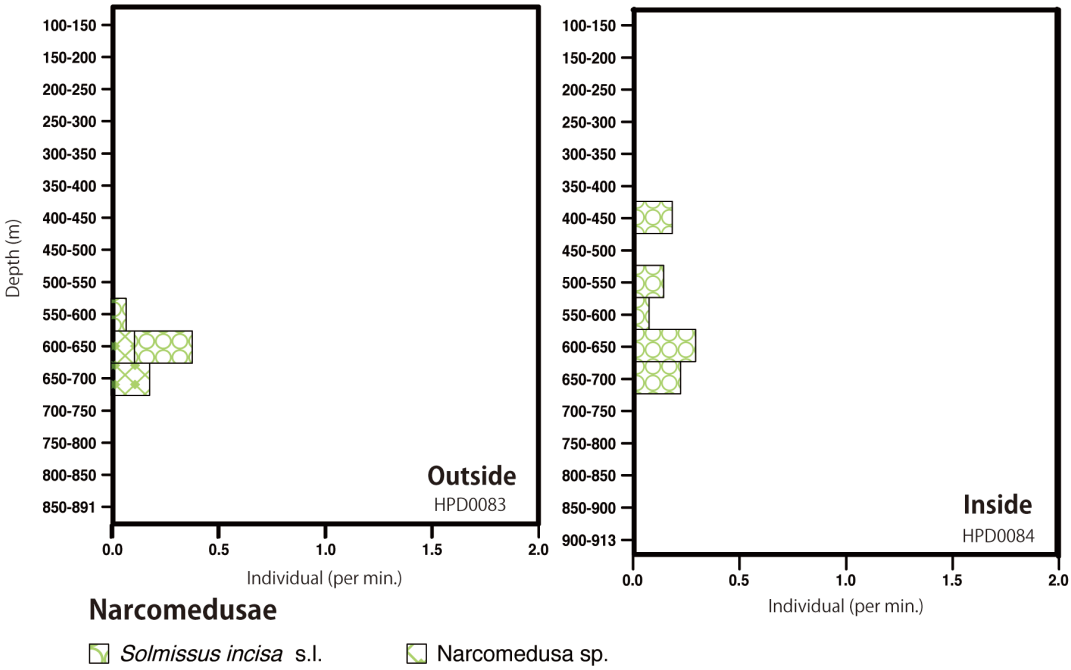


Fig. 29. Comparative vertical distribution of Narcomedusae for each 50-m depth stratum outside and inside the Sumisu caldera.

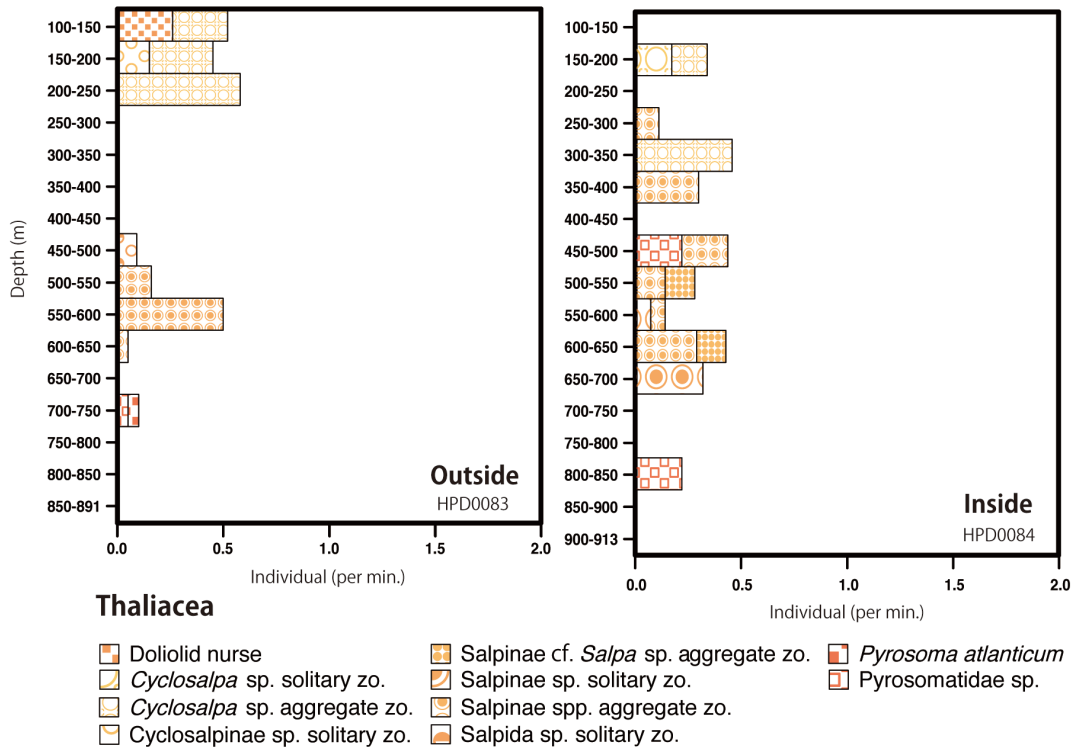


Fig. 30. Comparative vertical distribution of Thaliacea for each 50-m depth stratum outside and inside the Sumisu caldera.

Table. 2. The observation time for each 50-m depth stratum.

| HPD0083 (Outside) | | HPD0084 (Inside) | |
|---|---|---|---|
| Depth range (m) | Obs. Time (min.) | Depth range (m) | Obs. Time (min.) |
| 100-150 | 3.88 | 100-150 | 2.83 |
| 150-200 | 6.63 | 150-200 | 5.85 |
| 200-250 | 3.47 | 200-250 | 8.20 |
| 250-300 | 6.93 | 250-300 | 8.80 |
| 300-350 | 6.82 | 300-350 | 4.38 |
| 350-400 | 6.80 | 350-400 | 6.57 |
| 400-450 | 3.65 | 400-450 | 5.42 |
| 450-500 | 10.98 | 450-500 | 4.48 |
| 500-550 | 6.23 | 500-550 | 7.30 |
| 550-600 | 14.07 | 550-600 | 14.97 |
| 600-650 | 18.70 | 600-650 | 7.00 |
| 650-700 | 5.42 | 650-700 | 9.28 |
| 700-750 | 20.50 | 700-750 | 5.45 |
| 750-800 | 10.98 | 750-800 | 2.95 |
| 800-850 | 11.73 | 800-850 | 9.27 |
| 850-891 | 3.30 | 850-900 | 4.08 |
| - | - | 900-913 | 2.22 |

# General Discussion

## GELATINOUS ZOOPLANKTON AROUND THE IZU-BONIN ARC

A total of 109 gelatinous zooplankton morphotaxa were observed in the present study and their biodiversity and vertical distribution were revealed at three research sites on the Izu-Bonin Arc. This is noteworthy, novel knowledge about the gelatinous zooplankton communities at these sites. Four common species and two restricted species were identifiable, as described in below, and their habitats are described in Table 3. *Colobonema sericeum* (Hydromedusae) was characterised as the most common species without a doubt in the present study because it was observed during every dive (6 dives) and the habitat environments were quite varied, with temperatures from 4.9 to 14.6˚C, salinities 34.22–34.51 and depths 405–663 m. In addition, *Solmissus incisa* s.l. (Hydromedusae) and *Forskalia asymmetrica* (Siphonophora) were observed during 5 of the 6 dives, at temperatures of 4.1 to 14.7˚C (34.06–34.58, 352–758 m depth) and 4.8 to 14.1 ˚C (34.25–34.52, 469–631 m depth), respectively. *Bathocyroe fosteri* (Ctenophora) was observed during 4 of the 6 dives, at temperatures between 7.4 and 12.3 ˚C (34.14–34.41, 471–716 m depth). These four species were all distributed both inside and outside calderas, and they can be considered as common species at the study sites. By contrast, *Periphylla periphylla* was only observed outside calderas at water temperatures between 4.3–7.5˚C (34.29–34.32, 669–751 m depth), with it also having been reported from cold-water regions all over the world (e.g. Youngbluth and Båmstedt 2001, Lindsay et al 2004). *Earleria bruuni* was only observed within the warm-water masses inside the two calderas (10.2–11.3˚C, 34.34–34.40, 612–769 m depth). The above indicates

that some species are widely adapted to relatively varied physico-chemical conditions, while other species are restricted to relatively high or low water temperatures, even in essentially the same ecoregion. This is an important observation by the present study because water masses with extremely different water conditions (especially warm and cold) at similar depths are usually a long way from each other in the open ocean, with some notable exceptions such as the Sulu Sea and Celebes Sea (Grossmann et al. 2015). This implies that the Izu-Bonin Arc is an optimal region for investigating thermal adaptations and habitat preferences of gelatinous zooplankton.

## CALDERAS AS HABITATS FOR GELATINOUS ZOOPLANKTON

Four comparative ROV dives, which were conducted inside and outside inactive (Chapter 2, Kurose Hole) and active (Chapter 3, Sumisu Caldera) calderas made it possible to compare the biodiversities in four different environmental regimes in relation to the gelatinous zooplankton community. When comparing the number of taxa divided by the number of observed individuals, the value inside the inactive caldera was extremely low (0.14), compared to inside the active caldera (0.33), with outside the active caldera (0.39) and outside the inactive caldera (0.60) following (pie-graph of biodiversity inside and outside Sumisu Caldera is illustrated in Fig. 31). However, the total observation time divided by the counted number of individuals was lowest inside the inactive caldera (0.62), compared to inside the active caldera (0.87), outside the inactive caldera (1.13) and outside the active caldera (1.32). The former index can be considered as an index of biodiversity, and the latter index indicates the population density of gelatinous zooplankton.

According to these indices, biodiversity is relatively lower inside the calderas, but the concentrations of gelatinous zooplankton were higher inside the calderas, with this phenomenon being especially pronounced in the inactive caldera. Discussion about the considerably higher population densities of gelatinous zooplankton inside both the Kurose Hole and the Sumisu Caldera was introduced in Chapters 2 and 3; therefore this section chiefly discusses the diversities of the gelatinous zooplankton.

The diversity of gelatinous zooplankton was low within the uniform warm water masses inside the calderas, while higher diversities were observed outside the calderas where water column physico-chemical parameters varied to a greater degree (warm to cold) through the entire water column from the surface to the bottom (Figs. 19, 25). These results indicate that higher variability in water column physico-chemical parameters could result in a more diverse gelatinous zooplankton community, and this could be one of the reasons why gelatinous zooplankton diversity was high outside the two calderas (Kurose Hole and Sumisu Caldera).

From the point of view of their geology/topography, the inactive caldera of the "Kurose Hole" possesses a shallower caldera rim than the active Sumisu Caldera, and it also lacks channels like in the Sumisu Caldera (Fig 32), so the closedness of the caldera is much higher. Therefore, it is easily imagined that for deep-living species of gelatinous zooplankton it is harder to enter the inside of the Kurose Hole than the inside of the Sumisu Caldera, even if they ontogenetically or/and daily migrate vertically. This could be one of the reasons that the diversity of gelatinous zooplankton was much lower inside the Kurose Hole than anywhere else. Indeed, a corroborative research result backing up this hypothesis has been reported by Grossmann et al. (2015), comparing the gelatinous zooplankton communities

between the Sulu Sea and the Celebes Sea. The Sulu Sea is an isolated sea with shallow sills, while the Celebes Sea is linked to the Java, Molucca and Philippine Seas by deep channels. The hydrographic and geological/topological situation of the Sulu Sea is similar to the Kurose Hole, although it is at a much greater scale, with respect to being an isolated ocean with water conditions constant from 400 m to 1000 m depth and temperature at 10 ˚C (salinity, 34.50). Contrastingly, water temperature in the Celebes Sea gradually changed from 15.7 to 4.8 ˚C with depth. According to Grossmann et al. (2015), species richness was much lower inside the Sulu Sea than in the Celebes Sea and mature, cold-water species were absent inside the Sulu Sea. Furthermore, the authors also refer to the high water temperatures of the Sulu Sea at depth preventing colonization by cold-water species, even if the larvae were physically able to enter. This should also be the case with the area investigated in the present study.

To sustain a diverse gelatinous zooplankton community, variation in food resources should also be important. Therefore, the vertical distribution of gelatinous zooplankton inside and outside Kurose Hole and Sumisu Caldera, split by feeding types, were graphed in Figure 33. Crustacean-feeders and larva-feeders were widely observed at all dive locations. Filter-feeders and gelatinous zooplankton-feeders were absent inside the Kurose Hole, although they were present inside the Sumisu Caldera. This suggests that food diversity was much higher inside the Sumisu Caldera than in the Kurose Hole. In addition, hydrothermal vents could provide a greater amount and variety of food resources for the gelatinous zooplankton as discussed in Chapter 3, and this might also contribute to the greater diversity of predatory gelatinous zooplankton inside the Sumisu Caldera.

Based on the above, it is inferred that the "closedness" of a caldera is the principal factor that regulates the diversity of gelatinous zooplankton when comparing two different calderas, because it is directly linked to the diversity of water column habitats and linkages to immigrating populations – ie. the more closed the caldera, the lower the variability in water column habitats and the weaker the linkages to populations outside, also resulting in low diversity of food resources. Consequently, calderas would presumably be a harsh environment for the majority of deep-sea gelatinous zooplankton taxa.

## IMPORTANCE OF KEYS FOR TAXONOMIC IDENTIFICATION BASED ON IN-SITU IMAGES

By using in-situ images, new habitat records for 109 gelatinous zooplankton morphotaxa have been provided from the Izu-Bonin Arc in the present study. This clearly demonstrates how useful ROV in-situ image-based studies are for characterizing the gelatinous zooplankton fauna. However, colonial gelatinous zooplankton such as siphonophores and pyrosomes were usually only identifiable to higher taxa with respect to taxonomic identification during the present study, probably because of the general lack of published information regarding their colony morphology. Even in other taxa, when they were moving around or were too far away, they were also difficult to identify to lower taxonomic groups. To exponentially increase knowledge about their ecology based on captured stills or video images from ROVs, an innovative characterization approach for their species identification needs to be established, instead of relying on traditional taxonomic keys, in order to maximize the utilisation of archived ROV dive records.

Involving "Artificial Intelligence (AI)" and "Citizen Science (CS)" into the image analyses should provide powerful driving forces for future ROV image-based research. These two methods seem completely different, dealing with machines and humans, but both can be complementary and therefore provide us vastly better performance to deal with "big data" than a single researcher alone. In fact, both methods have already been introduced to identify terrestrial wild animals (Willi et al. 2019). To establish a classification key for the gelatinous zooplankton species usable for these new methods, interpretation by human engineering and machine engineering would be required. Colony morphology, behavioural morphology and/or three-dimensional information provided by video data would presumably play a crucial role to help distinguish each taxon.

**REFERENCES**

Grossmann MM, Nishikawa J, Lindsay DJ (2015) Diversity and community structure of pelagic cnidarians in the Celebes and Sulu Seas, southeast Asian tropical marginal seas. Deep-Sea Res I 100: 54–63. doi:10.1016/j.dsr.2015.02.005.

Lindsay DJ, Furushima Y, Miyake H, Kitamura M, Hunt JC (2004) The scyphomedusan fauna of the Japan Trench: preliminary results from a remotely-operated vehicle. Hydrobiologia 530/531: 537–547.

Willi M, Pitman RT, Cardoso AW, Locke C, Swanson A, Boyer A, Veldthuis M, Fortson L (2019) Identifying animal species in camera trap images using deep

learning and citizen science. Methods Ecol Evol, 10: 80-91

Youngbluth MJ, Båmstedt U (2001) Distribution, abundance, behavior and metabolism of *Periphylla periphylla*, a mesopelagic coronate medusa in a Norwegian fjord. Hydrobiologia, 451: 321-333.

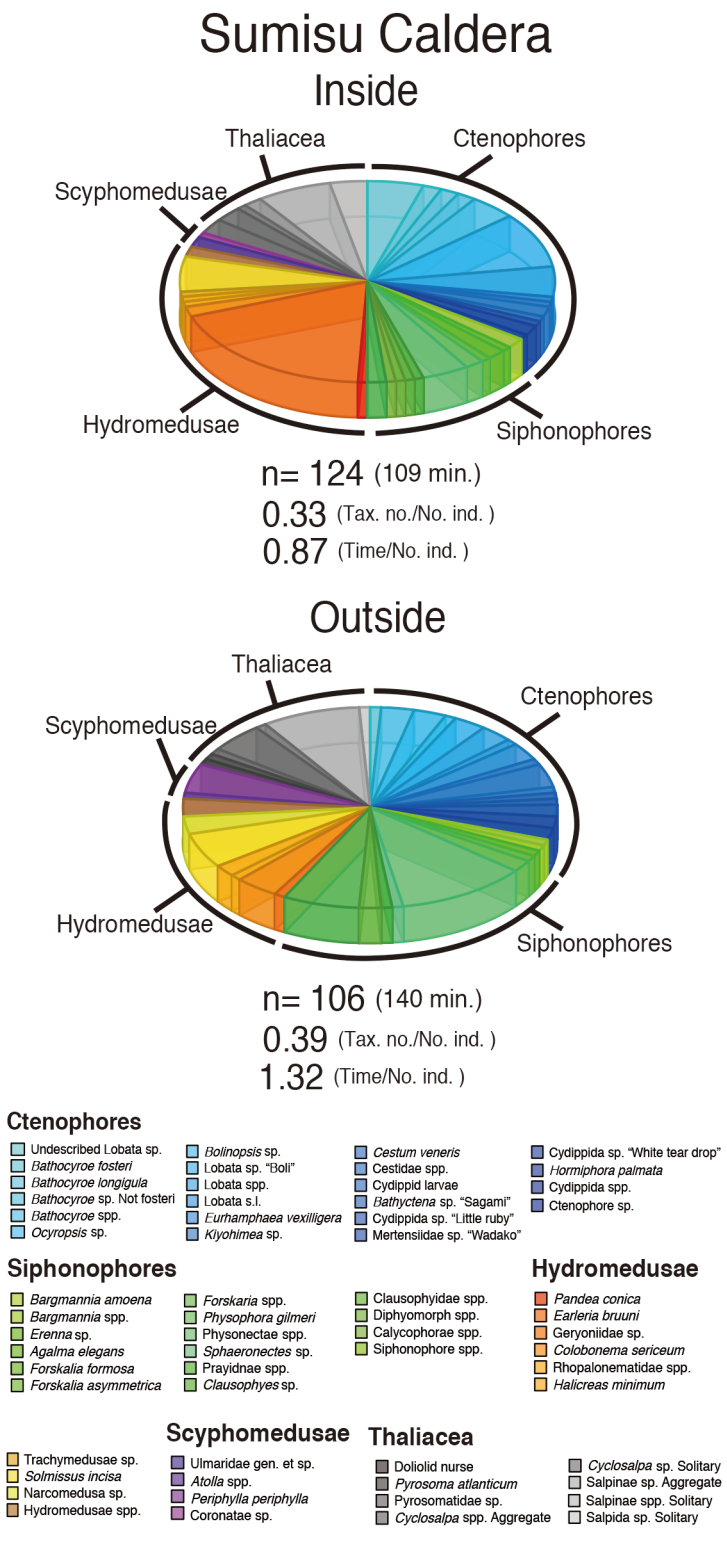


Fig. 31. Pie graphs comparing taxon richness and evenness of macrozooplankton between dives outside (HPD0083) and inside (HPD0084) the Sumisu Caldera.

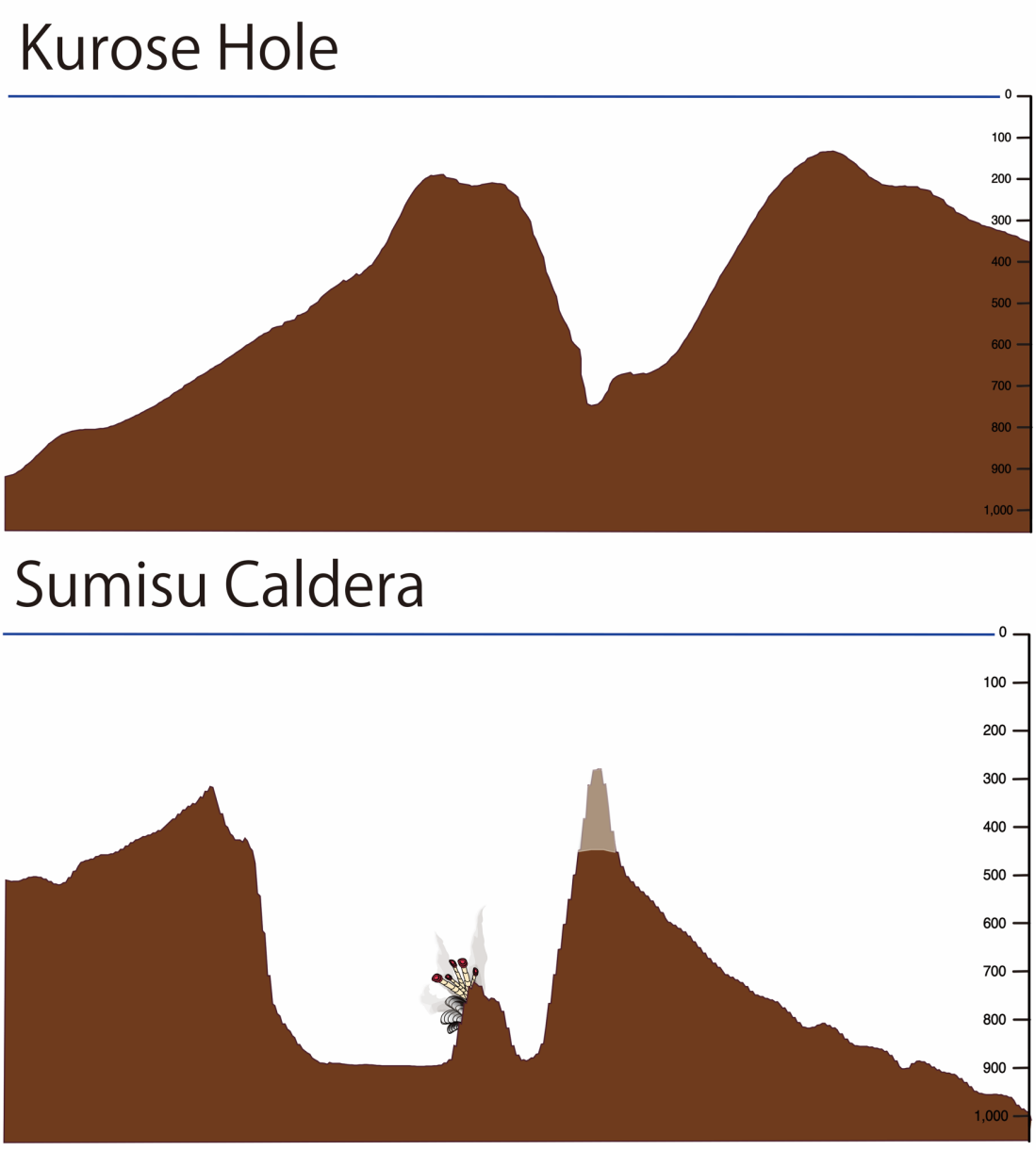


Fig. 32. The topological schematics of the Kurose Hole and the Sumisu Caldera.

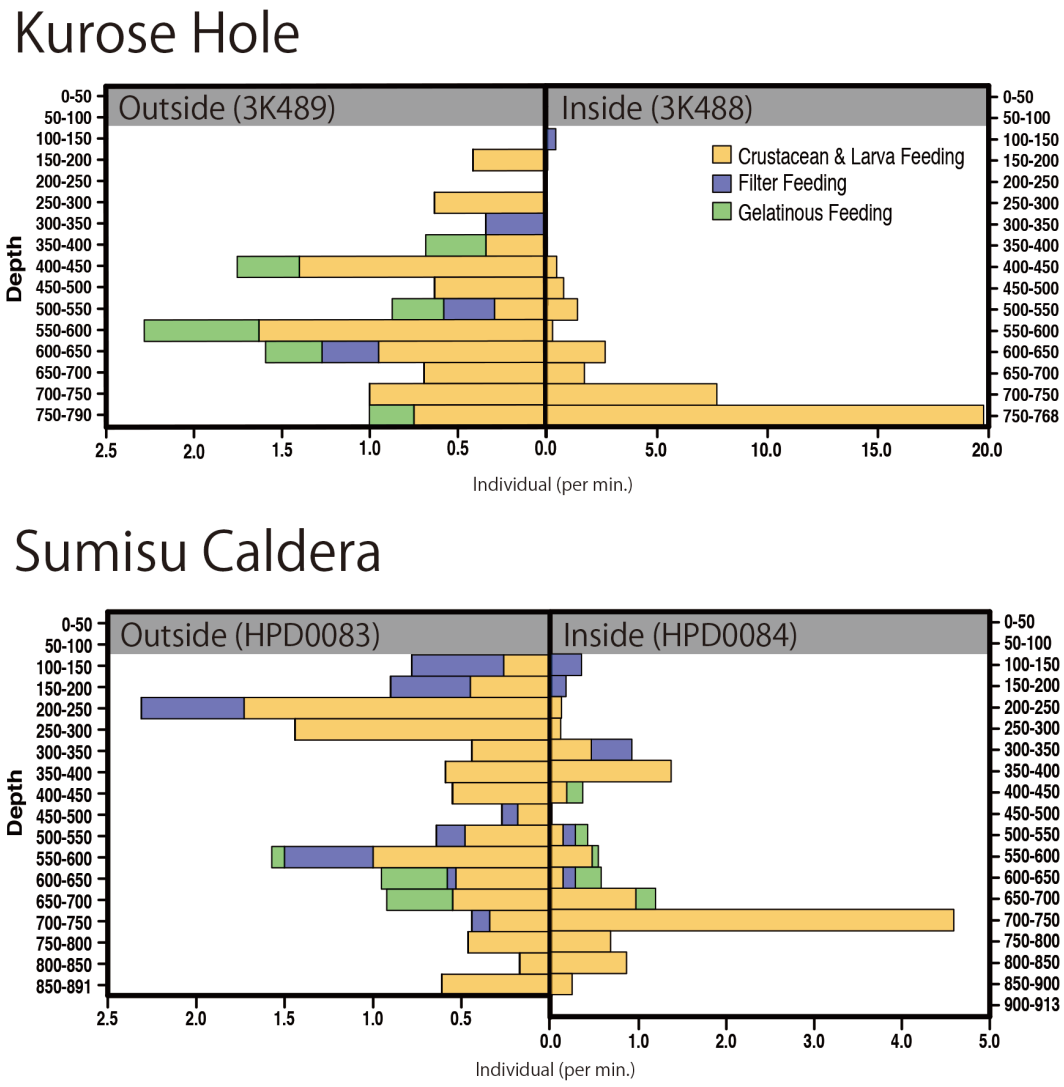


Fig. 33. Vertical distribution of gelatinous zooplankton sorted by feeding types. Orange: Crustacean- and larva-feeding, Blue: Filter-feeding, Green: Gelatinous zooplankton-feeding. Above: the Kurose Hole, Below: the Sumisu Caldera

Table. 3. List of the common species and the restricted species and their habitat environment.

**Common Species**

| ***Colobonema sericeum*** | Kurose Hole | | Kaikata Seamount | | Sumisu Caldera | |
|---|---|---|---|---|---|---|
| Dives | 3K488 (Inside) | 3K489 (Outside) | HPD0081 (Outside) | HPD0082 | HPD0083 (Outside) | HPD0084 (Inside) |
| Depth (m) | 491–649 | 584, 606 | 477–525 | 405, 470 | 468–644 | 581, 663 |
| Temperature (˚C) | 11.2–11.8 | 5.5, 4.9 | *9.1–10.3 | 14.6, 12.4 | 14.2–8.7 | 11.2, 10.6 |
| Salinity | 34.39–34.41 | 34.22, 34.24 | *34.18–34.27 | 34.60, 34.43 | 34.51–34.29 | 34.39, 34.32 |

| ***Solmissus incisa s.l.*** | Kurose Hole | | Kaikata Seamount | | Sumisu Caldera | |
|---|---|---|---|---|---|---|
| Dives | 3K488 (Inside) | 3K489 (Outside) | HPD0081 (Outside) | HPD0082 | HPD0083 (Outside) | HPD0084 (Inside) |
| Depth (m) | – | 352–758 | 497–574 | 469 | 578–614 | 448–688 |
| Temperature (˚C) | – | 4.1–9.7 | *9.28–11.89 | 12.9 | 9.6–11.1 | 10.5–14.7 |
| Salinity | – | 34.06–34.33 | *34.23–34.35 | 34.43 | 34.32–34.37 | 34.35–34.58 |

| ***Forskalia asymmertrica*** | Kurose Hole | | Kaikata Seamount | | Sumisu Caldera | |
|---|---|---|---|---|---|---|
| Dives | 3K488 (Inside) | 3K489 (Outside) | HPD0081 (Outside) | HPD0082 | HPD0083 (Outside) | HPD0084 (Inside) |
| Depth (m) | – | 631 | 504–549 | 469 | 602 | 495, 582 |
| Temperature (˚C) | – | 4.8 | *9.25–10.98 | 12.9 | 10.1 | 14.1, 11.2 |
| Salinity | – | 34.25 | *34.22–34.32 | 34.41 | 34.34 | 34.52, 34.40 |

| ***Bathocyroe fosteri*** | Kurose Hole | | Kaikata Seamount | | Sumisu Caldera | |
|---|---|---|---|---|---|---|
| Dives | 3K488 (Inside) | 3K489 (Outside) | HPD0081 (Outside) | HPD0082 | HPD0083 (Outside) | HPD0084 (Inside) |
| Depth (m) | – | – | 503–701 | 471 | 716 | 687, 688 |
| Temperature (˚C) | – | – | *7.7–9.2 | 12.3 | 7.4 | 10.5, 10.5 |
| Salinity | – | – | *34.14–34.21 | 34.41 | 34.28 | 34.35, 34.31 |

**Restricted Species**

| ***Periphylla periphylla*** | Kurose Hole | | Kaikata Seamount | | Sumisu Caldera | |
|---|---|---|---|---|---|---|
| Dives | 3K488 (Inside) | 3K489 (Outside) | HPD0081 (Outside) | HPD0082 | HPD0083 (Outside) | HPD0084 (Inside) |
| Depth (m) | – | 669, 725 | 763 | – | 704–751 | – |
| Temperature (˚C) | – | 4.6, 4.3 | ND | – | 6.7–7.5 | – |
| Salinity | – | 34.29, 34.32 | ND | – | 34.23–34.29 | – |

| ***Earleria bruuni*** | Kurose Hole | | Kaikata Seamount | | Sumisu Caldera | |
|---|---|---|---|---|---|---|
| Dives | 3K488 (Inside) | 3K489 (Outside) | HPD0081 (Outside) | HPD0082 | HPD0083 (Outside) | HPD0084 (Inside) |
| Depth (m) | 612–767 | – | – | – | – | 714–769 |
| Temperature (˚C) | 11.2–11.3 | – | – | – | – | 10.4–10.2 |
| Salinity | 34.40 | – | – | – | – | 34.36–34.34 |